QUANTUM LIQUID CRYSTAL PHASES AND UNCONVENTIONAL MAGNETISM IN ELECTRONIC AND ATOMIC FERMI SYSTEMS

BY

BENJAMIN MUNOZ FREGOSO

DISSERTATION

Submitted in partial fulfillment of the requirements
for the degree of Doctor of Philosophy in Physics
in the Graduate College of the
University of Illinois at Urbana-Champaign, 2010

Urbana, Illinois

Doctoral Committee:

Professor Philip W. Phillips, Chair
Professor Eduardo Fradkin, Director of Research
Professor John D. Stack
Professor S. Lance Cooper

Abstract

This thesis is devoted to the study of quantum liquid crystal phases in metallic systems and itinerant Fermi systems with dipole-dipole interactions. It is based on published works of Refs. [65, 193, 68, 67, 66]. In the first part of the Thesis, I present the construction of a generalization of the the McMillan- de Gennes theory of nematic-smectic thermal phase transition of classical liquid crystals to describe an analogous quantum phase transition in metallic systems. This theory qualitatively can also describe similar quantum phase transitions in high Tc superconductors. Recent experimental advances in cooling atoms with large electric or magnetic moment[125] make possible the study of novel quantum phases that arise due to the anisotropic and long-range nature of the dipole-dipole interactions. In the next part of the Thesis I present a Landau Fermi liquid theory of one-component Fermi systems with electric or magnetic dipolar interactions. I use this theory to construct an order parameter theory and predict elongated Fermi surface(FS) along the polarization axis. I calculate the temperature and interaction dependence of FS distortions. For a two-component system with magnetic dipole-dipole interactions I predict the existence of "spin textures" in *momentum space* and of prolate/oblate deformed FS's. This constitutes a new phase of matter I called *ferronematic*. Possible observation of this phase in ultracold Fermi gases with large mangnetic moments such as ^{163}Dy are discussed. The stability of Fermi gases under attractive interactions at unitarity was also studied.

I now briefly summarize the content of this thesis. Chapter 2 is based on Ref. [65]. I present a unified overview, from the mean-field to the unitarity regime, of the stability of a trapped Fermi gas with short range attractive interactions. Unlike in a system of bosons, a Fermi gas is always stable in these regimes, no matter how large the particle number. However, when the interparticle spacing becomes comparable to the range of the interatomic interactions, instability is not precluded.

Chapter 3 is based on Ref. [193]. I discuss the quantum phase transition between a quantum nematic metallic state to an electron metallic smectic state in terms of an order-parameter theory coupled to fermionic quasiparticles. Both commensurate and incommensurate smectic (or stripe) cases are studied. Close to the quantum critical point (QCP), the spectrum of fluctuations of the nematic phase has low-energy fluctuating

stripes. I study the quantum critical behavior and find evidence that, contrary to the classical case, the gauge-type of coupling between the nematic and smectic is irrelevant at this QCP. The collective modes of the electron smectic (or stripe) phase are also investigated. The effects of the low-energy bosonic modes on the fermionic quasiparticles are studied perturbatively. I find that at the nematic-smectic critical point, due to the critical smectic fluctuations, the dynamics of the fermionic quasiparticles near several points on the Fermi surface, around which it is reconstructed, are not governed by a Landau Fermi liquid theory. On the other hand, the quasiparticles in the smectic phase exhibit Fermi liquid behavior. I also present a detailed analysis of the dynamical susceptibilities in the electron nematic phase close to this QCP (the fluctuating stripe regime) and in the electronic smectic phase.

Chapter 4 is based on Ref. [68]. I demonstrate the possibility of a spontaneous symmetry breaking biaxial phase in these systems, which may be realized in, e.g., gases of ultracold polar molecules or strongly magnetic atoms. This biaxial nematic phase is manifest in a spontaneous distortion of the Fermi surface perpendicular to the axis of polarization. I describe these dipolar interaction induced phases using Landau Fermi liquid theory.

Chapter 5 is based on Ref. [67]. I show that a homogeneous two-component Fermi gas with long range dipolar and short-range isotropic interactions has a ferronematic phase for suitable values of the dipolar and short-range coupling constants. The ferronematic phase is characterized by having a non-zero magnetization and long range orientational uniaxial order. The Fermi surface of majority component is elongated while the minority component is compressed along the direction of the magnetization.

Chapter 6 is based on Ref. [66]. I study the magnetic structure of the ground state of a magnetic dipolar Fermi system of spin-$1/2$ particles in an imbalanced, partially polarized, state. I determine the distribution of quasiparticle spins states in momentum space. The $\mathbf{k}$-dependent spin quantization axis is not along the spin magnetization axis but develops instead spin textures in momentum space. I compute the shape of the Fermi surfaces, and the effective magnetic moment of the quasiparticles, at zero temperature and weak coupling. I discuss realizations of this state with ultracold magnetic atoms.

To my mother

Acknowledgements

I am immensely grateful to my advisor, Professor Eduardo Fradkin, who was extremely supportive and patient during all the years that we worked together. I thank the faculty at Illinois in particular Professor Gordon Baym, Anthony J Leggett and Benjamin Lev, my fellow group members in particular Dr. Kai Sun, Benjamin Hsu and Michael Lawler, who were very helpful to me; during all these years, chats during the coffee breaks, informal discussions, and group meetings helped me learn physics.

The works presented in this Thesis were supported in part by the National Science Foundation grants DMR 0442537 and DMR 0758462 at the University of Illinois and by the Department of Energy, Division of Basic Energy Sciences under Award DE-FG02-07ER46453 and DE-FG02-91ER45439 through the University of Illinois Frederick Seitz Materials Research Laboratory. Thanks to the University of Illinois Graduate College for awarding me a University of Illinois Fellowship for the Fall 2009 providing me with financial means to complete this project.

Table of Contents

List of Tables

List of Figures

Chapter 1

Introduction

In my thesis I worked on two aspects of quantum liquid crystal phases: 1) the quantum phase transition from a nematic to a smectic phase in metallic systems[193] and 2) the nematic phase and unconventional magnetism that, as I uncovered, arises in Fermi systems with dipole interactions[68, 67, 66]. I also worked on the stability of Fermi gases with attractive interactions[65], a topic somehow disconnected and more akin to atomic physics. This thesis is based on the published works [65, 193, 68, 67, 66] in which the author has collaborated. In the following, I briefly describe the need and importance of such studies but leave the details to the following chapters.

Quantum liquid crystals are quantum phases whose symmetries under rotations and translations are intermediate between those of a liquid and a crystalline solid. They were theoretically conceived in Ref. [104]. The nematic phase breaks the rotational invariance of space while keeping the translational invariance intact. The smectic or stripe phase is a charge density wave which breaks rotational and translational invariance of space. In my thesis I focused on the nematic and smectic phases. Phase transitions among classical liquid crystal phases have been extensively studied[48]. Quantum liquid crystal phases such as stripe phases have recently been investigated in high temperature superconductors and detailed and recent reviews are available on this subject[103, 197]. Stripe phases in high temperature superconductors have unidirectional order in both spin and charge (although not always) and it is typically incommensurate. In general the detected stripe order (by low-energy inelastic neutron scattering) in $La_{2-x}Sr_xCuO_4$, $La_{2-x}Ba_xCuO_4$ and $YBa_2Cu_3O_{6+y}$ (see Refs.[103] and [197] and references therein) is not static but "fluctuating". As emphasized in Ref.[103], "fluctuating order" means that there is no true long range unidirectional order. Instead, the system is in a (quantum) disordered phase, very close to a quantum phase transition to such an ordered phase, with very low-energy fluctuations that reveal the character of the proximate ordered state. On the other hand, in $La_{2-x}Ba_xCuO_4$ near $x = 1/8$ (and in $La_{1.6-x}Nd_{0.4}Sr_xCuO_4$ also near $x = 1/8$), the order detected by elastic neutron scattering[196], and resonant x-ray scattering in $La_{2-x}Ba_xCuO_4$ [6] also near $x = 1/8$, becomes true long-range static order.

It is interesting to investigate what is the interplay between fluctuating stripe, nematic and supercon-

ducting orders. Before my work there was no generalization of the classical nematic-smectic phase transition to the case of quantum metallic systems. In particular, it is not known how the presence of fermions will modify the critical point and hence we do no have experimental predictions of such a model. There is a clear need to pursue this line of reasoning further. Since electronic correlations are strong and despite the great amount of theoretical work, the mechanism of high Tc superconductivity is unknown. Finding the role of stripes or nematic order in high Tc superconductors is not the main purpose of my work; I refer the reader to excellent reviews on the subject. My work focuses on a narrower problem, i.e., to develop a quantum version of the nematic-smectic phase transition with a suitable chosen microscopic model of quasiparticle dynamics. Although the model is valid in the weak coupling limit it contains the full structure of symmetries of both phases and makes some predictions as to the form of the charge susceptibilities that can be compared with experiments.

I also explored quantum liquid crystal phases in Fermi systems with dipole interactions by developing Landau's Fermi liquid theory for polarized dipolar Fermi systems. Such systems can be engineered using atomic Fermi gases with dipole-dipole interactions.[125]. In general, atomic Fermi gases have the great advantage that interaction strengh can be controled, boundary shapes can be modified, etc. Condensed matter and, as we show, nuclear physics problems can be simulated using dipolar Fermi gases. Dipolar interactions are anisotropic and long-ranged[160]; when written in momentum space the dipole-dipole interaction resembles one type of non-central force between nucleons in dense nuclear matter. In fact, many of the effects that I will describe in the context of condensed matter and atomic systems were long studied theoretically in the nuclear physics literature from a phenomenological perspective[152] and references therein. However, we showed that the recent progress in trapping a Fermi gas with pure dipole-dipole interactions in Ben's Lev laboratory[125] opens the possibility of solving long standing puzzles such as non-Fermi liquid behavior at the isotropic-nematic quantum critical point, interesting unconventional magnetism with possible topological order. My research results opened a new and exiting venue not only in atomic physics but in the crossover to condensed matter.

The dipole-dipole interactions between polarized spins or electric dipoles are invariant under spatial rotations about the polarization axis. The anisotropy of the dipolar interaction breaks the invariance under full S0(3) spatial rotations. As we show, this fact leads to elliptically distorted ground state Fermi surface (FS) along the polarization axis. Moreover, magnetic dipole-dipole interactions are invariant under rotations in real and spin space ($\hat{\mathbf{J}} = \hat{\mathbf{L}} + \hat{\mathbf{S}}$)[160] and hence provide a novel type of spin-orbit coupling. Spin-orbit coupling are of much current interest since they are responsible for the so called band inversion in topological insulators. They are also important in spintronics and in theoretical studies of models with other topological

orders. My results suggests that magnetic dipolar systems provide a cleaner playground for the realization of this phases.

In chapter 2, I present a unified overview, from the mean-field to the unitarity regime, of the stability of a trapped Fermi gas with short range attractive interactions. Unlike in a system of bosons, a Fermi gas is always stable in these regimes, no matter how large the particle number. However, when the interparticle spacing becomes comparable to the range of the interatomic interactions, instability is not precluded.

In chapter 3, I discuss the quantum phase transition between a quantum nematic metallic state to an electron metallic smectic state in terms of an order-parameter theory coupled to fermionic quasiparticles. Both commensurate and incommensurate smectic (or stripe) cases are studied. Close to the quantum critical point (QCP), the spectrum of fluctuations of the nematic phase has low-energy fluctuating stripes. I study the quantum critical behavior and find evidence that, contrary to the classical case, the gauge-type of coupling between the nematic and smectic is irrelevant at this QCP. The collective modes of the electron smectic (or stripe) phase are also investigated. The effects of the low-energy bosonic modes on the fermionic quasiparticles are studied perturbatively, for both a model with full rotational symmetry and for a system with an underlying lattice, which has a discrete point group symmetry. I find that at the nematic-smectic critical point, due to the critical smectic fluctuations, the dynamics of the fermionic quasiparticles near several points on the Fermi surface, around which it is reconstructed, are not governed by a Landau Fermi liquid theory. On the other hand, the quasiparticles in the smectic phase exhibit Fermi liquid behavior. I also present a detailed analysis of the dynamical susceptibilities in the electron nematic phase close to this QCP (the fluctuating stripe regime) and in the electronic smectic phase.

In chapter 4, I demonstrate the possibility of a spontaneous symmetry breaking biaxial phase in these systems, which may be realized in, e.g., gases of ultracold polar molecules or strongly magnetic atoms. This biaxial nematic phase is manifest in a spontaneous distortion of the Fermi surface perpendicular to the axis of polarization. I describe these dipolar interaction induced phases using Landau Fermi liquid theory.

In chapter 5, I show that a homogeneous two-component Fermi gas with long range dipolar and short-range isotropic interactions has a ferronematic phase for suitable values of the dipolar and short-range coupling constants. The ferronematic phase is characterized by having a non-zero magnetization and long range orientational uniaxial order. The Fermi surface of majority component is elongated while the minority component is compressed along the direction of the magnetization.

In chapter 6, I study the magnetic structure of the ground state of a magnetic dipolar Fermi system of spin-$1/2$ particles in an imbalanced, partially polarized, state. I determine the distribution of quasiparticle spin states in momentum space. The k-dependent spin quantization axis is not along the spin magnetization

axis but develops instead spin textures in momentum space. I compute the shape of the Fermi surfaces, and the effective magnetic moment of the quasiparticles, at zero temperature and weak coupling. I discuss realizations of this state with ultracold magnetic atoms.

Chapter 2

Stability of trapped fermionic gases with attractive interactions

2.1 Introduction

The freedom to tune the interparticle interactions in dilute Fermi and Bose gases using Feshbach resonances raises the question of the stability of trapped atomic gases with attractive interactions against collapse. Weakly interacting Bose gases with attractive interactions become mechanically unstable once the particle number exceeds a critical value, of order the ratio of the oscillator length to the magnitude of the s-wave scattering length [23, 176, 17, 146]. The question is whether Fermi systems are always stabilized, and by what mechanisms, or can they ever be similarly unstable? The aim of this chapter of my Thesis is to present an overview of the problem in the different parameter regimes, putting together and extending the various arguments that have been given for the stability (and instability) of Fermi systems [70, 83, 135, 12, 31, 151, 22, 156, 157, 88, 191, 90, 160] within a unified framework.

At first, one might think that the Fermi energy of the atoms would be sufficient to support a trapped Fermi gas against collapse, in the way, for example, that electron degeneracy pressure supports white dwarfs against gravitational collapse. In a white dwarf the gravitational energy scales as the inverse of the system radius, $\mathcal{R}$, while the Fermi energy scales as $\mathcal{R}^{-2}$ non-relativistically; instability sets in only in the relativistic limit, when the Fermi energy begins to scale as $\sim \mathcal{R}^{-1}$. In a trapped Fermi gas with short range s-wave interactions between different components, the Fermi energy similarly scales as $\mathcal{R}^{-2}$, while the interaction energy scales, within mean-field theory, as $\mathcal{R}^{-3}$. Thus the Fermi energy is not, in itself, adequate to prevent an instability.

In the Fermi problem with low energy s-wave interactions, one must distinguish several regimes. The first is that of the weak interactions where the s-wave scattering length, a, is small compared with the interparticle spacing, and mean-field theory is valid. Calculating within mean-field theory one finds an instability at high density [191, 90, 160, 70], $k_F|a| > \pi/2$, or large particle number $N^{1/6} \gtrsim 0.6 d/|a|$ [83, 135], where k_F is the Fermi momentum, and $d = \sqrt{\hbar/m\omega}$ is the oscillator length, with ω the oscillator frequency (assumed isotropic); however, at such densities the interparticle spacing is comparable to the scattering

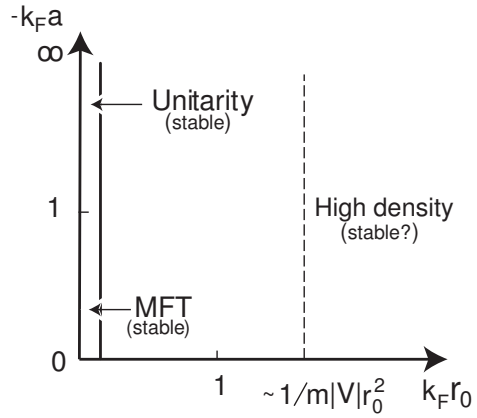

Figure 2.1: Regions of stability in the $k_F r_0$, $k_F|a|$ plane of a two component Fermi gas with short range interactions. Here k_F is the Fermi momentum, a the s-wave scattering length, and r_0 the range of the interactomic potential.

length, and the mean-field calculation becomes invalid. Indeed, in the mean-field regime ($k_F|a| << 1$) the system is always stable. The second – "unitary" – regime is when the scattering length is large compared with the interparticle spacing, itself large compared with the range of the interparticle potential. Here the system is again always stable, since the total energy remains positive [83, 70, 12, 31, 151, 22, 156, 157, 88, 16]. The third regime is when the interparticle spacing becomes comparable to the range, r_0, of the interparticle potential. In this regime the system can in principle become unstable. Figure 2.1 schematically illustrates these regimes in the $k_F r_0$, $k_F|a|$ plane.

I first study the stability of the Fermi gas in mean field theory, working in the local-density approximation in which the gas is assumed at each point to be locally homogeneous [28], and derive analytically the mean-field limits on the density and particle number. I do not include effects of pairing. As can be seen, the two instability conditions, $k_F|a| > \pi/2$, and number $N^{1/6} \gtrsim 0.6d/|a|$, are equivalent. I next discuss the unitary regime. By means of a simple interpolation formula for the density dependence of the energy, I show that the gas should be stable, with no limit to the number of particles in the system. I show, by using the Hartree-Fock approximation as a rigorous upper bound to the total energy of a system with an attractive square well interparticle interaction, how stability can break down in the high density regime.

2.2 Stability in mean-field

I consider a Fermi gas with equal numbers of two components (denoted by $\uparrow$ and $\downarrow$) in equilibrium at zero temperature in an isotropic harmonic trap, $V(r) = \frac{1}{2}m\omega^2 r^2$. The energy of the system in the local density

approximation is

$$E = \frac{3\hbar^2}{10m}(3\pi^2)^{2/3}\int d\mathbf{r}\ n^{5/3} + \frac{1}{2}m\omega^2\int d\mathbf{r}\ r^2\ n + g\int d\mathbf{r}\ n_\uparrow n_\downarrow, \tag{2.1}$$

where $g = 4\pi\hbar^2 a/m$ is the coupling constant, and $n = 2n_\uparrow = 2n_\downarrow$ is the total density of particles. The short range s-wave interactions between particles of the same species essentially vanish due to the antisymmetry of the many-fermion wave function.

The equilibrium density minimizes the total energy with respect to the density, at fixed particle number, $N = \int d\mathbf{r}\ n(r)$. Taking the constraint of fixed total number of particles into account via a chemical potential, $\mu = \mu_\uparrow = \mu_\downarrow$, I find that the first functional derivative of the energy is

$$\delta E - \mu\delta N = \int d\mathbf{r}\left((3\pi^2)^{2/3}\frac{\hbar^2}{2m}n^{2/3} + \frac{1}{2}m\omega^2 r^2 + \frac{g}{2}n - \mu\right)\delta n = 0, \tag{2.2}$$

which yields the density-position relation,

$$(3\pi^2)^{2/3}\frac{\hbar^2}{2m}n^{2/3} + \frac{1}{2}m\omega^2 r^2 + \frac{g}{2}n = \mu. \tag{2.3}$$

It is most convenient to regard this equation as determining r^2 in terms of n:

$$r^2 = -\left((3\pi^2 n)^{2/3} - 4\pi|a|n\right)d^4 + R^2(a, N), \tag{2.4}$$

where $d = \sqrt{\hbar/m\omega}$ is the oscillator length, and the radius of the cloud is $R = \sqrt{2\mu/m\omega^2}$. Equation (2.4) can be inverted either graphically, or by simply solving the cubic equation explicitly. The results are shown in Fig. (2.2). Note that when $a < 0$, $r(n)^2$ has a minimum as a function of density at

$$r_0^2 = -\frac{\pi^2}{12}\frac{d^4}{|a|^2} + R^2, \tag{2.5}$$

where

$$n_0 = \frac{\pi}{24|a|^3}. \tag{2.6}$$

In order for the density profile to be stable it must minimize, not maximize, the energy functional, i.e.,

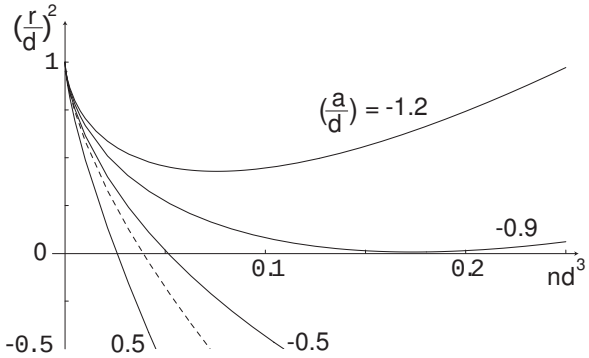

Figure 2.2: Distance from center of trap, squared, as a function of the density, n, Eq. (2.4), for the value $R = d$. For large negative a the curve does not intersect the n-axis, and the system becomes unstable. The dashed curve shows the characteristic radius squared vs. density calculated with the effective scattering length, Eq. (2.11).

the second variation of $E - \mu N$:

$$\delta^2 E - \mu \delta^2 N = \int d\mathbf{r} \left((3\pi^2)^{2/3} \frac{\hbar^2}{3m} n^{-1/3} + \frac{g}{2} \right) (\delta n)^2, \tag{2.7}$$

must be positive for all δn. This condition requires,

$$k_F(r)|a| < \frac{\pi}{2} \approx 1.57, \tag{2.8}$$

at all positions, or equivalently $n \leq \pi/24|a|^3$ (cf. Eq. (2.6)). As can be seen, Eq. (2.8) is the condition that the density profile corresponds to a minimum of the energy functional (2.1). Note that I have derived this result in terms of the Thomas-Fermi profile including interactions. This argument is similar to that of [160]. The result (2.8) has also been obtained heuristically by comparing the repulsive force on an atom arising from the kinetic energy term with the attractive force due to the mean field interaction energy [70], and derived via a field-theoretical approach [191].

When the minimum of r^2 vs. n is at negative r^2, the system is stable because then n is less than n_0, so that $k_F|a|$ is always $< \pi/2$. On the other hand, when the minimum is at positive values, the curve does not intersect the horizontal axis, and therefore there is no solution for the density at the center of the trap. (An unphysical solution for the density would have a hole of radius r_0 about the center of the trap.) However, in this case the density equals n_0 at $r = r_0$, and vanishes as $r \to R$. Then, $k_F(0)|a| = \pi/2$, and the solution is marginally stable, not actually minimizing the energy functional (2.1). I conclude that the system is stable

when $r_0^2 \leq 0$, and the critical point is $r_0 = 0$, corresponding to

$$R^2 = \frac{\pi^2}{12}\frac{d^4}{|a|^2}. \tag{2.9}$$

and then the density of the system at the center of the trap is given by Eq. (2.6).

When Eq. (2.9) is satisfied the system reaches its maximum number of particles in equilibrium, given by the area under the n vs r curve, $N_{max} = 4\pi \int_0^\infty n(r) r^2 dr$. Integrating with respect to the n, I find

$$N_{max} = \frac{\pi^5}{48}\frac{d^6}{|a|^6} I, \tag{2.10}$$

where

$$\begin{aligned} I &= \int_0^1 \left(\frac{2}{3}x^3 - x^2 + \frac{1}{3}\right)^{1/2} (1-x)x^4 dx \\ &= \frac{54}{5005} - \frac{40}{9009\sqrt{3}} \approx 0.00823. \end{aligned}$$

As long as the local density approximation is valid, the condition (2.10) is equivalent to the condition (2.8). However, the use of mean field is no longer valid for $k_F|a| \gtrsim 1$. From (2.10), the condition for stable equilibrium is $N^{1/6} \leq 0.612 d/|a|$, which agrees with that found numerically in Ref. [135].

Table 2.1 lists the number of particles in representative experiments on ^{6}Li gases with two-spin components. Since these experiments were not testing the maximum number of particles that could be trapped, they provide only lower bounds on the maximum number of particles. For small $k_F|a| < 1$, the experimental particle numbers are well within the bound (2.10). However fermionic systems at larger $k_F|a|$, exceeding $\pi/2$, do remain stable. See Fig. 2.3. The argument leading to Eq. (2.10) breaks down at large $k_F|a|$, for then correlations beyond mean field become important. In addition, when $n(0) \to n_0$, the local density approximation fails. A necessary condition for the local density approximation to be valid is that the density varies slowly over an interparticle spacing, or $|\partial \ln n/\partial r| \ll k_F$. From Eq. (2.4), I thus find the requirement, for $n(0) \simeq n_0$, that $1 - 2k_F|a|/\pi \gg (|a|/d)^2$ for the local density approximation to be valid, where I have taken r^2 to be bounded by the critical R^2 in Eq. (2.9). This condition clearly breaks down as $n(0) \to n_0$, where dn/dr diverges, as one sees in Fig. 2.2.

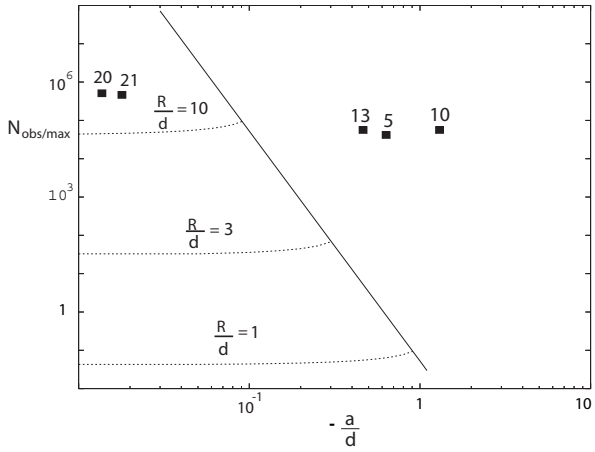

Figure 2.3: The maximum particle number vs. $-a/d$, as predicted by Eq. (2.10). The nearly horizontal lines are contours of constant chemical potential in the stable region; here $R/d = \sqrt{2\mu/\hbar\omega}$. Also shown are the particle numbers measured in the five experiments in Table 1. Data points are labelled by the corresponding reference numbers.

2.3 Near the unitary regime

When $k_F|a|$ becomes large perturbation methods fail, and the question of stability is more involved. In the unitarity regime ($k_F|a| \to \infty$), the energy of the ground state is bounded and can be written in the scale-free form [83, 31, 12, 22] $E_0 = (1+\beta)E_{FG}$, where β is universal constant ~ -0.5. To approach the problem, I interpolate the energy between small $|a|$ and $-\infty$ by calculating in mean field theory with a density dependent effective scattering length,

$$a_{\rm eff} = \frac{a}{1-\gamma k_F a}, \tag{2.11}$$

for $k_F a < 0$, and replacing the coupling g in Eq. (2.1) by the local coupling $g_{\rm eff} = 4\pi\hbar^2 a_{\rm eff}/m$. The choice

Table 2.1: Experimental measurements of particle numbers in ^{6}Li gases. In the regime $k_F|a| < 1$, Eq. (2.10) is satisfied; a_0 is the Bohr radius.

Expt.	T/T_F	$-a/a_0$	N_{obs}	N_{max}	$k_F\|a\|$
[97]	< 0.2	3500	9×10^5	$\sim 10^{12}$	< 1
[192]	< 0.1	~ 500	6×10^5	$\sim 10^9$	$<< 1$
[157]	~ 0.75	15600	$1.3-9\times10^4$	~ 7	$>> 1$
[70]	~ 0.15	10^4	8.0×10^4	~ 1	≈ 2.5
[151]	~ 0.1	10^4	7.5×10^4	~ 0	≈ 7.4

$\gamma = -20/9\pi\beta$ reproduces the known energies in the weakly interacting limit and in the unitary regime [1]. Pairing effects do not modify this approach since in the unitary regime pairing energies also scale with E_{FG}.

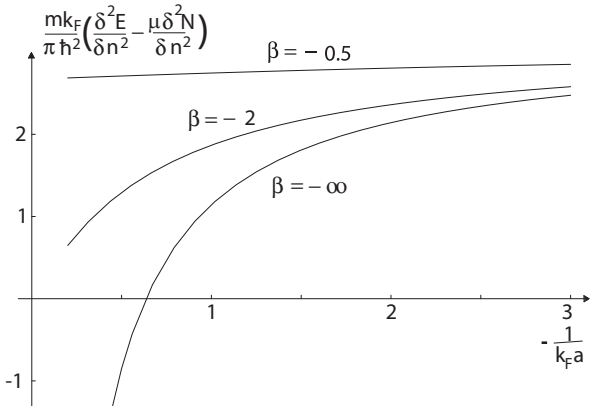

Figure 2.4: The second variation of $E - \mu N$, Eq. (2.13), as a function of $-1/k_F|a|$, calculated with the effective scattering length, $a_{\rm eff}$, Eq. (2.11).

Repeating the above Thomas-Fermi calculation with this density-dependent scattering length, I find, first, the position as a function of density,

$$r^2 = -\left[k_F^2 - 4\pi|a_{\rm eff}|n\left(1-\frac{\gamma}{6}k_F|a_{\rm eff}|\right)\right]d^4 + R^2. \tag{2.12}$$

The density profile is similar to that of the stable configurations shown in Fig. 2. I show in that figure, as a dashed line, the density profile calculated with Eq. (2.12) $a = -0.5$, and $\beta = -0.5$.

The second functional derivative of the energy with respect to n is,

$$\frac{\delta^2 E - \mu\delta^2 N}{(\delta n)^2} = \frac{\pi\hbar^2}{mk_F}\left(\pi + 2k_F a_{\rm eff} + \frac{10}{9}\gamma(k_F a_{\rm eff})^2 + \frac{2}{9}\gamma^2(k_F a_{\rm eff})^3\right). \tag{2.13}$$

In the limit $\gamma k_F|a| << 1$, $a_{\rm eff} \sim a$, and Eq. (2.13) predicts that the gas is stable for all $k_F|a|$, in distinction to the prediction of Eq. (2.8). In the opposite limit, $\gamma k_F|a| >> 1$, $|a_{\rm eff}| \to 9\pi\beta/20k_F$, a constant, and $\left(\delta^2 E - \mu\delta^2 N\right)/(\delta n^2) = (\pi^2\hbar^2)/(mk_F)(1+\beta/2)$. Hence the gas is stable for $\beta > -2$, as can be seen in Fig. 2.4, a plot of $(mk_F/\pi\hbar^2)(\delta^2 E - \mu\delta^2 N)/(\delta n)^2$ as a function of $-1/k_F|a|$ for various β. Experiments on ^{6}Li find[70, 22, 156], $\beta \sim -0.5$; for these values, the second variation is always positive, predicting that the gas should be stable for all $k_F|a|$, in agreement with experiment.

2.4 Even higher density

In the scale-free unitary regime the interparticle spacing is large compared with the range of the potential, and the system is stable. However, at higher densities when the interparticle spacing becomes comparable to

the range of the potential, the system can in fact become unstable, as can be seen from the following model calculation. Let us assume that the interparticle interaction is an attractive square well potential with range r_0 and depth $V(< 0)$. The energy calculated assuming a Hartree-Fock wave function is a rigorous upper bound to the exact total energy, E; thus

$$\frac{E}{N} \leq \frac{3\hbar^2 k_F^2}{10m} + \frac{2\pi r_0^3}{3} nV. \tag{2.14}$$

As n increases, the energy becomes unbounded below; the kinetic energy does not save the system from collapse. I note that at $V = -\hbar^2\pi^2/4mr_0^2$ the two body-scattering amplitude has a resonance, the scattering length diverges, and the interaction energy per particle becomes $E_{\rm int}/N = -(5\pi/27)k_F r_0 E_{FG}$. The instability in this model should not occur, however, for realistic interatomic potentials which have a repulsive core.

Chapter 3

Fluctuating stripes in strongly correlated electron systems and the nematic-smectic quantum phase transition

3.1 Introduction

I discuss the quantum phase transition between a quantum nematic metallic state to an electron metallic smectic state in terms of an order-parameter theory coupled to fermionic quasiparticles. Both commensurate and incommensurate smectic (or stripe) cases are studied. Close to the quantum critical point (QCP), the spectrum of fluctuations of the nematic phase has low-energy "fluctuating stripes". I study the quantum critical behavior and find evidence that, contrary to the classical case, the gauge-type of coupling between the nematic and smectic is irrelevant at this QCP. The collective modes of the electron smectic (or stripe) phase are also investigated. The effects of the low-energy bosonic modes on the fermionic quasiparticles are studied perturbatively, for both a model with full rotational symmetry and for a system with an underlying lattice, which has a discrete point group symmetry. I find that at the nematic-smectic critical point, due to the critical smectic fluctuations, the dynamics of the fermionic quasiparticles near several points on the Fermi surface, around which it is reconstructed, are not governed by a Landau Fermi liquid theory. On the other hand, the quasiparticles in the smectic phase exhibit Fermi liquid behavior. I also present a detailed analysis of the dynamical susceptibilities in the electron nematic phase close to this QCP (the fluctuating stripe regime) and in the electronic smectic phase.

The discovery of the high temperature superconductors in the quasi-two-dimensional copper-oxide materials in the late 1980s, and of novel correlated phases in other complex oxides, has brought to the forefront the problem of the physics of strongly correlated electron systems. To this date the understanding of the behavior of these systems remains one of the main open and challenging problems in condensed matter physics. The central conundrum in this field is the fact that these strongly coupled electron systems are best regarded as doped Mott insulators for which both the band theory of metals and the Landau theory of the Fermi liquid (FL) fail.

One characteristic feature of the physics of doped Mott insulators is their inherent tendency to electronic

phase separation, frustrated by the effects of Coulomb interactions.[56, 106] The ground states resulting from these competing tendencies typically break the translation invariance and/or the point group symmetry of the underlying lattice. From a symmetry point of view, the ground states of doped Mott insulators are charge-ordered phases[104], which share many similarities with classical liquid crystals, and should be regarded as electronic liquid crystal phases.[104] However, unlike classical liquid crystals, electronic liquid crystals are strongly quantum mechanical states whose transport properties range from insulating to metallic and even superconducting. In contrast with classical liquid crystals, whose ordered phases represent the spontaneous breaking of the continuous translation and rotational symmetry of space[48, 34], the electronic liquid crystal phases of strongly correlated systems are sensitive to the effects of the underlying lattice and the symmetry breaking patterns involve the point and space groups, as well as to disorder. More complex ordered states, involving simultaneously charge and spin degrees of freedom, may also arise.[212]

The sequence of quantum phase transitions described above, electron crystal $\rightarrow$ smectic (stripe) $\rightarrow$ nematic $\rightarrow$ isotropic fluid, representing the progressive restoration of symmetry, is natural from a strong correlation perspective. Indeed, the electron crystal state(s) are naturally insulating (much as in the case of a Wigner crystal), the smectic or stripe phases are either anisotropic metals or superconductors, and the charged isotropic fluids are either metallic or superconducting. While the isotropic metallic phase is essentially a FL (albeit with strongly renormalized parameters), the nematic and smectic metallic phases have a strong tendency to show non-FL character. Indeed, much of the theoretical description of the stripe or smectic phases is usually based on a quasi-one-dimensional analysis, which makes explicit use of this strong correlation physics. Such approaches give a good description of this state deep inside this phase and at energies high compared to a "dimensional crossover" scale below which the state is fully two-dimensional (and strongly anisotropic)[57, 30, 55, 204, 72, 11, 29]. Stripe phases (insulating, metallic, and superconducting) have been found in mean-field studies of generalized two-dimensional Hubbard and t-J models[222, 128, 100, 162, 183, 205, 206, 155, 181, 124, 85, 169].

The same pattern of quantum phase transitions can also be considered in reverse order, with a weak coupling perspective, as a sequence of symmetry breaking phase transitions beginning from the isotropic metal: FL $\rightarrow$ electron nematic $\rightarrow$ electron smectic $\rightarrow$ insulating electron crystal. In this case, one begins with a uniform isotropic metal, well described at low energies by the Landau theory of the FL, with well-defined quasiparticles and a Fermi surface (FS), and considers possible instabilities of the isotropic fluid into a nematic (or hexatic and other such states), as well as phase transitions into various possible charge-density-wave (CDW) phases. The unidirectional CDW-ordered states are the weak coupling analog of the smectic (or stripe) phases, and have the same order parameters as they break the same symmetries. The main

difference between a CDW and a smectic resides in the fact that while the CDW arises as a weak coupling (infinitesimal) instability of a FL in which parts of the FS are gapped[133] (which requires the existence of a FS with sharp quasiparticles), the stripe phases do not require such description. While a CDW phase at high energies is essentially a FL, the high-energy regime of a stripe phase is a quasi-one-dimensional Luttinger liquid.[30, 55] A direct quantum phase transition from a FL to a CDW phase is, naturally, possible and this quantum phase transition has been studied in some detail,[7, 39] as well as to a metallic spin-density wave (SDW)[202, 199].

The weak coupling description of an electron nematic phase uses a Pomeranchuk instability of a Fermi liquid state[163]. Oganesyan, Kivelson, and Fradkin[150] showed that the nematic quantum phase transition is a quadrupolar instability of the FS, and gave a characterization of the properties of the nematic Fermi fluid in a continuum model. An electron nematic quantum phase transition has also been found in lattice models[79, 136, 50], which show, however, a strong tendency to exhibit a first-order quantum phase transition[101, 102, 216]. Pomeranchuk instabilities in the Landau theory of the FL have also shown the existence of an electron nematic transition[149, 211]. Perturbative renormalization group analysis of the stability of the FL in Hubbard-type models[89], as well as high-temperature expansions[165], has also shown that in such models there is a strong tendency to a nematic state. An electron nematic state was shown to be the exact ground state in the strong coupling limit of the Emery model of the copper oxides at low hole doping[106].

The upshot of the work on the electron nematic quantum phase transition is that, at the QCP (if the transition is continuous) and in the nematic phase (in the continuum) the electron quasiparticle essentially no longer exists as an asymptotically stable state at low energies, except along symmetry determined directions in the ordered phase. A full solution of this QCP by bosonization methods has confirmed these results, which were gleaned from mean-field theory, and have also provided strong evidence for local quantum criticality at this QCP [114, 116].

In this chapter I will be interested in the quantum phase transition from an electron nematic phase to a charge stripe phase, a unidirectional CDW. For simplicity I will not consider here the spin channel, which plays an important role in many systems. I will only consider the simpler case of unidirectional order. Extensions to the more general case of multidirectional order are straightforward. Here I develop a quantum-mechanical version of the nematic-smectic transition in a metallic system. This is a quantum-mechanical version of the McMillan-deGennes theory for the quantum phase transition from a metallic nematic phase to a metallic smectic (or CDW) phase. The construction of such a generalization of the McMillan-deGennes theory is the main purpose of this chapter.

As it is discussed in detail in subsequent sections, here I will follow the "weak-coupling" sequence of quantum phase transitions described above, beginning with the transition from a FL to an electron nematic, and from the latter to a stripe or unidirectional CDW state. The main advantages of this approach are that it allows to address the fate of the electronic quasiparticles and non-Fermi liquid behaviors as the correlations that give rise to these electronic liquid crystal phases develop, as well as to study the quantum critical behavior following the standard Hertz-Millis approach [84, 137, 180]. However, the main disadvantage is that this approach does not do justice to the physics of strong correlation. For this reason, in spite of the important insights that are gained through this line of analysis, this approach cannot explain the physics of the "strange metal" regime observed in the "normal state" of high T_c superconductors where non-Fermi liquid effects are widely reported. To do that would require studying this problem as a sequence of quantum melting transitions. An important first step in this direction has been made by Cvetkovic and coworkers [45, 44, 43] who have studied a purely bosonic model of such quantum melting. The inclusion of fermionic degrees of freedom in this strong coupling approach is an interesting but challenging open problem.

I have both conceptual and phenomenological motivations for considering this problem. At the conceptual level the main question is to develop a theory of the quantum critical behavior at the electron nematic-smectic phase transition, and of the low-energy physics of both phases near quantum criticality. Although the static properties are the same as in the classical theory (as required by symmetry) the quantum dynamics changes the physics substantially. Thus, physical properties, which determine the transport properties and the fermion spectral function, cannot be gleaned from the classical problem. Provided that the quantum phase transition is continuous or, at most weakly first order, the low-energy fluctuations in one phase (say the nematic metal) must reflect the character of the nearby ordered stripe phase. In other words, under these assumptions, as the quantum phase transition is approached the metallic nematic phase behaves as a state with "fluctuating stripes". The ample experimental evidence in high temperature superconductors for "fluctuating stripe order" should be interpreted instead as evidence of a nematic phase proximate to a quantum phase transition to a stripe (or smectic)-ordered state[103].

3.2 Summary of results

I follow a phenomenological approach to study the quantum phase transition between an electronic nematic state and electronic smectic state. I postulate the existence of both an electron nematic and a smectic phases with a possible direct phase transition between them. This physics will be represented by an effective field theory involving the nematic and CDW order parameters. The static part of the effective action of

the order-parameter theory has the same form as in the classical theory of the nematic-smectic transition, the McMillan-deGennes theory. I will assume that aside from the effects of the coupling to the fermionic quasiparticles, this effective field theory is analytic in the order parameters and their derivatives as this dependence is determined by local physics. As shown below, this assumption implies a dynamical quantum critical exponent $z = 1$.

The fermionic quasiparticles couple to the nematic and smectic (CDW) order parameters in their natural symmetry-dictated way. The fermions will be assumed to be a normal FL, with well-defined quasiparticles and a FS. Thus, I will not attempt to explain why the phase transition exists, which requires a microscopic theory, but rather describe its character. One of our most important results is that this theory gives a description of a phase with fluctuating stripe (smectic) order, of much interest in current experiments. The effective theory that I consider also allows for a possible direct transition between the normal and isotropic FL state and a CDW phase, without going through an intermediate nematic phase, as in the direct transition between a FL and a CDW state, discussed by Altshuler, Ioffe, and Millis[7]. Thus, the theory I present here actually describes the behavior of a FL in the vicinity of a possible bicritical point which, as I shall show, is not directly accessible. The main results of our theory are summarized in Table 3.1,3.2, 3.3. In Sec.

	Nematic
Anisotropic Scaling $[q_x] : [q_y] : [\omega]$	1 : 1 : 3
Non-analyticity	
Gaussian Fixed Point	Stable
$\Sigma''(k_F, \omega)$	$\lvert\omega\rvert^{2/3}$

Table 3.1: Summary of results: nematic phase.

	$Q_S < 2k_F$	$Q_S = 2k_F$ commensurate	$Q_S = 2k_F$ incommensurate	inflection point
Anisotropic Scaling $[q_x] : [q_y] : [\omega]$	1 : 1 : 2	1 : 2 : 3	1 : 2 : 2	1 : 3 : 3
Non-analyticity		$\Phi^{5/2}$	$\Phi^{5/2}$	$\Phi^{9/4}$
Gaussian Fixed Point	Stable	Unstable/First Order	Stable	Stable
$\Sigma''(k_F, \omega)$	$\lvert\omega\rvert^{1/2}$		$\lvert\omega\rvert$	$\lvert\omega\rvert^{13/12}$

Table 3.2: Summary of results: smectic mode at the electronic nematic-smectic QCP.

3.3 I discuss the current experimental status of electronic liquid crystal phases in a number of different materials. In Sec. 3.4 we set up the order parameter theory for the electronic liquid crystal phases based on symmetry and analyticity. The static part of this phenomenological theory is (as it should be) similar

	continuous rotational group	discrete rotational group
Anisotropic scaling $[q_x] : [q_y] : [\omega]$	$1 : 2 : 2$	$1 : 1 : 1$
Non-analyticity		
Gaussian fixed point	stable	Stable
$\Sigma''(k_F, \omega)$	$\omega^2 \log \lvert\omega\rvert$ or $\lvert\omega\rvert^{3/2}$	$\omega^2 \log \lvert\omega\rvert$ or $\lvert\omega\rvert^2$

Table 3.3: Summary of results: smectic phase.

to its classical counterpart, but I add proper dynamics to describe the quantum fluctuations. I next couple the order parameter theory to the fermionic quasiparticles, in Sec. 3.5. The coupling between the fermionic quasiparticles and the order parameters is completely determined by symmetry. This is a standard approach to study quantum phase transitions in metallic systems [180]. It is a consistent scheme for the study of the quantum phase transition provided the effective dimension $d+z$ is close to 4 (here d is the dimensionality of space). Several different non-analytic dependences on the order parameters in the effective action appear as a consequence of their coupling to the fermions. I show that these nonanalytic dynamical terms dominate over the dynamics prescribed phenomenologically. Hence, the dynamics of fermionic liquid crystal phase is very different from that of the simple phenomenological theory. I present a detailed analysis of the behavior of the dynamical susceptibilities in both phases and at the QCP.

The nematic-smectic QCP is studied in Sec. 3.6. In classical liquid crystals, the Goldstone mode of the nematic phase plays a very important role at the nematic-smectic transition. There, this relevant coupling drives the transition weakly first order through a fluctuation-induced first order transition[81]. However, in the case of the electronic liquid crystals, I find that the coupling between the nematic Goldstone mode and the smectic field is actually irrelevant at the electronic nematic-smectic QCP. Therefore, these two modes can be treated separately, as they are weakly coupled to each other. Several different nematic-smectic critical theories are studied, depending on the relation between the magnitude of the ordering wave vector of the CDW, Q_S, and the Fermi wave vector, k_F. For $Q_S < 2k_F$ (Fig. 3.2(a)), I find that the critical smectic field has a dynamic critical exponent $z = 2$, which will result in a $C \sim T$ contribution to the heat capacity. This is a correction to the conventional linear T behavior of Fermi liquids. These quantum fluctuations lead to the existence of four points on the FS where the assumptions of FL theory are violated (Fig. 3.2(a)). At these points the imaginary part of the fermion self-energy correction $\Sigma''(k_F, \omega) \sim |\omega|^{1/2}$. For $Q_S = 2k_F$ (Fig. 3.2(b)), the system exhibits anisotropic scaling: $[q_x] = 1$, $[q_y] = 2$ and $[\omega] = 3$ for the incommensurate CDW, while $[q_x] = 1$, $[q_y] = 2$ and $[\omega] = 2$ for the commensurate case. Besides, a non-analytic $\Phi^{5/2}$ term, where Φ is the smectic order parameter, is generated in the action of the low-energy effective theory. This non-analytic

term is relevant under the renormalization group (RG) for the incommensurate case, suggesting a weak, fluctuation-induced, first-order transition. This coupling is irrelevant in the commensurate case. Here I also find two points on the FS (Fig. 3.2(b)), where the system has marginal FL behavior, with a quasiparticle scattering rate $\Sigma''(k_F, \omega) \sim |\omega|$, and a low temperature correction to the heat capacity $C \sim T^{3/2}$, which is subleading. I also consider the special case of a CDW caused by a nearly nested FS, for which I find that the low-temperature heat capacity correction $C \sim T^{4/3}$, which is also subleading, and the fermions form a FL, with $\Sigma''(k_F, \omega) \sim |\omega|^{13/12}$. I also calculated the dynamic CDW susceptibility $\chi_S(q, \omega)$ for both cases. The $Q_S > 2k_F$ case will not be discussed here. In the presence of a lattice this case is quite trivial (see Sec. 3.6) while for it to occur in a continuum system, where it is non-trivial, requires unphysical assumptions.

The smectic phase is discussed in Sec. 3.7. In the smectic phase the anisotropic scaling associated with the Goldstone fluctuations are $[q_x] = 1$, $[q_y] = [\omega] = 2$. I find that the low-temperature heat capacity correction $C \sim T^{3/2}$, which is also subleading. The quasiparticle scattering rate in this case is $\Sigma''(k_F, \omega) \sim \omega^2 \log |\omega|$ for much of the FS while $\Sigma''(k_F, \omega) \sim |\omega|^{3/2}$ at the two special points where the Fermi velocity is parallel to the ordering wave vector. Thus, in this case fermions behave as a FL. I also calculated both the longitudinal and transverse dynamic CDW susceptibilities in the smectic phase.

Lattice effects are also discussed. For the case of an incommensurate smectic phase, I show that there is an unpinned smectic phase close to the nematic-smectic critical point. In this phase, the smectic Goldstone mode has a dynamic critical exponent $z = 1$ and the system is a FL with $\Sigma''(\omega) \sim \omega^2 \log |\omega|$ at most of the FS and $\Sigma''(\omega) \sim \omega^2$ at some special point on the FS described below. Due to the unpinned smectic ordering, the system receives a correction to the low-temperature heat capacity $C \sim T^2$, and I also computed the dynamic transverse CDW susceptibility. Deep into the smectic phase, an incommensurate CDW may be pinned down by lattice distortion. As expected, the fermions in a pinned smectic are in a conventional FL state.

In Sec. 3.8 I present a brief discussion of the role of thermal fluctuations for these phases and of the classical-to-quantum crossovers. I conclude with a summary of our main results and a discussion of open questions in Sec. 3.9. Details of the calculations are presented in several appendices. In Appendix A.1 I discuss the tensor structure of the order parameters. In Appendix A.2 I present details of the nematic-smectic QCP for the case $Q_S < 2k_F$, while the nonanalytic terms induced for the $Q_S = 2k_F$ case are presented in Appendix A.3. In Appendix A.4 I present details of the calculation of the spectrum of Goldstone modes in the smectic phase. In Appendix A.5 I summarize the random phase approximation (RPA) calculation of the fermion self-energy at the nematic-smectic QCP and in the smectic phase.

3.3 Experimental status of electronic liquid crystal phases

During the past decade or so experimental evidence has been mounting of the existence of electronic liquid crystal phases in a variety of strongly correlated (as well as not as strongly correlated) electronic systems. I will be particularly interested in the experiments in the copper oxide high temperature superconductors, in the ruthenate materials (notably $Sr_3Ru_2O_7$), and in two-dimensional electron gases (2DEG) in large magnetic fields. However, as I will discuss below, our results are also relevant to more conventional CDW systems such as the quasi-two-dimensional dichalcogenides.

3.3.1 High temperature superconductors

In addition to high temperature superconductivity, the copper oxide materials display a strong tendency to have charge-ordered states, such as stripes. The relation between charge ordered states[105], as well as other proposed ordered states[35, 200], and the mechanism(s) of high temperature superconductivity is a subject of intense current research. It is not, however, the focus of this chapter.

Stripe phases have been extensively investigated in high temperature superconductors and detailed and recent reviews are available on this subject[103, 197]. Stripe phases in high temperature superconductors have unidirectional order in both spin and charge (although not always) and it is typically incommensurate. In general the detected stripe order (by low-energy inelastic neutron scattering) in $La_{2-x}Sr_xCuO_4$, $La_{2-x}Ba_xCuO_4$ and $YBa_2Cu_3O_{6+y}$ (see Refs.[103] and [197] and references therein) is not static but "fluctuating". As emphasized in Ref.[103], "fluctuating order" means that there is no true long range unidirectional order. Instead, the system is in a (quantum) disordered phase, very close to a quantum phase transition to such an ordered phase, with very low-energy fluctuations that reveal the character of the proximate ordered state. On the other hand, in $La_{2-x}Ba_xCuO_4$ near $x = 1/8$ (and in $La_{1.6-x}Nd_{0.4}Sr_xCuO_4$ also near $x = 1/8$), the order detected by elastic neutron scattering[196], and resonant x-ray scattering in $La_{2-x}Ba_xCuO_4$ [6] also near $x = 1/8$, becomes true long-range static order.

In the case of $La_{2-x}Sr_xCuO_4$, away from $x = 1/8$, and particularly on the more underdoped side, the in-plane resistivity has a considerable temperature-dependent anisotropy[9], which has been interpreted as an indication of electronic nematic order. From these experiments it has been suggested that this phase be identified as an electron nematic[9]. The same series of experiments also showed that very underdoped $YBa_2Cu_3O_{6+y}$ is an electron nematic as well. The most striking evidence for electronic nematic order in high temperature superconductors are the recent neutron scattering experiments in $YBa_2Cu_3O_{6+y}$ at $y = 6.45$[87]. In particular, the temperature-dependent anisotropy of the inelastic neutron scattering in $YBa_2Cu_3O_{6+y}$ shows that there is a critical temperature for nematic order (with $T_c \sim 150K$) where the inelastic neutron

peaks also become incommensurate. Similar effects were reported by the same group[86] at higher doping levels ($y \sim 6.6$) who observed that the nematic signal was decreasing in strength suggesting the existence of a nematic-isotropic quantum phase transition closer to optimal doping. Fluctuating stripe order in underdoped $YBa_2Cu_3O_{6+y}$ has been detected earlier on in inelastic neutron scattering experiments [143, 190] which, in hindsight, can be reinterpreted as evidence for nematic order. However, as doping increases the strength of the temperature-independent anisotropic background, due to the increased orthorhombicity of the crystal, also increases thus making this phase transition difficult to observe.

Recent inelastic neutron scattering experiments have found similar effects in $La_{2-x}Sr_xCuO_4$ materials where fluctuating stripes where in fact first discovered[195]. Matsuda *et al* [131] have given qualitatively similar evidence for nematic order in underdoped $La_{2-x}Sr_xCuO_4$ ($x = 0.05$) which was known to have "fluctuating diagonal stripes". In the same doping range it has also been found by resonant x-ray scattering experiments that 5% Zn doping stabilizes a static diagonal stripe-ordered state with a very long persistence length which sets in at quite high temperatures[177].

These recent results strongly suggest that the experiments that had previously identified the high temperature superconductors as having "fluctuating stripe order" (both inside and outside the superconducting phase) were most likely detecting an electronic nematic phase, quite close to a state with long-range stripe (smectic) order. In all cases the background anisotropy (due to the orthorhombic distortion of the crystal structure) acts as a symmetry breaking field that couples linearly to the nematic order, thus rounding the putative thermodynamic transition to a state with spontaneously broken point group symmetry. These effects are much more apparent at low doping where the crystal orthorhombicity is significantly weaker.

The nature of the fluctuating spin order changes substantially as a function of doping: in the very underdoped systems there is no spin gap while inside much of the superconducting dome there is a finite spin gap. In fact in $La_{2-x}Ba_xCuO_4$ at $x = 1/8$ there is strong evidence for a complex stripe-ordered state which combines charge, spin and superconducting order[119, 19]. These experiments have also established that static long-range stripe charge and spin orders do not have the same critical temperature, with static charge order having a higher T_c.

An important caveat to our analysis is that in doped systems there is always quenched disorder, and has different degrees of short range "organization" in different high temperature superconductors. Since disorder also couples linearly to the charge order parameters it ultimately also rounds the transitions and renders the system to a glassy state (as noted in Refs.[104, 103]). Such effects are evident in scanning tunneling microscopy (STM) experiments in $Bi_2Sr_2CaCu_2O_{8+\delta}$ which revealed that the high-energy (local) behavior of the high temperature superconductors has charge order and it is glassy[93, 103, 82, 107, 203].

Finally, I note that in the recently discovered iron pnictides based family of high temperature superconductors, such as La $(O_{1-x}F_x)$FeAs [99, 145], a unidirectional spin-density wave has been found. It has been suggested[59] that the undoped system LaOFeAs may have a high-temperature nematic phase and that quantum phase transitions also occur as a function of fluorine doping[213]. This suggests that many of the ideas and results that I present here may be relevant to these still poorly understood materials.

3.3.2 Other complex oxides

The existence of stripe-ordered phases is well established in other complex oxide materials, particularly the manganites and the nickelates. In general, these materials tend to be "less quantum mechanical" than the cuprates in that they are typically insulating (although with interesting magnetic properties) and the observed charge-ordered phases are very robust. These materials typically have larger electron-phonon interactions and electronic correlations are comparatively less dominant in their physics. For this reason they tend to be "more classical" and less prone to quantum phase transitions. However, at least at the classical level, many of the issues I discussed above, such as the role of phase separation and Coulomb interactions, also play a key role[46]. The thermal melting of a stripe state to a nematic has been seen in the manganite material $Bi_xCa_xMnO_3$[175].

3.3.3 Ruthenates

Recent magneto-transport experiments in the quasi-two-dimensional bilayer ruthenate $Sr_3Ru_2O_7$ by the St. Andrews group[21] have given strong evidence of a strong temperature-dependent in-plane transport anisotropy in these materials at low temperatures $T \lesssim 800$ mK and for a window of perpendicular magnetic fields around 7.5 Tesla. These experiments provide strong evidence that the system is in an electronic nematic phase in that range of magnetic fields[21, 64]. The electronic nematic phase appears to have preempted a metamagnetic QCP in the same range of magnetic fields[75, 138, 159, 73]. This suggests that proximity to phase separation may be a possible microscopic mechanism to trigger such quantum phase transitions, consistent with recent ideas on the role of Coulomb-frustrated phase separation in 2EDGs[95, 123].

3.3.4 2DEGs in large magnetic fields

To this date, the best documented electron nematic state is the anisotropic compressible state observed in 2DEGs in large magnetic fields near the middle of a Landau level, with Landau index $N \geq 2$[121, 120, 53, 154]. In ultrahigh-mobility samples of a 2DEG in AlAs-GaAs heterostructures, transport experiments in the second Landau level (and above) near the center of the Landau level show a pronounced anisotropy of the

longitudinal resistance rising sharply below $T \simeq 80$ mK, with an anisotropy that increases by orders of magnitude as the temperature is lowered. These experiments were originally interpreted as evidence for a quantum Hall smectic (stripe) phase [110, 142, 62, 127, 15]. Further experiments[41, 42, 40] did not show any evidence of pinning of this putative unidirectional CDW as the $I-V$ curves are strictly linear at low bias and no broadband noise was detected. In contrast, extremely sharp threshold electric fields and broadband noise in transport was observed in a nearby reentrant integer quantum Hall phase, suggesting a crystallized electronic state. These facts, together with a detailed analysis of the experimental data, suggested that the compressible state is in an electron nematic phase[62, 63, 208, 170, 51], which is better understood as a quantum melted stripe phase.

3.3.5 Conventional CDW materials

CDWs have been extensively studied since the mid-seventies and there are extensive reviews on their properties[77, 78]. From the symmetry point of view there is no difference between a CDW and a stripe (or electron smectic). The CDW states are usually observed in systems which are not particularly strongly correlated, such as the quasi-one-dimensional and quasi-two-dimensional dichalcogenides, and the more recently studied tritellurides. These CDW states are reasonably well described as FLs which undergo a CDW transition, commensurate or incommensurate, triggered by a nesting condition of the FS[133, 134]. As a result, a part or all of the FS is gapped in which case the CDW may or may not retain metallic properties. Instead, in a strongly correlated stripe state, which has the same symmetry breaking pattern, at high energy has Luttinger liquid behavior[104, 55, 29].

What will interest us here is that conventional quasi-2D dichalcogenides, the also quasi-2D tritellurides and other similar CDW systems can quantum melt as a function of pressure in $TiSe_2$[188], or by chemical intercalation as in Cu_xTiSe_2[144, 14] and Nb_xTaS_2[47]. Thus, CDW phases in chalcogenides can serve as a weak-coupling version of the problem of quantum melting of a quantum smectic. Interestingly, there is strong experimental evidence that both $TiSe_2$[188] and Nb_xTaS_2[47] do not melt directly to an isotropic Fermi fluid but go instead through an intermediate phase, possibly hexatic. (Cu_xTiSe_2 is known to become superconducting[144].) Whether or not the intermediate phases are anisotropic is not known as no transport data is available in the relevant regime.

The case of the CDWs in tritellurides is more directly relevant to the theory I present in this chapter. Tritellurides are quasi-2D materials which for a broad range of temperatures exhibit a unidirectional CDW (*i.e.* an electronic smectic phase) and whose anisotropic behavior appears to be primarily of electronic origin[26, 113, 179, 178, 58]. However, the quantum melting of this phase has not been observed yet.

Theoretical studies have also suggested that it may be possible to have a quantum phase transition to a state with more than one CDW in these materials[217].

3.4 Order-parameter theory

In this section I will construct, using phenomenological arguments, an effective order parameter theory that will describe both the electron nematic and the electron smectic (or unidirectional CDW) phases. Although by symmetry the order parameter theory must be very similar to the ones used in classical liquid crystal phases, I will go through the construction of the phenomenological theory in some detail for several reasons. In 2D the rotation group $SO(2)$ is Abelian which allows for a significant simplification of the formulas by using a complex order parameter for the nematic phase, instead of a tensor expressions commonly used for 3D classical liquid crystals. Proper dynamical terms now need to be included to describe the quantum fluctuations at zero-temperature. Besides, in order to provide a clear relation between this work and earlier studies of the CDW state of fermions, I would like to discuss also the relation between the smectic phase and the CDW state.

3.4.1 The normal-electronic nematic transition

The nematic order parameter in 2D is a $l = 2$ representation of the $SO(2)$ rotational group [150]. It is defined as a symmetric traceless tensor of rank two.

$$\mathbf{N} = \begin{pmatrix} n_{11} & n_{12} \\ n_{12} & -n_{11} \end{pmatrix}. \tag{3.1}$$

The 2D rotational group $SO(2)$ is isomorphic to $U(1)$. Hence, I define instead the complex order-parameter field $N(\vec{r}, t)$

$$N(\vec{r}, t) = n_{11}(\vec{r}, t) + i n_{12}(\vec{r}, t), \tag{3.2}$$

where $\vec{r}$ and t are the space and time coordinates. I will use this complex order parameter field in this chapter to take the advantage of the Abelian nature of $SO(2)$.

The conjugate field is $N^\dagger(\vec{r}, t) = n_{11}(\vec{r}, t) - i n_{12}(\vec{r}, t)$. Under a global rotation by an angle θ, the fields $N(\vec{r}, t)$ and $N^\dagger(\vec{r}, t)$ transform, respectively, as $N(\vec{r}, t) \to e^{2i\theta}\, N(\vec{r}, t)$ and $N^\dagger(\vec{r}, t) \to e^{-2i\theta} N^\dagger(\vec{r}, t)$. Hence, N and $N^\dagger$ carry the angular momentum quantum numbers $l_z = 2$ and $l_z = -2$, respectively.

This complex order parameter can be generalized easily to other angular momentum channels $l \neq 2$, but not to higher dimensions $d > 2$, since it relies heavily on the special property of the 2D rotational group $SO(2)$. In higher dimensions, the rotational group will no longer be Abelian, so one will need to use the tensor formula as in the classical liquid crystal theories. In Appendix A.1, formulas using the complex order parameter are translated into the conventional tensor form for comparison.

The order-parameter field I just defined is invariant under spatial-inversion and time-reversal

$$PN(\vec{r},t)P^{-1} = N(-\vec{r},t), \tag{3.3}$$

$$TN(\vec{r},t)T^{-1} = N(\vec{r},-t). \tag{3.4}$$

In even spatial dimensions, including 2D in which our system lives, a chiral transformation is different from a space inversion. To change the chirality in 2D, I can reverse the y direction and keep the x direction unchanged. Under this chiral transformation, the nematic field will be changed into the conjugate field

$$CN(x,y,t)C^{-1} = N^{\dagger}(x,-y,t). \tag{3.5}$$

Here, C is the chiral transformation operator.

The effective action must preserve the symmetries of the system, both continuous, as the translational and rotational symmetries, and discrete, as the time reversal, spatial inversion and chiral symmetries. With the assumption of analyticity, the action must be

$$S_N = \int \mathrm{d}\vec{r}\mathrm{d}t \left(|\partial_t N|^2 - |\vec{\nabla} N|^2 - \Delta_N |N|^2 - u_N |N|^4 \right). \tag{3.6}$$

Here the dynamical term is quadratic in time derivatives. This is because the term linear in time derivatives $-iN^{\dagger}\partial_t N + h.c.$ is not allowed by the chiral symmetry. It is the imaginary part of $N^{\dagger}\partial_t N$. It corresponds to a pseudoscalar, and is not allowed.

In 2D, cubic terms in the nematic field N are not allowed. Hence, if $u_N > 0$, the normal-nematic transition is second order, instead of a first-order transition as in the 3D case [48, 34]. For $u_N > 0$ and $\Delta_N > 0$, the rotational invariant ground state will be stable. When Δ_N becomes negative, N will develop an expectation value $\bar{N}$ with module $\sqrt{-\Delta_N/(2u_N)}$, which breaks the $SO(2)$ rotation symmetry. The residual rotational symmetry would be Z_2. The argument of $\bar{N}$ determines the direction of the nematic order parameter.

The action of Eq. (3.6) has an internal $U(1)$ symmetry associated with the phase of the complex field

N, which is not physical. By symmetry, terms of the form

$$-\kappa \left(N^{\dagger}(\partial_x + i\partial_y) N^{\dagger}(\partial_x + i\partial_y) N + h.c. \right) \tag{3.7}$$

are allowed [150, 2]. This kind of terms are irrelevant at the QCP and in the isotropic phase, which leads to the existence of an "emergent" internal $U(1)$ symmetry at quantum criticality. But it will be important in the nematic phase, as it makes the two Frank constants to attain different values. (This effect is formally analogous to the role of spin-orbit interactions in the Schrödinger equation: in their absence spin is an internal degree of freedom.) This emergent symmetry of the normal phase and at the critical point is very important for the classical normal-nematic transition, especially in the study about the fluctuation effects [164, 108, 148].

3.4.2 The electronic nematic phase

In the nematic phase, the $SO(2)$ rotational symmetry is broken. Hence, I expect the fluctuations of the amplitude of the nematic order parameter, δN, to correspond to a massive mode with an energy gap of $-2\Delta_N$ ($\Delta_N < 0$), and the fluctuations of the phase, ϕ_N, constitute the gapless Goldstone mode. Without loss of generality, throughout this chapter, I assume that $\bar{N}$ is real and positive. This state corresponds to a nematic order in the main axis direction. In this state, the action of ϕ_N is

$$S_{\phi_N} = \bar{N}^2 \int d\vec{r}dt \ \left((\partial_t \phi_N)^2 - K_1 (\partial_x \phi_N)^2 - K_2 (\partial_y \phi_N)^2 \right) \tag{3.8}$$

where $K_1 = 1 + 2\kappa\bar{N}$ and $K_2 = 1 - 2\kappa\bar{N}$ are the two Frank constants. This action is only valid for small nematic fluctuations. It cannot be used to study topological defects of the nematic phase, known as disclinations[48]. The field ϕ_N has dynamic critical exponent $z = 1$. This makes the effective dimension of this system 3, which is above the lower critical dimension of the theory $d = 2$, and nematic order will not be destroyed by fluctuations.

3.4.3 CDW multi-critical point

The smectic order is a unidirectional CDW, described by a single complex order parameter field. If I assume analyticity, the effective low-energy theory of the bosonic field ρ can be determined as:

$$S_{\mathrm{CDW}} = \int \mathrm{d}\vec{r}\mathrm{d}t \ (\partial_t \rho)^2 + S_2 + S_3 + S_4, \tag{3.9}$$

where S_2 is the term in the quadratic order of ρ, S_3 and S_4 are the cubic and quartic terms respectively.

The term S_2 in the momentum space is,

$$S_2 = -\int \frac{\mathrm{d}\vec{k}\mathrm{d}\omega}{(2\pi)^3} f(|k|)\rho(\vec{k},\omega)\rho(-\vec{k},-\omega). \tag{3.10}$$

The function $f(|k|)$ has the physical meaning of the inverse of the CDW susceptibility. If I assume the ordering wave-vector of the CDW is $\vec{Q}_S$ (with $|\vec{Q}_S| = Q_S$ its magnitude), $f(|\vec{k}|)$ will have the form

$$f(|\vec{k}|) = \Delta_{\mathrm{CDW}} + C(|\vec{k}|^2 - Q_S^2)^2 + \dots \tag{3.11}$$

where Δ_{CDW} is the energy gap of the CDW excitations [24], and C is a positive constant.

When the energy gap Δ_{CDW} decreases to zero, all the density wave modes with $|\vec{k}| = Q_S$ will become soft and critical when $\Delta_{\mathrm{CDW}} = 0$. This is very different from an ordinary ϕ^3- or ϕ^4-theory, where I only need to consider one mode (or two modes for a complex field) at small momentum. Here, I need to consider all the modes with the wave vector $\vec{k}$ whose magnitude is close to Q_S. In other words, the point $\Delta_{\mathrm{CDW}} = 0$ is not a critical point but a multi-critical point with an infinite number of critical modes. Even if a lattice background is present, the $\Delta_{\mathrm{CDW}} = 0$ point may still be a multi-critical point of n critical modes, if the lattice has a n-fold rotational symmetry for $n > 2$. For a multi-critical point, higher-order terms become important. Without a detailed knowledge of these higher-order terms, it is not possible to determine whether the transition is first or second order, or how many CDWs will be formed in the ordered phase.

Brazovskii [24] studied the classical version of this problem, considering only the isotropic interactions. Chubukov and co-workers [39] studied the quantum problem in a fermionic system in the high-density regime where the cubic and quartic terms of ρ can be ignored.

In general, depending on the non-Gaussian terms, the ordered phase may have only one or several CDWs [24]. For a rotational invariant system, it is often assumed that 3 CDWs form a triangular lattice to minimize the breaking of the rotational symmetry, as the 2D Wigner crystal state [210]. For systems with a strong lattice potential, the system is often assumed to become an electron crystal state which preserves the point group rotational symmetry of the background lattice, *e.g.* the rare-earth tritellurides[217].

For isotropic systems, outside the nematic phase, the ρ^3 term in Eq. (3.9) favors that three CDWs form by a first-order transition [24]. However, inside a nematic phase, as I will show below, the nematic order parameter, which is coupled to ρ^2, favors only one CDW and will compete with the ρ^3 term. For a continuous quantum phase transition, ρ^3 will be a subleading perturbation compared to ρ^2, at least close enough to the transition. Hence, the smectic phase, a unidirectional CDW, will be energetically favorable. On the other

hand, in the case of a first-order transition, depending on microscopic details either the smectic phase or the state with three CDWs would be preferred. I represent these different possibilities in the schematic phase diagram shown in Fig. 3.1.

On a square lattice, due to the point group symmetry of the lattice, the electron crystal phase usually consists of 2 CDWs perpendicular to each other. The phase transition between this phase and the FL may be second order due to the absence of the cubic term ρ^3 which, in contrast to isotropic systems, is prohibited by momentum conservation. I have confirmed this structure of the phase diagram in a microscopic mean-field calculation. However, at the multi-critical point where both the CDW modes and the nematic mode are critical (the $(0,0)$ point in Fig. 3.1), the coupling between CDWs and the nematic order parameter (Eq. (3.12)) is relevant. This suggests a fluctuation driven first-order transition near the multi-critical point. Hence, this multi-critical point is essentially unreachable.

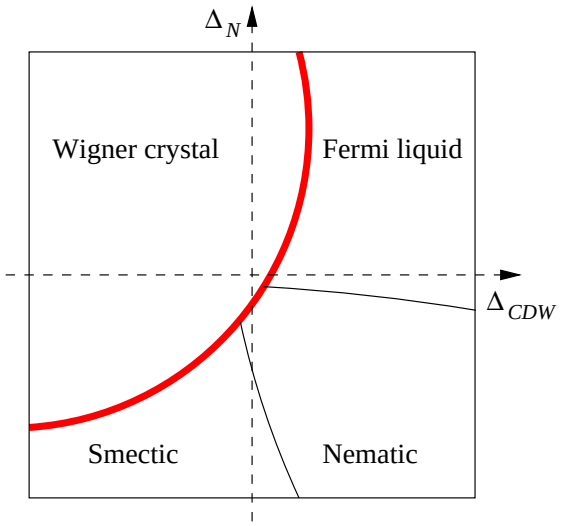

Figure 3.1: Schematic phase diagram at $T = 0$ as a function of Δ_N and Δ_{CDW} defined in Eqs.(3.6) and (3.11). The cross point of the two dash lines is the multi-critical point $\Delta_N = \Delta_{CDW} = 0$. The red thick lines stand for first order phase boundaries. Other phase boundaries may be first or second order. More complex electron crystal phases are possible, for example, an anisotropic electron crystal phase where more than one CDWs and nematic coexist, but they are beyond the discussion of this chapter.

In this chapter, I study the nematic-smectic phase transition and the smectic phase using a weak coupling approach by perturbing about a FL state. This approach is consistent provided the nematic phase is narrow enough in coupling constant space so that the nematic-smectic transition is not too far from the FL phase.

It is useful to compare to the classical version of this problem. The theory of classical (thermal) melting in two dimensions, the Kosterlitz-Thouless-Halperin-Nelson-Young theory[147, 221] (see Ref.[34]), is a theory of a phase transition driven by the proliferation of topological defects: a dislocation unbinding transition

in the case of melting of a 2D Wigner crystal (a triangular lattice) into a hexatic phase, and disclination unbinding transition in the hexatic-isotropic phase transition. (The case of the square lattice was discussed only recently in Ref.[129]). The reason for the success of the classical theory of melting in two dimensions is that, as in all Kosterlitz-Thouless phase transitions[109, 34], at finite temperatures the classical ordered state with a spontaneously broken continuous symmetry is not possible in two dimensions. Instead, there is a line (or region) of classical critical behavior with exactly marginal operators. The defect-unbinding phase transition appears as an irrelevant operator becoming marginally relevant.

In the case of the quantum phase transitions in two dimensions that I am interested in, there are no such exact marginal operators available at zero temperature, and hence, no lines of fixed points available. Thus, the $T = 0$ quantum phase transition is not triggered by a defect-unbinding operator becoming marginal, but instead by making the coupling constant of an irrelevant operator large (as in standard continuous phase transitions, classical or quantum). Instead, the quantum phase transition is closer to Landau-type (or, rather, Hertz-Millis like) description in that it is governed (as I will show) by a quantum-mechanical analog of the celebrated McMillan-deGennes theory for a nematic-smectic phase transition in classical liquid crystals in three dimensions[48, 34]. The approach that I will pursue here does not contain much of the physics of strong correlations as it begins with a state with well-defined fermionic quasiparticles. It also does not treat correctly the tendency of strongly correlated systems to exhibit inhomogeneous states and phase separation. The only way to account for this physics correctly is to use the opposite approach, a strong coupling theory of quantum melting of the crystal and stripe phases, as advocated in Ref.[104]. So far, this theory only treats the physics deep inside a stripe phases, and the theory of their quantum melting to a nematic phase does not yet exist. Thus, although from a strong-coupling perspective it would be highly desirable to have such a defect unbinding theory of this quantum phase transition (such a description does exist for an insulating system[223] but its extension to a metallic state is not available and it is highly non-trivial), I will pursue instead a Hertz-Millis approach [84, 137, 180] to this quantum phase transition.

3.4.4 The electronic nematic-smectic transition

Nematic order will remove the degeneracy of CDW modes in different directions and select one CDW. As a result, the Brazovskii CDW multi-critical point becomes just a critical point. For simplicity, I assume that the nematic order parameter is small enough so that a Landau-type expansion still makes sense, which is equivalent to assuming that the system is still "close enough" to the nematic-isotropic QCP. However, as I will show later, the critical theory I get using these assumptions has the only form allowed by symmetry, assuming analyticity.

By symmetry, the coupling between the CDW and the nematic field is

$$S_{\text{int}} = -g \int \frac{\mathrm{d}\vec{k}\mathrm{d}\Omega}{(2\pi)^3} \int \frac{\mathrm{d}\vec{q}\mathrm{d}\omega}{(2\pi)^3} N(\vec{q},\omega) e^{-2i\theta_k} \rho(\vec{k}-\vec{q},\Omega-\omega)\rho(-\vec{k},-\Omega) + \text{h.c.} \tag{3.12}$$

whose tensor form is shown in Appendix A.1. Here, θ_k is the polar angle of $\vec{k}$. This term is irrelevant in the isotropic phase, but in the nematic phase, where N gets the expectation value $\bar{N}$; this term will be of the same order as S_2, which was defined in Eq. (3.10), and hence it becomes important.

Inside the nematic phase the amplitude fluctuations of the nematic order parameter are gapped while the orientational fluctuations, the nematic Goldstone modes, are gapless, at least strictly in the absence of a lattice and other orientational symmetry breaking couplings. Thus, deep enough in the nematic phase it is possible to integrate out the gapped nematic amplitude fluctuations and derive an effective theory involving the gapless nematic Goldstone mode. However, as the nematic-smectic phase transition is approached, the gap of the fluctuations of the smectic order parameter will get smaller and will approach zero at the QCP. Thus, in this regime, the nematic phase has low-energy "fluctuating stripes". This regime is the analog of that in conventional liquid crystals where the McMillan-deGennes classical theory applies . I will now show how this theory arises in the quantum case.

The leading term in S_{int} of Eq. (3.12) will be

$$-2g \int \frac{\mathrm{d}\vec{k}\mathrm{d}\omega}{(2\pi)^3} \bar{N} \cos(2\theta_k)\rho(\vec{k},\omega)\rho(-\vec{k},-\omega). \tag{3.13}$$

This term will stabilize the density wave in either x or y direction and destabilize the other, depending on the sign of g. As a result, the nematic order will select a special direction along which only one CDW will form. Past this phase transition the system will be in a smectic state, a unidirectional CDW. For simplicity, I assume $g > 0$, which selects $\vec{Q}_S$ in the y direction.

Only the density fluctuations close to $\vec{k} = \pm\vec{Q}_S$ matter for the low-energy theory. I define a complex field Φ, describing the density fluctuations around $\vec{k} = \pm\vec{Q}_S$ as

$$\Phi(\vec{q},\omega) = \rho(\vec{q}+\vec{Q}_S,\omega), \tag{3.14}$$

where q is small. The real part of $\Phi(\vec{r},t)$ measures the density fluctuations.

Under a spatial inversion, $\Phi(\vec{r},t)$ will become its conjugate field $\Phi^\dagger(-\vec{r},t)$. Hence, the term $-i\Phi^\dagger\partial_t\Phi + h.c.$ is not allowed in the Lagrangian, and the dynamical term for Φ is at least quadratic in time derivatives.

The cubic term of the field in the isotropic-CDW transition vanishes in the nematic-smectic transition,

due to momentum conservation. By expanding Eq. (3.12) around $q \sim 0$, $\vec{k} \sim \vec{Q}_S$ and $\phi_N \sim 0$, I obtain

$$\begin{aligned} S =& S_{\phi_N} + \int \mathrm{d}\vec{r}\mathrm{d}t \Big(|\partial_t \Phi|^2 - C_y |\partial_y \Phi|^2 \\ & - C_x |(\partial_x - i\frac{Q_S}{2}\phi_N)\Phi|^2 - \Delta_S |\Phi|^2 - u_S |\Phi|^4 \Big). \end{aligned} \tag{3.15}$$

Here S_{ϕ_N} is the action of the nematic Goldstone mode defined in Eq. (3.8).

The action of Eq. (3.15) is just a 2D version McMillan-de Gennes theory of the nematic-smectic transition in the classical liquid crystals but with $z = 1$ quantum dynamics. The constants in Eq.(3.15) are

$$\begin{aligned} C_x &= \frac{4g\bar{N}}{Q_S^2}, & C_y &= C \\ \Delta_S &= \Delta_{\mathrm{CDW}} - 2g\bar{N}, & u_S &= u_{\mathrm{CDW}} - \frac{4g^2}{\Delta_N}. \end{aligned} \tag{3.16}$$

Here Δ_S is the energy gap of Φ field, which mainly comes from the CDW gap defined in Eq. (3.11). The correction term $-2g\bar{N}$ comes from the nematic ordering. The u_S term comes from the interactions between CDWs and it gets a correction from the amplitude fluctuations of the nematic order, which has been integrated out. The nematic Goldstone field ϕ_N couples to the CDW field Φ as a gauge field with a "charge" $Q_S/2$. Here the two in the denominator comes from the fact that the nematic order parameter has an angular momentum $l = 2$. This gauge-like coupling is required by the rotational symmetry since, under spatial rotation by a small angle θ, the fields transform as $\Phi \to \exp(iQ_S\ x\ \theta)\ \Phi$ and $\phi_N \to \phi_N + l\theta$ (for the angular momentum channel l). In fact, with the symmetry constrain and the assumption of analyticity, the action I show in Eq. (3.15) is the only allowed form for the effective low-energy theory, provided the topological excitations of ϕ_N are ignored [172]. Therefore, although I only keep linear terms of $\bar{N}$ in our calculations above, which is valid close to the normal-nematic critical point, the action in Eq. (3.15) will have the same form even deep inside the nematic phase.

The theory with the effective action given in Eq.(3.15) has a critical field Φ and gapless Goldstone boson ϕ_N. A naive mean-field theory would suggest that this is a continuous phase transition. In the case of the theory of classical liquid crystals, where the same naive argument also holds, Halperin, Lubensky and Ma [81] used the $4 - \epsilon$ expansion to show that there is a run-away behavior in the renormalization group flows, similar to that of superconducting transition coupled to a fluctuating electromagnetic field. They concluded that in both cases the transition is probably weakly first order, a fluctuation-induced first-order transition. In other terms, in the classical theory the coupling of the smectic to the nematic Goldstone mode (which

has the same form as a coupling to a gauge field) is relevant. To ascertain what happens in the case of the metallic nematic-smectic QCP I will also need to take into account the effects of the fermionic degrees of freedom. I will show that the fermionic fluctuations change the critical behavior in an essential way.

3.4.5 The electronic smectic phase: a unidirectional CDW

In the smectic phase, the amplitude fluctuations of the order parameter, $\delta\Phi$, are gapped but the phase fluctuations, ϕ_Φ, are gapless, as required by the Ward-identity. This happens in systems for which lattice effects can be neglected, and hence are described formally in a continuum, or if the smectic order is sufficiently incommensurate. Therefore, upon integrating out the gapped amplitude fluctuations $\delta\Phi$, the effective low-energy theory of the Goldstone mode becomes

$$S_{\phi_\Phi} = \int \mathrm{d}\vec{r}\mathrm{d}t \ \left[\kappa_0(\partial_t\phi_\Phi)^2 - \kappa_1(\partial_x^2\phi_\Phi)^2 - \kappa_2(\partial_y\phi_\Phi)^2\right], \tag{3.17}$$

When I are close to the nematic-smectic critical point, the coefficients of this effective action are

$$\kappa_0 = |\bar{\Phi}|^2, \qquad \kappa_1 = \frac{4K_1\bar{N}^2}{Q_S^2}, \qquad \kappa_2 = C_y|\bar{\Phi}|^2, \tag{3.18}$$

with $\bar{\Phi}$ being the expectation value of the CDW order parameter. The vanishing of the stiffness $(\partial_x\phi_\Phi)^2$ term [158, 112] is required by the Ward identity of rotational invariance. Thus, an underlying lattice, which will break the continuous rotational symmetry down to its discrete point group, will lead to a non-vanishing stiffness. Nevertheless, in many cases and particularly away from situations in which the FS is strongly nested, the breaking of rotational invariance can be parametrically small enough that at low temperatures its effects to a first approximation can be neglected and treated perturbatively afterward.

A simple scaling analysis of the effective action of Eq. (3.17) shows that, at the tree level, the scaling dimensions of space and time $[x]$, $[y]$ and $[t]$, are -1, -2 and -2, respectively. Although the time direction and the y direction scales in the same way, the x and y directions now scale differently. This is a typical phenomenon for anisotropic states. Now the effective dimensions of this quantum theory is 5. Hence, our theory is above its (upper) critical dimension. So the higher-order interactions of the smectic Goldstone mode will be irrelevant, if I don't consider topological defects. The fact that I am above the critical dimension also tells us that the quantum fluctuations in the quantum smectic phase will not destroy the long-range order.

This scaling is very different from the classical smectic phase of 3D, where $[x] = [y] = -1$ and $[z] = -2$, if the modulation is on the z direction. This classical theory is at its lower critical dimension, and long-range order is destroyed by fluctuations [158, 112], resulting in a power-law quasi-long-range order. This system

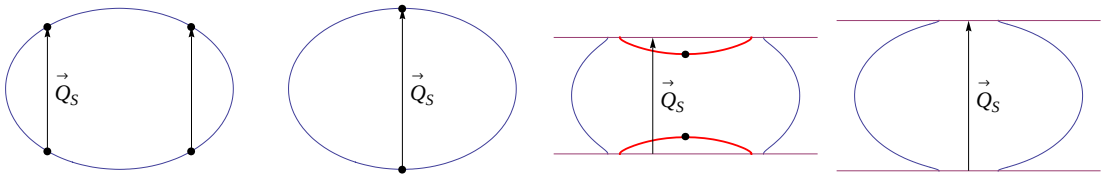

(a) $Q_S < 2k_F$ (b) $Q_S = 2k_F$ (c) $Q_S < 2k_F$ (d) $Q_S = 2k_F$

Figure 3.2: The FS of the nematic phase (a and b) and the reconstructed FS in the smectic phase (c and d). (a) and (c) are for $Q_S < 2k_F$ at the QCP and in the smectic phase respectively, while (b) and (d) are $Q_S = 2k_F$, also at the QCP and in the smectic phase respectively. In (a) and (b), the black dots marked the non-FL points on the FS caused by the smectic mode fluctuations at the nematic-smectic QCP. The relevance of the points in (c) is explained in Sec. 3.7. In (c) I have show the case of Q_S to be comparable to $2kF$ so as to keep the FS reconstruction simple. Here I show the effective Brillouin Zone with an open orbit and a closed pocket. The reconstructed FS of case (d) is partially gapped and the FS has an open orbit.

has a line of critical points, so the higher order terms of the action that need to be considered were found to lead to logarithmic corrections to the power-law behavior [76].

The above analysis implies that our quantum problem is above the lower critical dimension. Therefore all these effects of the 3D classical smectic phase will not be present in the 2D quantum case. The scaling behavior of a 2D quantum system is similar to the columnar state of the classical liquid crystals, instead of that of classical smectics. The classical columnar state has two density waves so that it is a solid in two directions but a liquid in the third direction. The Goldstone fluctuations of this state scale as $[x] = -1$ and $[y] = [z] = -2$ [48], which is the same as in the present case, if I consider the time direction in our problem as the z direction. The difference between the classical columnar state and the 2D quantum smectic state is that in the 3D columnar state, the Goldstone mode is a planar vector but in the present case it is a scalar.

3.5 Coupling the order parameter theory to fermions

I will now proceed to couple the phenomenological theory of the nematic and smectic phases to a system of *a priori* well-defined fermionic quasiparticles described by the Landau theory of the FL. In a fermionic liquid crystal state, the bosonic order-parameter fields, defined above, will couple to the fermions.

Let us define $\psi^\dagger(x,t)$ and $\psi(x,t)$ to be the fermion creation and annihilation operators of a FL. I will assume that the FL has a well-defined FS, which for simplicity I will assume is circular. (For lattice systems the FS will have the symmetry of the point group of the lattice.) The Fermi wave vector is k_F. The Fermi velocity is set to 1 so that the energy and momentum have the same units. Consistent with the assumptions of the Landau theory of the FL[18] the effective Hamiltonian of the fermionic quasiparticles will be taken to

be that of a free Fermi system, with a well-defined FS, and a set of quasiparticle interactions parametrized by the Landau parameters. These interactions are irrelevant in the low-energy limit of the FL but play an important role in the physics of electronic liquid crystal phases [150]. In any case in our discussion it will be unnecessary to include the Landau parameters explicitly since their effects will already be taken into account through the coupling to the liquid crystal order parameters.

By symmetry, the nematic order-parameter field, N, couples to the fermion density quadrupole [150]

$$\mathbf{Q}(\vec{r},t) = \frac{1}{k_F^2}\psi^\dagger(\vec{r},t)\begin{pmatrix} \partial_x^2 - \partial_y^2 & 2\partial_x\partial_y \\ 2\partial_x\partial_y & -\partial_x^2 + \partial_y^2 \end{pmatrix}\psi(\vec{r},t). \tag{3.19}$$

In 2D, since the rotational group is $SO(2)$, the density quadrupole can be defined in terms of a two-component real director field (*i.e.* a headless vector) or, in terms of complex field

$$\begin{aligned} Q(\vec{r},t) &= Q_{11}(\vec{r},t) + iQ_{12}(\vec{r},t) \\ &= \psi^\dagger(\vec{r},t)\frac{(\partial_x + i\partial_y)^2}{k_F^2}\psi(\vec{r},t). \end{aligned} \tag{3.20}$$

Same as the nematic order parameter, Q is also invariant under rotations by π.

The coupling between Q and N is

$$-g_N \int \mathrm{d}\vec{r}\mathrm{d}t(Q^\dagger N + h.c.). \tag{3.21}$$

Here g_N is a coupling constant. Again, the chiral symmetry of the system requires that the effective action depends only on the real part of $Q^\dagger N$, and that there is no dependence on the imaginary part, since it is a pseudo scalar. The tensor form of this coupling is shown in Appendix A.1. In what follows I choose the sign of g_N to be negative, so that a positive expectation value of the nematic order parameter $\bar{N}$ means a FS stretched along the x direction and compressed in the y direction, as shown in Figs. 3.2(a) and (b).

The sign of g_N alone is not important. What matters is the relative sign between g_N and the coupling constant g defined in Eq. (3.12). Under a redefinition of N becoming $-N$, both g_N and g change sign. If $g \times g_N > 0$, $\vec{Q}_S$ prefers the direction in which the FS is stretched, but when $g \times g_N < 0$, it prefers the direction where the FS is compressed. In general, the sign of $g \times g_N$ is determined by microscopic details of the system to which this model may apply.

If $Q_S = 2k_F$, very close to a nesting condition the curvature of the FS controls the CDW instability as it controls how singular the charge susceptibility is near the nesting wave vector. In this case one finds that it

leads to the condition $g \times g_N < 0$, when Q_S connects two points on the Fermi surface where the curvature is smallest, as shown in Fig.3.2(b). In general, far from a nesting condition, the curvature of the FS alone is not the dominant factor, and the sign of $g \times g_N$ may be positive or negative, depending on the microscopic details.

The smectic order-parameter field should be coupled to the CDW of the fermions. The CDW operator of the fermions, close to the ordering wave vector Q_S, is

$$n(\vec{q},\omega) = \int \frac{\mathrm{d}\vec{k}\mathrm{d}\Omega}{(2\pi)^3}\, \psi^\dagger(\vec{k}+\vec{Q}_S+\vec{q},\Omega+\omega)\, \psi(\vec{k},\Omega), \tag{3.22}$$

where $q \sim 0$. The smectic order-parameter field Φ couples to this fermion density wave n as

$$-g_S \int \mathrm{d}\vec{r}\mathrm{d}t(n^\dagger\Phi + h.c.). \tag{3.23}$$

Integrating out the bosons, attractive four-fermion interactions are generated of the form

$$\frac{g_N^2}{\Delta_N}|Q|^2 + \frac{g_S^2}{\Delta_S}|n|^2. \tag{3.24}$$

Hence, the order-parameter fields can be regarded as Hubbard-Stratonovich fields used to decouple four-fermion interactions. In this picture, the couplings between the order-parameter fields and fermions are measuring the strength of the attractive four-fermion term.

Gapless fermions will introduce nonanalytic terms to the low-energy effective theory of the nematics and smectics. For the case of the nematic order parameter, it was shown by Oganesyan and co-workers [150] that the fermions generate nonanalytic Landau damping terms[84, 137], so the theory of the isotropic-nematic metallic QCP becomes

$$S_N = g_N^2 N(0) \int \frac{\mathrm{d}\vec{q}\mathrm{d}\omega}{(2\pi)^3} \left(\frac{i|\omega|}{q} - \kappa_N q^2\right) N^\dagger(\vec{q},\omega) N(\vec{q},\omega), \tag{3.25}$$

The nematic susceptibility at this FL-nematic QCP is[150]

$$\begin{aligned} \chi^N(\vec{q},\omega) = &\quad -i\langle N^\dagger(\vec{q},\omega)N(\vec{q},\omega)\rangle_{\mathrm{ret}} \\ = &\quad \frac{1}{g_N^2 N(0)\left(\frac{i\omega}{q} - \kappa_N q^2\right)}. \end{aligned} \tag{3.26}$$

The phase mode of the nematic order-parameter field in the nematic phase, the nematic Goldstone mode,

has an effective action of the form

$$S_{\phi_N} = g_N^2 \bar{N}^2 N(0) \times \int \frac{\mathrm{d}\vec{q}\mathrm{d}\omega}{(2\pi)^3} \left(\frac{i|\omega|}{q} \sin^2 2\varphi_q - K_1 q_x^2 - K_2 q_y^2 \right) |\phi_N(\vec{q},\omega)|^2 \tag{3.27}$$

where $\bar{N}$ is the expectation value of the nematic order parameter and φ_q is the angle between $\vec{q}$ and the main axis direction of the nematic ordering. The stiffnesses K_1 and K_2 (the Frank constants) are given in Ref.[150]. With this action, it follows that the transverse nematic susceptibility in the electron nematic phase is[150]

$$\begin{aligned} \chi_\perp^N(\vec{q},\omega) = & \quad -i\bar{N}^2 \langle \phi_N(\vec{q},\omega)\phi_N(-\vec{q},-\omega)\rangle_{\mathrm{ret}} \\ = & \quad \frac{1}{g_N^2 N(0)\left(\frac{i\omega}{q} \sin^2 2\varphi_q - K_1 q_x^2 - K_2 q_y^2 \right)} \end{aligned} \tag{3.28}$$

For the case of a nematic order parameter aligned along the x-axis, the angular factor becomes $\sin^2 2\varphi_q = 4(q_x^2 q_y^2/q^4)$.

For the case of a charged smectic, a unidirectional CDW, a similar effect will be observed. Besides, if Q_S connects to points on the FS which have just the opposite Fermi velocity as shown in Fig. 3.2(b), the discontinuity leads to another type of nonanalytic terms as will be shown in Sec. 3.6.2.

3.6 The nematic-smectic metallic quantum critical point

In this section, I study the metallic nematic-smectic QCP. The two cases shown in Figs. 3.2(a) $Q_S < 2k_F$, and (b) $Q_S = 2k_F$, are studied separately.

Deep in the nematic phase, the amplitude fluctuations of the nematic order parameter are gapped, and the low-energy fluctuations are due to the nematic Goldstone mode, ϕ_N, whose action is given in Eq. (3.27). However, as the nematic-smectic QCP is approached (from the nematic side) the fluctuations of the smectic order parameter become progressively softer and, provided the quantum phase transition is continuous, become gapless at this QCP. In this scenario, the nematic phase looks like a "fluctuating stripe" phase qualitatively similar to the phenomenology of the cuprate superconductors, as discussed in Sec. 3.3.1.

The case $Q_S > 2k_F$ will not be discussed here. The reason is that since now the CDW fluctuations with $Q_S > 2k_F$ cannot decay into particle-hole pairs, in this case fermions only renormalize the coefficients of the smectic effective action, while the nematic fluctuations will still be Landau damped. For isotropic

systems and for $Q_S > 2k_F$, the CDW (Lindhard) susceptibility $\chi(Q_S)$ in general decreases faster than linear as $\chi(2k_F) - A\sqrt{Q_S - 2k_F}$, where A is a constant. This implies that a CDW with $Q_S > 2k_f$ is unlikely to be realized as it would require an anomalously attractive interaction at a large Q_S. However, for a lattice system the phase fluctuations of the nematic mode ϕ_N get gapped by lattice anisotropies and in this case the fermions only yield the trivial effect of renormalizing the coefficients of the effective action at the CDW transition.

3.6.1 $Q_S < 2k_F$

For $Q_S < 2k_F$, the leading contribution to the effective action of the order parameter field, resulting from integrating out the fermions, has the form

$$g_S^2 \int \frac{\mathrm{d}\vec{q}\mathrm{d}\omega}{(2\pi)^3}\, \Pi(\vec{Q}_S + \vec{q}, \omega)\, |\Phi(\vec{q}, \omega)|^2, \tag{3.29}$$

Here $\Pi(\vec{Q}_S + \vec{q}, \omega)$ is the CDW susceptibility of the fermions, given by the fermion loop integral (bubble)

$$\Pi(\vec{k}, \omega) = -\int \frac{\mathrm{d}\vec{p}}{(2\pi)^2}\, \frac{n_F[\epsilon(\vec{p}+\vec{k})] - n_F[\epsilon(\vec{p})]}{\omega - \epsilon\left(\vec{p}+\vec{k}\right) + \epsilon\left(\vec{p}\right) + i0^+\,\mathrm{sign}(\omega)}, \tag{3.30}$$

where $n_F(k)$ is the Fermi-Dirac distribution function.

The static part of the fermion CDW susceptibility depends on the details of the dispersion relation from way above the FS to the bottom of the band. However, since $\Pi(\vec{k}, \omega = 0)$ is analytic for $k < 2k_F$, the static part, $\Pi(\vec{Q}_S + \vec{q}, \omega = 0)$, will not change the analytic structure of Eq. (3.15), but just renormalize the coefficients, in particular the critical value of the coupling constant. The important contribution comes from the dynamical part, $\Pi(\vec{Q}_S + \vec{q}, \omega) - \Pi(\vec{Q}_S + \vec{q}, 0)$. The singular contributions to this integral are dominated by the behavior of the integrand around the four points on the FS, which are connected by the ordering wave vector $\vec{Q}_S$, as marked with black dots on Fig. 3.2(a). If I expand the dispersion relation of the fermions around these four points, $\epsilon(\vec{q}) = \pm v_x q_x \pm v_y q_y$, to leading order I get a Landau damping contribution

$$\Pi(\vec{q} + \vec{Q}_S, \omega) - \Pi(\vec{q} + \vec{Q}_S, 0) = \frac{i|\omega|}{2\pi v_x v_y}, \tag{3.31}$$

which is linear in $|\omega|$. The formula above can be checked by taking the limit of $Q_S \ll 2k_F$ or $Q_S \lesssim 2k_F$. In these two regimes, the fermion loop integral can be computed by RPA without expanding the dispersion relations around the four points. After setting $v_F = 1$, for $Q_S \ll 2k_F$, one finds $\Pi(\vec{q}+\vec{Q}_S, \omega) = iN(0)|\omega|/Q_S$ with $N(0)$ being the density of states and for $Q_S \lesssim 2k_F$, $\Pi(\vec{q} + \vec{Q}_S, \omega) = i|\omega|\sqrt{k_F}/(2\pi\sqrt{2k_F - Q_S})$, which

can be reached by expanding Eq. (3.37). Both of them agree with the general formula given above.

The term linear in ω in the effective action for the smectic field Φ of Eq. (3.31), which is due to the contributions of the fermions, dominates over the "naive" dynamical term proportional to ω^2 of the phenomenological theory. I can thus write an effective action for the electron nematic-smectic quantum phase transition of the form

$$\begin{aligned} S &= \int \frac{\mathrm{d}\vec{q}\mathrm{d}\omega}{(2\pi)^3} C_0 i|\omega| \, |\Phi(\vec{q},\omega)|^2 \\ &\quad - \int \mathrm{d}\vec{r}\mathrm{d}t \left(C_y |\partial_y \Phi|^2 + C_x |(\partial_x - i\frac{Q_S}{2}\phi_N)\Phi|^2 + \Delta_S |\Phi|^2 + u_S |\Phi|^4 \right) \\ &\quad + \int \frac{\mathrm{d}\vec{q}\mathrm{d}\omega}{(2\pi)^3} \left(\widetilde{K}_0 \frac{i|\omega|}{q} \sin^2 2\varphi_q - \widetilde{K}_1 q_x^2 - \widetilde{K}_2 q_y^2 \right) |\phi_N(\vec{q},\omega)|^2, \end{aligned} \tag{3.32}$$

where $C_0 = g_s^2/(2\pi v_x v_y)$, $\widetilde{K}_0 = g_N^2 \bar{N}^2 N(0)$ and $\widetilde{K}_{1,2} = g_N^2 \bar{N}^2 N(0) K_{1,2}$. The point $\Delta_S = 0$ and $u_S > 0$ is the nematic-smectic critical point. With the nonanalytic dynamical term, the dynamic critical exponent of the field Φ becomes $z = 2$, instead of $z = 1$ as it would generally be in the absence of fermions (or, if the fermions were gapped as in the case of an insulator).

The nematic Goldstone mode ϕ_N has a dynamic critical exponent $z = 3$ [150], larger than the $z = 2$ exponent for the smectic fluctuations. Thus, the Goldstone mode of the nematic order parameter ϕ_N and the smectic Φ fluctuate on very different energy scales, with ϕ_N being the low-energy mode. If I only focus on the asymptotic low-energy theory, I should integrate out the high-energy mode Φ. This process will lead to an effective theory of ϕ_N. In turn, the low-energy mode ϕ_N will mediate interactions of the field Φ. However, I will show by a scaling argument that in the case of the quantum metallic system the coupling between the smectic field and the nematic Goldstone mode is irrelevant.

The action of Eq.(3.32) is invariant under a rescaling parametrized by a factor b

$$\begin{aligned} &t \to b^{-3} t, && \vec{r} \to b^{-1}\vec{r}, \\ &\Phi(\vec{r},t) \to b^{3/2}\Phi(b^{-1}\vec{r}, b^{-3}t), && C_0 \to b^{-1} C_0, \\ &C_{x,y} \to C_{x,y}, && Q_S \to b Q_S, \\ &\Delta_S \to b^2 \Delta_S, && u_S \to b^{-1} u_S, \\ &\widetilde{K}_{0,1,2} \to b^3 \widetilde{K}_{0,1,2}. \end{aligned} \tag{3.33}$$

where C_x, C_y, K_0, K_1, and K_2 are the stiffness in Eq. (3.32).

When $\Delta_S = 0$, at the tree level and in the long-wavelength regime, both the gauge-like "coupling

constant" Q_S and $\widetilde{K}_{0,1,2}$ scale to infinite, but the ratio $Q_S^2/\widetilde{K}_{0,1,2}$ scales to 0 as a function of b^{-1}. This implies that the gauge-like coupling is irrelevant. Quantum fluctuations may change the tree-level scaling behavior as I include loop corrections. However, for large enough $\widetilde{K}_{0,1,2}$ or small enough Q_S, the irrelevancy of the gauge-like coupling will not be changed. As a byproduct, I notice that C_0 and u_S scale to zero in the long-wavelength regime, which means that these two terms are irrelevant also. However, I should keep in mind that these operators are actually dangerous irrelevant, in the sense that C_0 is necessary to find the proper equal-time correlation function for Φ and u_S is necessary for stability in the ordered phase, and they are only irrelevant at this QCP.

Notice that at the QCP there are two critical modes: the amplitude of the CDW order parameter, which has $z = 2$, and the transverse (Goldstone) mode of the nematic phase, which has $z = 3$ (and it is clearly dominant at low enough energies). Thus, I also need to check the scaling behavior of $t \to b^{-2}t$ and $\vec{r} \to b^{-1}t$ for the high-energy mode. Under this rescaling,

$$\begin{aligned}
&\Phi(\vec{r},t) \to b\Phi(b^{-1}\vec{r}, b^{-2}t), && C_{0,x,y} \to C_{0,x,y},\\
&Q_S \to bQ_S, && \Delta_S \to b^2\Delta_S,\\
&u_S \to u_S, && \widetilde{K}_0 \to b^3\widetilde{K}_0,\\
&\widetilde{K}_{1,2} \to b^2\widetilde{K}_{1,2}. &&
\end{aligned} \tag{3.34}$$

At the critical point where $\Delta_S = 0$, it can be seen that $Q_S^2/\widetilde{K}_0$ also scales to 0 as b^{-1} in the long-wavelength limit, which means, for the $z = 2$ mode, the gauge-like coupling is still irrelevant.

These conclusions are confirmed by one-loop perturbation theory calculations, presented in Appendix A.2, where I show that integrating out Φ (or ϕ_N) does not change the action of ϕ_N (or Φ). This is one of our main results.

In conclusion, there are two essentially decoupled soft modes at the nematic-smectic QCP. The nematic Goldstone mode is governed by the same action as in the nematic phase, Eq. (3.27). Since as the nematic-smectic QCP is approached from the nematic side, the nematic Goldstone mode and the smectic order parameters effectively decouple; the effective action for the smectic field Φ in this limit reduces to

$$S_S = \int \frac{\mathrm{d}\vec{q}\mathrm{d}\omega}{(2\pi)^3} \left(iC_0|\omega| - C_x q_x^2 - C_y q_y^2 - \Delta_S\right) |\Phi(\vec{q},\omega)|^2, \tag{3.35}$$

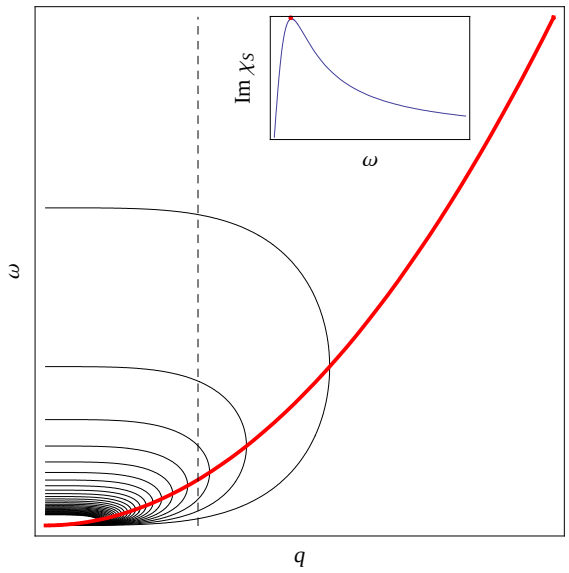

Figure 3.3: The spectral density of the smectic susceptibility at the nematic-smectic QCP, $Im\chi_S$, as a function of q and ω for $Q_S < 2k_F$. The spectral density is singular near the origin (lower right corner) and decays monotonically away from there. Here I show contour plots at constant spectral density with values from 0 up to 2000. The red line, $\omega = C_x q_x^2/C_0 + C_y q_y^2/C_0$, marks the peak of the spectral density as a function of momentum $\vec{q}$ parallel to the nematic orientation. The inset is the energy dependence of Imχ_S at a fixed small momentum (along the dashed vertical line).

which implies that the dynamic smectic susceptibility is

$$\begin{aligned}\chi^S =& -i\langle\Phi^\dagger(\vec{q},\omega)\Phi(\vec{q},\omega)\rangle_{\rm ret}\\ =&\frac{1}{iC_0\,\omega - C_x q_x^2 - C_y q_y^2 - \Delta_S},\end{aligned} \tag{3.36}$$

where $\vec{q}$ is the momentum measured from the ordering wave vector $\vec{Q}_S$. Here $\Delta_S > 0$ on the nematic side of this QCP. On the smectic (stripe) side of the quantum phase transition the Φ^4 coupling, which is (dangerous) irrelevant at this QCP, cannot be ignored as it stabilizes the smectic ground state. The smectic susceptibility in the ordered smectic phase differs from that of Eq.(3.36) in two standard ways: a) it acquires the usual delta function term peaked at the ordering wave vector, $\bar{\Phi}^2\delta(\vec{q})$, where $\bar{\Phi}$ is the expectation value of the smectic order parameter and $\vec{q}$ is measured from the ordering wave vector $\vec{Q}_S$, and b) the "mass term" (Δ_S) in the denominator of the susceptibility becomes $2|\Delta_S|$. At the nematic-smectic QCP, $\Delta_S = 0$, the smectic fluctuations are described by an overdamped critical mode with $z = 2$. The spectral density of χ_S at the QCP is shown in Fig. 3.3. It shows that most of the spectral weight is at small ω and q, which is typical for a critical mode, and the energy distribution curve at fixed momentum has a broad peak marked by the red line ($\omega = C_x q_x^2/C_0 + C_y q_y^2/C_0$), indicating an overdamped critical mode with $z = 2$.

The low-energy physics of the system will be dominated by ϕ_N, the Goldstone mode of the nematic field, whose behavior has been studied extensively in Ref. [150, 114]. On the other hand, at higher energy scales ($\omega \sim q^2$), the effects of field Φ, the amplitude mode of the smectic (or stripe) fluctuations, will become observable and, in this range, the system effectively has "fluctuating stripes". Notice that if the nematic Goldstone mode becomes gapped, say by the effects of the lattice, the smectic amplitude fluctuations become the only low-energy modes left. Finally, since the field Φ at the critical point has $z = 2$, the effective total dimension of this theory is 4. A standard Hertz-Millis type argument[84, 137, 180] implies that in this case the $|\Phi|^4$ term is marginally irrelevant. Therefore, the Gaussian fixed point will have the correct scalings, up to logarithmic corrections. In particular, contrary to what happens in the classical case where this transition becomes weakly first order, at the nematic-smectic QCP the electron smectic susceptibility will acquire logarithmic corrections to scaling in the $\omega \to 0$ and $\vec{q} \to 0$ limit, as can be deduced from standard arguments in classical and quantum critical phenomena[8, 180].

The gapless smectic amplitude mode Φ, the *fluctuating stripe*, can be detected in inelastic light scattering experiments, much in the same way as in the case of conventional CDW materials. The existence of this mode also has observable effects on thermodynamic properties such as the low-temperature heat capacity. Since the dynamic exponent now is $z = 2$, the fluctuation of the amplitude of the smectic mode leads to a $C \sim T$ contribution, which is subleading compared to the $C \sim T^{2/3}$ contribution of the nematic Goldstone mode ϕ_N.

Besides the subleading contribution to the heat capacity, the critical fluctuations of the smectic order parameter also have an observable effect on the fermions as they profoundly change the character of these excitations. As pointed out by Oganesyan and coworkers [150], the fermionic states in the nematic phase will become a non-FL due to the effects of the fluctuations of the nematic Goldstone mode, an overdamped mode with dynamic critical exponent $z = 3$. To leading order in perturbation theory, these authors found that for the most of the FS, the imaginary part of the fermion self-energy (the quasiparticle scattering rate) $\Sigma''(k_F, \omega) \sim |\omega|^{2/3}$, which, as $\omega \to 0$ (*i.e.* as the FS is approached) vanishes *slower* than ω. Thus, in almost all of the FS the fermionic quasiparticle is no longer a well-defined state as the quasiparticle pole in the fermion Green function is lost. This is the signature of a non-FL. However, for fermionic excitations propagating along the four main-axis directions of the nematic FS, the quasiparticle scattering rate now scales as $\Sigma''(k_F, \omega) \sim |\omega|^{3/2}$. Although this is not the conventional ω^2 behavior expected in an ordinary FL, nevertheless it is still consistent with the existence of a pole on the fermion spectral function, and a well-defined quasiparticle. Hence, in the nematic phase, except along these four special directions, the quasiparticles are not well defined.

The $|\omega|^{2/3}$ behavior of the quasiparticle rate is in clear conflict with conventional FL behavior. It also implies that perturbation theory is breaking down in this system. Two approaches have been proposed to assess the non-perturbative behavior of the system. Using the non-perturbative approach of higher dimensional bosonization [80, 92, 91, 32, 33], Lawler and Fradkin showed that at the non-perturbative level the $|\omega|^{2/3}$ perturbative correction to the quasiparticle rate leads to a dramatic change in the behavior of the fermion propagator, which they found to have a vanishing quasiparticle residue and to exhibit a form of "local quantum criticality" as it scales in frequency but not in momentum[114, 116]. On the other hand, Chubukov and Khveshchenko[38] used a resummed perturbation theory approach (on a similar problem) and argue that the $|\omega|^{2/3}$ behavior persists to all orders in perturbation theory. Although it is presently an open problem how to reconcile these two results, both analysis lead to the conclusion that the fermionic quasiparticles do not exist as well-defined excitations at the nematic-FL QCP and throughout the nematic phase (provided the nematic Goldstone modes remain gapless and overdamped).

At the nematic-smectic QCP, the fluctuations of the smectic field Φ (*i.e.* the "fluctuating stripe" mode) will also contribute to the fermion self-energy corrections (See Appendix A.5.1 for details). For most points on the FS, the contribution to the quasiparticle rate $\Sigma''(k_F, \omega)$ of the fluctuations of the smectic field Φ is proportional to ω^2, which is consistent with a conventional Landau behavior and a well-defined quasiparticle. However, at special points on the FS satisfying $\epsilon(\vec{k}) = \epsilon(\vec{k} + \vec{Q}_S)$ (shown in Fig. 3.2(a) as the four black dots), the contributions of the fluctuations of the smectic order-parameter field Φ to the quasiparticle rate scale as $\Sigma''(k_F, \omega) \sim |\omega|^{1/2}$. This $|\omega|^{1/2}$ behavior dominates even over the $|\omega|^{2/3}$ contribution of the nematic Goldstone mode. Hence, at the nematic-smectic QCP the quasiparticle residue will vanish at these special points of the FS. Note that these special points are precisely the positions on the FS where FS reconstruction will take place due to the development of CDW order, as shown in Figs. 3.2 (a) and (c). Hence, it is not surprising to see that strong derivations from the Landau FL picture appear at these points at the QCP. This non-FL behavior is just the prelude of the FS reconstruction in the ordered phase.

Finally, if the continuous rotational symmetry is broken explicitly by the anisotropic effects of the underlying lattice (say through an anisotropic band structure) or by external fields, at very low energies the nematic Goldstone mode of the nematic phase will have a finite gap (generally $z = 1$). If this gap is small enough, sufficiently close to the FS the fermion quasiparticle rate will show a crossover from the above mentioned $|\omega|^{2/3}$ above this gap to a conventional ω^2 characteristic of a Landau FL. (Note that at the nematic-FL QCP the $|\omega|^{2/3}$ behavior is still obtained even for a lattice system[50].) Nevertheless, at the nematic-smectic QCP, the quantum critical fluctuations of the smectic mode still generate $|\omega|^{1/2}$ corrections to the quasiparticle rate of the fermions at the special points where the FS is going to be reconstructed.

3.6.2 $Q_S = 2k_F$

I now consider the special case of $Q_S = 2k_F$. For the same reason as mentioned above, the coupling between the nematic Goldstone mode and the smectic field is irrelevant. Hence, at sufficiently low energies and close enough to the QCP, I can ignore their coupling and consider the effective theory of the smectic order-parameter field alone. The effects of the irrelevant coupling to the nematic Goldstone mode can be put back in perturbatively *a posteriori*.

When $Q_S = 2k_F$, Eq. (3.29) is still valid, although the structure of the fermion loop integral is very different. I can compute the effective theory of the bosonic modes by evaluating the fermion loop integral in the same way as I did in the previous section for the $Q_S < 2k_F$ case. Again, I find that $\Pi(\vec{Q}_S, 0)$ depends on the microscopic details of the fermion dispersion relation, but $\Pi(\vec{Q}_S + \vec{q}, \omega) - \Pi(\vec{Q}_S, \omega = 0)$ are dominated by the behavior of the integrand around the two points on the FS connected by Q_S as marked in Fig. 3.2(b). I expand the dispersion relation around these two points as $\epsilon = \mu \pm \delta k_y + \kappa \delta k_x^2/2$, where μ is the chemical potential, κ is the local curvature of the FS and $\delta\vec{k}$ is the momentum measured from these two points. By evaluating the fermion loop integral using this dispersion relation, I can determine the low-energy Lagrangian density of the field Φ to quadratic order

$$\mathcal{L}_\Phi(\vec{q}, \omega) = -\left(\zeta \left\{ \sqrt{q_y + \frac{\kappa q_x^2}{4} + \omega} + \sqrt{q_y + \frac{\kappa q_x^2}{4} - \omega} \right\} + \alpha_1 q_y + \alpha_2 q_x^2 \right) |\Phi(\vec{q}, \omega)|^2 \tag{3.37}$$

which implies that the smectic susceptibility at the QCP of this case is

$$\begin{aligned} \chi^S(\vec{q}, \omega) &= -i\langle \Phi^\dagger(\vec{q}, \omega)\Phi(\vec{q}, \omega)\rangle_{\text{ret}} \\ &= \frac{-1}{\zeta \left\{ \sqrt{q_y + \frac{\kappa q_x^2}{4} + \omega + i0^+} + \sqrt{q_y + \frac{\kappa q_x^2}{4} - \omega - i0^+} \right\} + \alpha_1 q_y + \alpha_2 q_x^2}. \end{aligned} \tag{3.38}$$

Here $\zeta = g_S^2/(2\pi\sqrt{\kappa})$ and $\alpha_{1,2}$ are determined by microscopic details. Notice that ζ diverges as κ vanishes, which is related the fact that a flat FS has a logarithmically divergent CDW susceptibility. In Sec. 3.6.4 I will show that at an inflection point of the FS, where $\kappa = 0$, there is a stronger non-analytic behavior of the form $\sqrt[4]{q_y + \omega}$.

For this Lagrangian density, a naive dimension counting suggests the scaling dimensions $[q_x] = 1$, $[q_y] = [\omega] = 2$. Under this scaling, α_1 and α_2 are irrelevant. However, if I take a small ω expansion for $q_y + \kappa q_y^2/4 < 0$,

the Lagrangian density becomes

$$\mathcal{L}_\Phi = \left(\frac{i\zeta|\omega|}{\sqrt{|q_y + \frac{\kappa}{4}q_x^2|}} - \alpha_1 q_y - \alpha_2 q_x^2 \right) |\Phi(\vec{q},\omega)|^2, \tag{3.39}$$

since $\sqrt{q_y + \kappa q_x^2/4 + \omega}$ and $\sqrt{q_y + \kappa q_x^2/4 - \omega}$ cancel each other in the $\omega \to 0$ limit when $q_y + \kappa q_x^2/4 < 0$. This Lagrangian density has scaling law $[q_x] = 1$, $[q_y] = 2$, and $[\omega] = 3$. This scaling is only valid inside the particle-hole continuum, while the naive scaling, $[q_x] = 1$, $[q_y] = [\omega] = 2$, is valid outside. This different behavior arises because $Q_S = 2k_F$ is located at the edge of the particle-hole continuum. Hence, the long wave length fluctuations may be inside or outside the particle-hole continuum, which leads to two possible different scaling behaviors. Among these two different scaling behaviors, the $[q_x] = 1$, $[q_y] = 2$, and $[\omega] = 3$ is the low energy mode in the long-wavelength limit. Hence, this mode dominates the low-energy physics and the scaling behavior.

The fact that q_x, q_y, and ω have different scaling dimensions is typical of anisotropic systems. For instance, in the smectic (stripe) phase of the quantum Hall state, a similar scaling was found in Ref. [15]. (This scaling behavior was later on proved to be unstable [115] due to the existence of an infinite set of marginal operators in that system.) Although the problem I am discussing here and the smectic quantum Hall state share the same scaling dimensions, they are actually quite different. In the case of the theory I am discussing in this section, it is the theory of the QCP of the nematic-smectic transition, while in the quantum Hall case, the same scaling is found in the smectic phase. Second, the different scaling dimensions in the x and y directions in our case are due to the existence of the FS, which results in two different scaling dimensions depending on whether the momentum is perpendicular or parallel to the FS. In contrast, in the quantum Hall smectic phase, it is due to the residue symmetry of the broken rotational symmetry, which is the same as in the smectic phase of the classical liquid crystals. Third, the scaling dimension 3 in the time direction is due to the nonanalytic dynamical term in the present problem I am discussing, but in the quantum Hall smectic, it is due to the explicitly broken time-reversal symmetry. Most importantly, the quantum Hall smectic is essentially an insulator in the direction perpendicular to the stripes. In our case, however, the stripe has not yet formed at the QCP, and the system is an anisotropic conductor in all directions. For our system, even inside the smectic phase, the FS is just partially gapped, so the conductivity in the direction perpendicular to the stripes is still non-zero. This difference is very important, since it means that in the quantum Hall smectic, the system is actually a $1D$ sliding Luttinger liquid, but in our case, the system is a full 2D structure. It is precisely the existence of the sliding symmetry that makes the $[q_x] = 1$,

$[q_y] = 2$, and $[\omega] = 3$ scalings unstable for the quantum Hall smectic phase. For our system instead, due to the absence of the sliding symmetry, our $[q_x] = 1$, $[q_y] = 2$, and $[\omega] = 3$ scalings will not experience the same instability as the quantum Hall smectic phase.

On the other had, non-Gaussian terms play an important role in our problem. The leading non-quadratic term is not the naive $|\Phi|^4$ term as in an ordinary Φ^4 bosonic theory. Instead, the discontinuity at the FS introduces a non-analytic term $|\Phi|^{5/2}$, as shown in Appendix A.3. A similar non-analytical term has been found in the FL-ferromagnets transition by Maslov, Chubukov, and Saha [130], where a non-analytic term $|m|^3$ in the thermodynamic potential, with m being the ferromagnetic order parameter, results in non-analytic behaviors for the specific heat coefficient and the spin susceptibility. It is also reported in the same reference that this $|m|^3$ term will be replaced by a term $\propto |m|^{7/2}$ at the QCP. Our theory will have effective dimension 6 at the Gaussian fixed point with scaling $[q_x] = 1$, $[q_y] = 2$, and $[\omega] = 3$, where $|\Phi|^4$ is irrelevant ($[\Phi] = 2$), but $|\Phi|^{5/2}$ is relevant. This relevant $|\Phi|^{5/2}$ term changes the scaling behavior of the critical theory away from the Gaussian theory.

Hence, in contrast with the case $Q_S < 2k_F$, the quantum critical theory at $Q_S = 2k_F$ is not controlled by the Gaussian fixed point. This conclusion agrees with the results of the "small momenta" regimes ($Q_S = 2k_F$ incommensurate CDW critical point) of the theory of a CDW-FL QCP of Altshuler *et al* [7], who also found a relevant perturbation at the Gaussian fixed point and hence a runaway RG flow. Therefore, the Gaussian theory fails. As a result, the irrelevant terms, which I ignored in this study, will determine the fate of this transition. In general, there are two possible situations. If the runaway RG flow has a (non-perturbative) discontinuity fixed point, the phase transition will become first order. This scenario is known as the "fluctuation-driven first order transition". However, there is also the possibility that the runaway RG flow has a non-trivial (and also non-perturbative) quantum critical fixed point, in which case the transition is still second order but has a different scaling. It may even be possible to change from a first-order transition to a second one by tuning some control parameters and going through a quantum tricritical point. In any case, although it is generally assumed that a fluctuation-induced first-order transition normally results, actually it is not possible to determine which one of these two scenarios actually holds by the perturbative arguments I am using here (and in Ref.[7]).

3.6.3 Commensurate CDW on a lattice

Our analysis can be used for the case of a commensurate CDW QCP as well, *i.e.* the "large momenta" regime of Ref. [7]. In this case, the Gaussian part of the effective Lagrangian density will become

$$\begin{aligned}\mathcal{L}_\Phi &= -\zeta\Big(\sqrt{q_y+\frac{\kappa q_x^2}{4}+\omega}+\sqrt{q_y+\frac{\kappa q_x^2}{4}-\omega}+\sqrt{-q_y+\frac{\kappa q_x^2}{4}+\omega}\\ &+ \sqrt{-q_y+\frac{\kappa q_x^2}{4}-\omega}\Big)\,|\Phi(\vec{q},\omega)|^2, \end{aligned} \tag{3.40}$$

which leads to the smectic susceptibility

$$\begin{aligned}\chi^S(\vec{q},\omega) &= -i\langle\Phi^\dagger(\vec{q},\omega)\Phi(\vec{q},\omega)\rangle_{\rm ret}\\ &= \frac{-1}{\zeta}\Big[\sqrt{q_y+\frac{\kappa q_x^2}{4}+\omega+i0^+}+\sqrt{q_y+\frac{\kappa q_x^2}{4}-\omega-i0^+}+\sqrt{-q_y+\frac{\kappa q_x^2}{4}+\omega+i0^+}\\ &+\sqrt{-q_y+\frac{\kappa q_x^2}{4}-\omega-i0^+}\Big]^{-1}. \end{aligned} \tag{3.41}$$

The last two terms in the Lagrangian density appear, due to the mirror effect between momentum $\vec{k}$ and $\vec{G}-\vec{k}$ introduced by the band structure, where $\vec{G}=2\vec{Q}_S$ is a reciprocal lattice vector. The static part of the Lagrangian density does not have a full cancellation as the incommensurate case in Eq. (3.39) due to the fact that $\pm q_y+\kappa q_x^2/4$ can not be negative at the same time. Hence, the naive scaling law, $[q_x]=1$, $[q_y]=2$, and $[\omega]=2$, is always valid, which makes the effective dimension of this theory 5. At the tree level, since Φ has dimension 2, $|\Phi|^{5/2}$ is marginal. In Ref. [7], it is shown that in this regime the coupling between the CDW order parameter and the fermions is marginal at the tree level and, at one-loop level it becomes marginal irrelevant. Therefore, the $|\Phi|^{5/2}$ term should be marginal irrelevant here too. I conclude that the quantum critical theory of the commensurate CDW critical point is Gaussian, with logarithmic corrections to scaling.

In this case, the contribution of the quantum critical smectic field to the low-temperature specific heat is proportional to $T^{3/2}$. The quasiparticle scattering rate $\Sigma''(k_F,\omega)$ acquires a contribution (due to the quantum smectic fluctuations) throughout most of the FS proportional to ω^2 , which can be ignored in low-energies and it is consistent with a finite quasiparticle pole. However, for the fermionic excitations close to $\pm k_F\vec{e}_y$, $\Sigma''(k_F,\omega)\sim|\omega|$, which suggests a marginal FL behavior. Details of this analysis can be found in Appendix A.5.1. The result $\Sigma''(k_F,\omega)\sim|\omega|$ for $\vec{k}=\pm k_F\vec{e}_y$ agrees with the findings of Ref. [7].

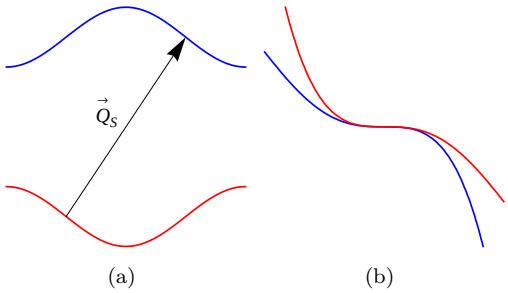

Figure 3.4: The FS near the inflection points. (a) a FS with 4 inflection points and only the two connected by $\vec{Q}_S$ will be considered; (b) the FS near the two inflection points by shifting them together and rotated.

3.6.4 The special case of a FS with inflection points

In the case of a two-dimensional system the FS is a curve. The point on the FS where the curvature vanishes is geometrically an inflection point (Fig. 3.4). In the $Q_S = 2k_F$ case, if the two points connected by Q_S happen to be two inflection points, the scaling behavior will become even more non-analytic than the cases I discussed above. Very close to the FS, I can assume that near the inflection points the dispersion relation of the fermions has an expansion of the form

$$\epsilon(\vec{q}+\vec{Q}_S/2) = \mu + q_y + aq_x^3 + bq_x^4 + \dots \tag{3.42}$$

Here μ is the chemical potential, the wave vector $\vec{q}$ has components q_x and q_y, which are the components perpendicular and tangent to the FS, all measured from the inflection point, and a and b are two constants. Assuming that the band structure has inversion symmetry, to obtain the dispersion relation around the other inflection point, I just need to reverse the vector $\vec{q}$. The term quadratic in q_x and q_y is set to zero since the curvature of the FS vanishes at the inflection point. The quartic term of q_x controls the FS nesting. Hence, if I decrease the coefficient b to zero, the CDW susceptibility will diverge, and a phase transition to a CDW state will be accessed by tuning the parameter b. If I start from a nematic phase, b can be used to control the nematic-smectic transition.

The Gaussian terms in the effective Lagrangian density of the smectic order parameter field is

$$\mathcal{L}_\Phi = -\gamma \left(\sqrt[4]{q_y + \frac{aq_x^3}{4} + \frac{bq_x^4}{8} + \omega} + \sqrt[4]{q_y + \frac{aq_x^3}{4} + \frac{bq_x^4}{8} - \omega} \right) |\Phi(\vec{q},\omega)|^2, \tag{3.43}$$

which implies the smectic susceptibility

$$\begin{aligned}\chi^S(\vec{q},\omega) &= -i\langle\Phi^\dagger(\vec{q},\omega)\Phi(\vec{q},\omega)\rangle_{\rm ret} \\ &= \frac{-1/\gamma}{\sqrt[4]{q_y+\frac{aq_x^3}{4}+\frac{bq_x^4}{8}+\omega+i0^+}+\sqrt[4]{q_y+\frac{aq_x^3}{4}+\frac{bq_x^4}{8}-\omega-i0^+}}.\end{aligned} \tag{3.44}$$

Here the constant $\gamma = (2/b)^{1/4}/(2\pi)$. As I just mentioned, $b = 0$ implies a nested FS and this is the reason that γ diverges as $b \to 0$. In contrast to the ordinary $Q_S = 2k_F$ incommensurate case studied before, there is no cancellation inside the particle-hole continuum for the inflection points, so that the naive scaling law, $[q_x] = 1$,$[q_y] = 3$, and $[\omega] = 3$, is always valid. The non-Gaussian terms now start at the order $|\Phi|^{9/4}$ as shown in Appendix A.3. This term is irrelevant at tree level.

The low-energy heat capacity contributed by this mode has $C \sim T^{4/3}$. The fermions near the inflection points have $\Sigma'' \sim |\omega|^{13/12}$, which means the fermionic quasiparticles near the inflection point will remain well defined, even when the nematic-smectic QCP is reached.

3.7 The electronic smectic phase

In the electronic smectic phase, *i.e.* in a conducting stripe phase, the electronic structure of the FL quasiparticles is changed by the modulation imposed by the smectic order parameter, and an energy gap will develop at the locus of the former FS. As a result new electronic bands along the direction of the ordering wave vector will be formed, with a gap in the electronic energy spectrum $\Delta_S \propto g_S\Phi$. As shown in Fig. 3.2(c), if $2k_F/Q_S$ is not close to an integer value, the highest band will have a closed FS, *i.e.* an electron (or hole) pocket, while the lower band (or bands) has instead an open FS (an "open orbit"). For $2k_F/Q_S$ close to an integer, as shown in Fig. 3.2(d), there will only be an open FS. The reconstruction of the FS of the effective quasiparticles of a stripe phase in the cuprate high temperature superconductors has been discussed recently[139] as a possible explanation of the observation of Shubnikov-deHaas and deHaas-van Alphen oscillations at relatively high magnetic fields[52].

I divide our discussion into two cases of interest: a) a smectic state in the continuum and b) a smectic state on a two-dimensional lattice.

3.7.1 The electronic smectic phase in a continuum system

I consider first a system with continuous rotational and translational symmetries which are partially and spontaneously broken by the smectic order parameter. I consider only the collective modes of the smectic

order. The nematic collective modes will be added *a posteriori* using symmetry considerations. In this section I derive the effective order-parameter theory for the electronic smectic. The details of the calculation are presented in Appendix A.4.

Let us consider a configuration of the complex smectic order-parameter field Φ, which is a small deformation of the ground-state configuration with expectation value $\bar{\Phi}$,

$$\Phi = \bar{\Phi}\left(1 + \frac{\delta\Phi}{|\bar{\Phi}|}\right) e^{i\phi_\Phi}. \tag{3.45}$$

Here $\delta\Phi$ measures the amplitude fluctuations of $\bar{\Phi}$ and ϕ_Φ measures the phase fluctuations.

At the mean-field level, *i.e.* ignoring fluctuations, the main effect of the presence of a non-vanishing $\bar{\Phi}$ is that the original FS becomes folded along the direction determined by the ordering wave vector and a more complex electronic band structure results. The inter-band and the intra-band scatterings of the fermions will have different contributions to the effective low-energy theory. For the smectic Goldstone mode, ϕ_Φ, in the static limit, the intra-band scatterings have no contributions but the inter-band scatterings will give a constant, which will cancel the constant coming from the terms $\Delta_S|\Phi|^2 + u_S|\Phi|^4$ for $Q_S < 2k_F$, or $\Delta_S|\Phi|^2 + u_S|\Phi|^{5/2}$ for $Q_S = 2k_F$, provided the expectation value of $\bar{\Phi}$ satisfies the self-consistency equation of the mean-field theory. This exact cancellation of the constant term for the Goldstone mode is required by the Ward identity for translations along the ordering wave vector. The amplitude mode however will not have this cancellation, and a term proportional to $\delta\Phi^2$ will appear in its effective action.

For $\omega \neq 0$ and $\vec{q} \neq \vec{0}$, the intra-band and inter-band scatterings also yield different contributions. The effective low-energy Lagrangian density of the smectic Goldstone mode ϕ_Φ (a real field in position space and time) takes the form (see Appendix A.4)

$$\mathcal{L}_{\phi_\Phi} = g_S^2|\bar{\Phi}|^2 N_S(0)\left(B(\varphi_q)\frac{\omega^2}{k_F g_S|\bar{\Phi}|} + iA(\varphi_q)\frac{|\omega|q}{k_F g_S|\bar{\Phi}|} - \kappa_S(\varphi_q)q^2\right)|\phi_\Phi(\vec{q},\omega)|^2, \tag{3.46}$$

where φ_q is the angle between $\vec{q}$ and the stripe direction and $N_S(0)$ is the density of states in the smectic phase. $A(\varphi_q)$, $B(\varphi_q)$, and $\kappa_S(\varphi_q)$ are coupling constants that depend on microscopic details and the direction of $\vec{q}$, which reflects the anisotropic nature of the smectic phase. I will neglect the direction dependence of these three coefficients since they result in irrelevant contributions at low energies and long distances. The first term $\propto \omega^2$ in Eq. (3.46) is due to inter-band scattering, while the second, $\propto i|\omega|q$, is due to intra-band scattering. The intra-band contribution does not have the typical $i|\omega|/q$ form, because the contributions from the intra-band scattering vanish in the $q = 0$ limit (see Appendix A.4.) The dynamic critical exponent is $z = 2$ at the QCP but $z = 1$ in the smectic phase. This discontinuity is reflected in the singularity of Eq.

(3.46) at $\bar{\Phi} = 0$.

This behavior of the smectic Goldstone mode is very similar to that of the spin Goldstone mode in the commensurate antiferromagnetic phase (commensurate SDW) of a 2D FL studied by Sachdev, Chubukov, and Sokol [182]. In fact, although they are studying the commensurate SDW, while I am studying incommensurate CDW, if the nematic fluctuations in our system are gapped by a lattice background or external fields which breaks the continuous rotational symmetry, the nematic-smectic transition I study here shares many common features with their work (especially "type B" in Ref. [182]). Both these two transitions are driven by FL instabilities with a finite ordering wave vector and fermions provide similar non-analytic damping terms for low-energy bosonic excitations in both systems. For both cases, the QCP has $z = 2$ and the ordered phase has a Goldstone mode with $z = 1$.

An RPA calculation (see also Appendix A.4) shows that the amplitude mode fluctuations $\delta\Phi$ of the electronic smectic order parameter has an effective low-energy Lagrangian density of the form

$$\mathcal{L}_{\delta\Phi} = g_S^2 N_S(0) \left(i\frac{|\omega|}{q} - |\Delta_S| \right) |\delta\Phi(\vec{q},\omega)|^2. \tag{3.47}$$

The dynamical term $i|\omega|/q$ comes from the intra-band scattering. In contrast with the case of the Goldstone mode ϕ_Φ, there is no cancellation of the intra-band contributions at $q = 0$ for the amplitude mode $\delta\Phi$. Inter-band scattering contributes an irrelevant $\sim \omega^2$ dynamical term which is ignored. The longitudinal CDW susceptibility in the smectic ordered phase is

$$\begin{aligned} \chi_\parallel^S(\vec{q},\omega) =& -i\langle \delta\Phi(\vec{q},\omega)\delta\Phi(-\vec{q},-\omega)\rangle_{\rm ret} \\ =& \frac{1}{g_S^2 N_S(0)\left(\frac{i\omega}{q} - |\Delta_S|\right)}, \end{aligned} \tag{3.48}$$

where $\vec{q}$ is measured from the ordering wave vector $\vec{Q}_S$

Hence, in the electron smectic phase both the phase and amplitude modes of the smectic order parameter scale with a dynamical exponent $z = 1$. This result is interesting, because in most other examples of continuous symmetry breaking, the amplitude mode is either gapped or has a smaller dynamic critical exponent z than the Goldstone mode. As a result, at lower energies, the amplitude mode will become weaker, and can be ignored from the effective low-energy theory. However, in this case, since both the amplitude mode and the Goldstone mode have the same dynamic critical exponent, no matter how low the energy scale is these two modes can no longer be separated.

Nevertheless, in our problem, the amplitude mode is irrelevant for the following reasons. Using Eqs.

(3.23) and (3.45), I see that both the amplitude CDW fluctuations $\delta\Phi$ and the CDW Goldstone modes ϕ_Φ couple to fermionic CDW operator $n(\vec{q},\omega)$ in the form:

$$\begin{aligned} &g_S\ n(\vec{q},\omega)\ \delta\Phi(-\vec{q},-\omega) + h.c., \\ &ig_S\ \bar{\Phi}\ n(\vec{q},\omega)\ \phi_\Phi(-\vec{q},-\omega) + h.c., \end{aligned} \tag{3.49}$$

but the coefficients in the action of $\delta\Phi$ ($g_S^2 N_S(0)$) and ϕ_Φ ($g_S|\bar{\Phi}|N_S(0)A/k_F$, $g_S|\bar{\Phi}|N_S(0)B/k_F$ and $g_S^2|\bar{\Phi}|^2 N_S(0)\kappa_S$) have different scaling behaviors. With $z=1$, the coefficients for $\delta\Phi$ have dimension 3, but the coefficients ϕ_Φ's coefficients have dimension 1. As a result, the coupling between the smectic Goldstone mode ϕ_Φ and the fermions is actually more relevant than the coupling to the amplitude mode $\delta\Phi$. Hence, I will not consider $\delta\Phi$ in what follows.

Finally, I need to couple the smectic Goldstone mode, ϕ_Φ, with the nematic Goldstone mode ϕ_N. Similar to the classical case, ϕ_N couples to the electronic smectic field Φ as a gauge field (Eq. (3.15)). Hence, in the electron smectic phase, upon substituting Eq. (3.45) into Eq. (3.15), the nematic Goldstone mode ϕ_N develops a mass term $\sim |\bar{\Phi}|^2\phi_N^2$, *i.e.* it acquires a gap. As in the classical case, the fluctuations of the nematic order produce bending of the smectic order, which costs energy. Thus, here too, this effect leads to the expulsion of the nematic Goldstone mode.

Since the dynamics of the nematic Goldstone mode ϕ_N has the structure $i|\omega|/q$, the mass term $|\bar{\Phi}|^2\phi_N^2$ of the nematic Goldstone mode in the smectic phase makes this mode to have $z=1$ dynamics, just as the smectic Goldstone mode ϕ_Φ has. However, if I am close to the QCP, where the smectic amplitude fluctuation $\bar{\Phi}$ is small, the energy scale of the smectic Goldstone mode ϕ_Φ will be lower than that of ϕ_N. Hence, upon integrating out the nematic Goldstone mode ϕ_N, I obtain an effective low-energy action for ϕ_Φ of the form

$$\mathcal{L}_{\phi_\Phi} = g_S^2|\bar{\Phi}|^2 N_S(0)\left(B\frac{\omega^2}{k_F g_S|\bar{\Phi}|} + iA\frac{|\omega|\sqrt{\kappa_1\kappa_2^{-1}q_x^4+q_y^2}}{k_F g_S|\bar{\Phi}|} - \kappa_1 q_x^4 - \kappa_2 q_y^2\right)\ |\phi_\Phi(\vec{q},\omega)|^2. \tag{3.50}$$

where A, B are two coefficients, and κ_1 and κ_2 are the defined in Eqs. (3.17) and (3.18). Here, as in the classical case, the coefficient of the q_x^2 term vanishes by rotational invariance.

By inspection of Eq. (3.50) I see that the scaling dimensions now are $[q_x]=1$ and $[q_y]=[\omega]=2$. Hence, I can conclude that the fluctuations of ϕ_Φ contributes to the low-temperature specific heat which scales with temperature as $C\sim T^{3/2}$. It follows from this scaling analysis that in this case the system is above its upper critical dimension. Hence, true long-range order exists. The logarithmic corrections generated by the higher-order terms in classical smectics [76] will not be present. Notice that these scaling dimensions are

the same as what I got from the phenomenological theory in Sec. 3.4, before it was coupled to the fermions. However, the physics is now very different. Most important of all, in the presence of fermions, the smectic Goldstone mode is damped, which is not the case in the phenomenological theory.

A one-loop calculation of the fermion self-energy shows that the fermionic quasiparticles in the electronic smectic phase is a FL (Appendix A.5.2). Indeed, for most of the FS, the quasiparticle scattering rate at low frequency is $\Sigma''(k_F, \omega) \sim \omega^2 \log|\omega|$. At the special points on the FS where the Fermi velocity is parallel to the ordering wave vector $\vec{Q}_S$ (*i.e.* perpendicular to the stripes) (marked in Fig. 3.2(c)), $\Sigma''(k_F, \omega) \sim |\omega|^{3/2}$ for small ω. However, this $|\omega|^{3/2}$ scaling will not be observed for $2k_F/Q_S$ close to an integer, since no point on the FS will have $\vec{v}_F \parallel \vec{Q}_S$ as shown in Fig. 3.2(d).

3.7.2 The electronic smectic phase on a lattice

For most physical electronic systems the continuous rotational symmetry is reduced to a discrete point group symmetry of the underlying lattice. As it is well known[104, 150] the explicit breaking of rotational invariance by the lattice has important consequences for an electron nematic state. For the simple square lattice, the $O(2)/\mathbb{Z}_2$ symmetry of the continuum nematic state reduces to an Ising-like $\mathbb{Z}_2$ symmetry, an "Ising nematic." On the other hand, at the nematic-FL QCP symmetry breaking by the underlying lattice are irrelevant[50], provided the quantum phase transition remains continuous which, in many instances does not appear to be the case[101, 102]. Lattice effects manifest in the electronic structure and hence on the allowed shape of the FS of the FL state. Lattice anisotropies will then break the continuous rotational symmetry and act as explicit symmetry breaking fields. In this case, the nematic phase does not have a true Goldstone boson which now becomes gapped. At the level of the effective theory this effect shows up by the presence of a term proportional to ϕ_N^2 in the effective action of the nematic Goldstone mode, which is just an allowed mass term since there is no Ward identity to prevent it. This term makes ϕ_N a $z = 1$ mode, in contrary to $z = 3$ without lattice. Hence, the "pseudo-Goldstone" mode ϕ_N has now become irrelevant at low energies. This changes a number of things. For one, the non-FL behavior of the nematic phase in the continuum is replaced by an anisotropic FL state with well-defined quasiparticles. Naturally if the effects of the lattice are weak enough, at sufficiently high energies (or temperatures) they can be neglected and the non-FL effects become detectable above this crossover. On the other hand, as the quantum phase transition to the electronic smectic phase is approached the gapped nematic Goldstone modes become irrelevant and the low-energy physics is dominated instead by the fluctuations of the smectic mode, which in the continuum case is a higher-energy excitation. In other terms, one now obtains a "fluctuating stripe" regime close enough to the nematic-smectic QCP.

In the electronic smectic phase, the lattice anisotropy makes the nematic Goldstone mode irrelevant, which can now be neglected in the effective low-energy theory. As a result, I only need to consider the smectic Goldstone mode to understand the low-energy physics of the smectic phase. Depending on whether the smectic (CDW) is pinned down by the lattice or not, the physics of the smectic Goldstone mode behaves very differently. In the absence of lattice pinning, the Lagrangian density shown in Eq. (3.46) will be the proper low-energy theory of the smectic Goldstone fluctuations, so the scaling behavior is $[q_x] = [q_y] = [\omega] = 1$ and the transverse smectic susceptibility is

$$\begin{aligned} \chi^S_\perp(\vec{q},\omega) &= -i\bar{\Phi}^2\langle\phi_\Phi(\vec{q},\omega)\phi_\Phi(-\vec{q},-\omega)\rangle_{\rm ret} \\ &= \frac{1}{g_S^2 N_S(0)}\frac{1}{B(\varphi_q)\frac{\omega^2}{k_F g_S|\bar{\Phi}|}+iA(\varphi_q)\frac{\omega q}{k_F g_S|\bar{\Phi}|}-\kappa_S(\varphi_q)q^2}, \end{aligned} \tag{3.51}$$

where $\vec{q}$ is measured from the ordering wave vector $\vec{Q}_S$. This low-energy behavior is different from the electronic smectic in the continuum. If the lattice effects are weak enough, I expect a crossover with increasing energy scales from the behavior of a smectic coupled to the lattice to one without this coupling.

By following the same type of analysis used in the previous subsections I can conclude that the heat capacity has a contribution due to the fluctuations ϕ_Φ with a T^2 temperature dependence. To the one-loop level, the fermionic quasiparticles at the FS will have a scattering rate $\Sigma''(k_F,\omega) \sim \omega^2 \log|\omega|$ for $\omega \to 0$ at most part of the FS, while $\Sigma''(k_F,\omega) \sim \omega^2$ for some special points on the FS discussed in Appendix A.5.2. This observation is consistent with a FL behavior (Appendix A.5.2).

For a pinned CDW, the cancellation of the intra-band scattering for ϕ_Φ no longer holds. Therefore, the dynamical term is $\sim i|\omega|/q$ with $z = 1$. The coupling between ϕ_Φ and the fermions is irrelevant in the pinned smectic phase, and the FL picture will hold.

In general, there are two sources for pinning the CDW: lattice and impurities. I will consider the lattice pinning first. Lattice pinning is relevant for commensurate CDWs. For incommensurate CDWs, however, some lattice distortions will be required to pin the CDWs. A distorted lattice can pin down an incommensurate CDW only if the CDW order parameter is large enough. This is because the energy gain by pinning vanishes as $|\bar{\Phi}|$ goes to 0. On the other hand, the energy needed to distort the lattice will not go to zero with decreasing $|\bar{\Phi}|$. For most conventional CDW materials, the CDW ordering is very strong at low T so that incommensurate CDWs will always be pinned down by distorted lattice [69, 60, 117, 77] and unpinned CDW only appears at finite T above a phase transition [134].

However, for our systems, there is a second-order phase transition from nematic to smectic. When I am close to the nematic-smectic QCP, the smectic order parameter will be small, so that an unpinned

incommensurate CDW phase is stable against a lattice background at least when it is close to this QCP. When I am far from the critical point, the smectic order parameter becomes large, so the energy gain by pinning may exceed the energy cost of distortion. Hence, a pinned CDW phase may form.

Throughout this chapter I ignore the effects of quenched disorder. Impurities, and more generally disorder, affect strongly all electronic liquid crystal phases as they couple linearly to the their order parameters, leading to the destruction of these ordered phases and to glassy-type states[104]. For the case of the CDW phases this problem was studied extensively in the 1980s, for which pinning is relevant for $d < 4$ for systems with short-range interactions [186, 94] and $d < 3$ for long-range Coulomb interactions [20]. In the case of these quantum phase transitions the effects of quenched disorder, even in the clean limit, are only poorly understood and I will not explore these problems in this work.

3.8 Finite-temperature crossovers and thermal phase transitions

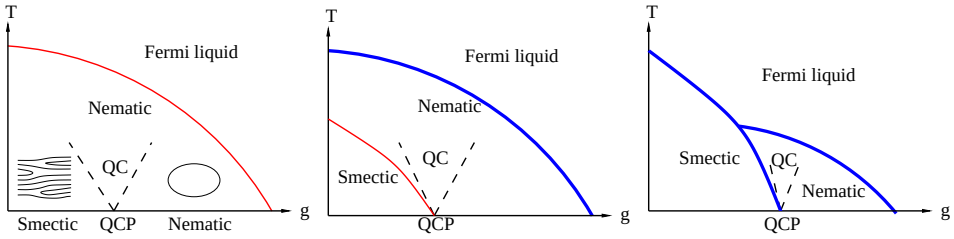

(a) isotropic system (b) with a lattice background (c) pinned CDW

Figure 3.5: The schematic phase diagrams at finite T for (a) an isotropic system, (b) a system with a lattice background, and (c) systems with a pinned CDW in the smectic phase. The horizontal axis is a control parameter that drives the quantum phase transitions: Fermi liquid $\rightarrow$ nematic $\rightarrow$ smectic at $T = 0$. The vertical axis is the temperature T. The thick (blue) lines are phase transitions belong to the Ising (or q-state Potts model) universality class while thin (red) lines are KT transition phase boundaries. The dashed lines mark the crossover to the quantum critical regime (QC). In panel (a) I show that the nematic phase (in the absence of lattice symmetry breaking) only has long range order at $T = 0$, and it is a critical KT phase at all temperatures below the KT transition. In panel (b) the lattice reduces the symmetry to $\mathbb{Z}_2$ and there is long-range Ising nematic order at finite temperatures. In this case there is also a finite-temperature smectic phase which is critical (KT) if the smectic (CDW) order is unpinned and has long-range order in the latter case (shown in panel c).

I now discuss the effects of a finite-temperature on the electronic nematic and smectic phases and on their quantum phase transition. In Fig. 3.5, I present schematic phase diagrams for the three cases of interest: a) the isotropic case (no lattice), b) the system with a lattice background (a square lattice in this case) and an unpinned electron smectic (CDW) and in c) the case of a lattice with pinned CDW.

In the nematic phase and at the nematic-smectic QCP, the nematic Goldstone modes have a finite

temperature equal-imaginary time correlation function, *i.e.* the transverse nematic susceptibility,

$$\begin{aligned}\chi_{\perp}^{N}(\vec{q}) =& \bar{N}^2 \langle \phi_N(\vec{q},\tau)\phi_N(-\vec{q},\tau)\rangle_{\rm ret} \\ =& \frac{1}{\beta g_N^2 N(0)} \sum_{\omega_n} \frac{1}{\frac{|\omega_n|}{q}\sin^2 2\varphi_q + K_1 q_x^2 + K_2 q_y^2}\end{aligned} \tag{3.52}$$

where I have set k_B to 1 so $\beta = 1/T$ and the sum runs over all bosonic Matsubara frequencies, $\omega_n = 2\pi n T$, where $n \in \mathbb{Z}$. The susceptibility $\chi_{\perp}^{N}(\vec{q})$ is singular as $\vec{q} \to 0$ (due to the $\omega_n = 0$ mode, where it takes the asymptotic form $\sim T/q^2$. This behavior suggests that the nematic order parameter field has power-law correlations at finite T. This conclusion agrees with the classical theory of a 2D nematic phase, which belongs to the Kosterlitz-Thouless (KT) universality class[194, 34].

By comparing the T/q^2 term with the equal-time correlation function at $T = 0$, which is $\sim q\log(E_F/q)$ where E_F is the Fermi energy, which enters the calculation as a high energy cutoff, I see that $T = 0$ behavior becomes dominant when $q \gg T^{1/3}$.

From the theory of classical liquid crystals[48, 34], I know that in a fully translationally invariant system, *e.g.* in the absence of a lattice, there is no stable finite-temperature smectic phase in two space dimensions[194], which implies that the equal-time correlation function of the smectic order parameter decays exponentially fast as a function of distance at any finite T. Due to the effects of the proliferating dislocations of the smectic the actual finite-temperature phase is a nematic.

In the nematic phase and at the nematic-smectic QCP, the finite T equal-time correlation function of the smectic fields, *i.e.* the smectic susceptibility, is

$$\begin{aligned}\chi^{S}(\vec{q}) &= \langle \Phi(\vec{q},\tau)\Phi(-\vec{q},\tau)\rangle_{\rm ret} \\ &= \frac{1}{\beta}\sum_{\omega_n} \left(C_0|\omega_n| + C_x q_y^2 + C_y q_y^2 + \Delta\right)^{-1}\end{aligned} \tag{3.53}$$

Here, $\vec{q}$ is measured from the ordering wave vector $\vec{Q}_S$ and $\Delta = \Delta_S + f(T)$, where $f(T)$ is a function of temperature which vanishes at $T = 0$. The leading term in $f(T)$ comes from the quartic term of the smectic field $\sim u_S T$ and the gauge-like couplings between the nematic Goldstone mode and the smectic fields $\sim Q_S^2 T$, where the ordering wave vector Q_S represents the strength of the gauge-like coupling. The absence of a finite-T smectic-ordered phase implies that $\Delta \neq 0$ for $T > 0$. Hence, on the nematic side, at low enough temperatures $\Delta > 0$ and it is essentially equal to $\Delta_S > 0$. However, in the quantum critical region (denoted by QC in Fig. 3.5), the singular behavior of $\chi^S(\vec{x})$ is regulated purely by finite temperature. Notice that $f(T)$ depends on irrelevant operators of the QCP; I conclude that the infrared divergence is regulated

by irrelevant operators, including the gauge-like coupling between smectic and the nematic Goldstone mode, which implies that this gauge-like coupling is a dangerous irrelevant term near the QCP and become relevant at finite T. This conclusion agrees with the theory of the classical nematic-smectic transition at finite T, where the gauge coupling is known to be relevant. The boundary between the nematic and the quantum critical regime is determined by the condition $f(T) \sim \Delta_S$, which is $T \sim \Delta_S$.

On the smectic side, the equal-time correlation function of the smectic Goldstone mode fluctuations, *i.e.* the transverse smectic susceptibility $\chi_\perp^S(\vec{q})$ (where $\vec{q}$ is the momentum measured from the ordering wave vector $\vec{Q}_S$ of the smectic phase) is

$$\begin{aligned} \chi_\perp^S(\vec{q}) &\equiv |\bar{\Phi}|^2 \langle \phi_S(\vec{q},\tau)\phi_S(-\vec{q},\tau)\rangle_{\rm ret} \\ &= \frac{1}{\beta g_S^2 N_S(0)} \sum_{\omega_n} \frac{1}{B\frac{\omega_n^2}{k_F g_S|\bar{\Phi}|} + A\frac{|\omega_n|\sqrt{\kappa_1\kappa_2^{-1}q_x^4+q_y^2}}{k_F g_S|\bar{\Phi}|} + \kappa_1 q_x^4 + \kappa_2 q_y^2} \end{aligned} \tag{3.54}$$

The most divergent term in $\chi_\perp^S(\vec{q})$ has the asymptotic behavior $T/(\kappa_1 q_x^4 + \kappa_2 q_y^2)$, which implies that the Fourier transform of $\chi_\perp^S(\vec{q})$, the transverse susceptibility of the smectic Goldstone mode, is infrared divergent at finite T. This divergence implies that the equal-time correlation functions of the smectic order parameter field $\langle \Phi(\vec{x})^\dagger \Phi(\vec{y})\rangle$ exactly vanishes, for all $\vec{x} \neq \vec{y}$. Thus, this system exhibits a form of "local quantum criticality", *i.e.* where the correlation length of the equal-time correlation function essentially vanishes but the equal-position auto-correlation function scales as a function of time. In Fourier space, this means that the finite temperature dynamical susceptibility scales in frequency but not in momentum. This behavior was discussed recently in the context of the FL-nematic QCP[116] and in the quantum critical behavior of quantum dimer models[71].

The vanishing of the equal-time correlation length however invalidates the assumption of small smectic Goldstone fluctuations, where topological defects (dislocations) become important. With dislocations, the smectic order parameter vanishes (as translation invariance has been restored) and the equal-time correlation functions of the smectic order parameter become short ranged. This physics proceeds, as usual, by the non-perturbative Kosterlitz-Thouless mechanism of defect proliferation. At low temperatures, where the density of the dislocations is low, the correlation length diverges, which recovers the proper behaviors of the zero-temperature quantum smectic phase.

For systems with a lattice background, the nature of the thermal nematic phase transition is determined by the point group symmetry of the lattice, *e.g.* for the square lattice it is an Ising transition. Also in

the presence of a lattice there is a stable electronic smectic phase at finite temperature. In this case the finite-temperature nematic-smectic transition is in the KT universality class for an unpinned CDW. With a lattice background, the 2D unpinned smectic will be at its lower critical dimension. Therefore, the smectic phase has quasi long-range order and a finite-temperature KT transition is expected. For smectics pinned by lattice, the transition instead belongs to the universality class of the q-state Potts model, with q equals to n for a lattice with n-fold rotational symmetry [14]. On the nematic side, Eq. (3.53) is still valid, but $\Delta \to 0$ as I approach the finite-temperature phase transition. On the unpinned smectic side, the most singular term of the correlation function of its Goldstone mode will be $\sim T/q^2$, which now will be unaffected by topological defects in the finite-T smectic phase since in the case of a lattice the dislocations are confined. This behavior of a phase smectic phase mode leads, as usual, to an equal-time correlation functions of the order parameter with power-law behavior as a function of distance. In the high-temperature phase, where the dislocations become deconfined, the order parameter has only short-ranged spatial correlations.

3.9 Discussion and conclusions

In this chapter I present a phenomenological theory of quantum phase transitions in electronic liquid crystal phases. For simplicity I have only considered the charge channel and discussed the behavior of two charge-ordered phases: the electron nematic and the electron smectic. The latter phase has the same symmetries as a charge stripe phase and a unidirectional CDW. I have not discussed the behavior of spin excitations and the associated magnetic phases, *i.e.* a spin stripe. The main results are summarized in Table 3.1,3.2,3.3.

I discuss in detail how to describe a fluctuating charge stripe phase, a metallic electron nematic phase close to a quantum phase transition to an electronic smectic (or stripe) phase. I analyzed the nature of the fluctuations of the bosonic collective modes in the nematic as this quantum phase transition is approached: it is described by a low-energy Goldstone nematic mode (with dynamic critical exponent $z = 3$) and a higher energy smectic collective mode (with dynamic critical exponent $z = 2$), and discussed in detail the behavior of the nematic and smectic correlation functions in this regime. I also gave a detailed analysis of the electron smectic phase and of the behavior of the correlation functions in this phase. In particular I give explicit form of the dynamical susceptibilities at zero temperature, including the dynamics induced by the fermionic fluctuations. This analysis was also done in the electron smectic phase. The behavior of the nematic and smectic susceptibilities should be useful to interpret experiments that can probe this dynamics, particularly light-scattering experiments. With some minor changes the form of these correlation functions and susceptibilities also apply to the analysis of magnetic fluctuations, such as neutron scattering

experiments in the fluctuating stripe regime.

I also developed a description of the quantum critical behavior at this phase transition to an electronic smectic phase. This effective critical theory is a quantum-mechanical generalization of the classical McMillan-deGennes theory for the nematic-smectic liquid crystals to quantum-mechanical metallic phases with the same pattern of symmetry breaking. It is a theory at zero temperature and it includes the effects of strong quantum fluctuations which turn out to have a very different character than their classical counterpart. Due to the non-trivial effects of the fermionic fluctuations, this quantum phase transition is continuous whereas the classical finite-temperature transition is weakly first order.

I presented an extensive discussion of the fate of the fermionic quasiparticles in each phase and at the quantum phase transition, and of the resulting non-FL behaviors. The resulting non-FL effects are quite rich. These results were obtained within a perturbative expansion in powers of the coupling between the fermions and the order-parameter fluctuations. As such, the obtained non-FL behaviors represent primarily a breakdown of perturbation theory rather than asymptotically exact results. The reliability of these low-order results will be checked in the near future using non-perturbative approaches such as higher dimensional bosonization. In any case our perturbative analysis of the quasiparticle self-energy shows once again that electronic liquid crystal phases are naturally compatible with non-FL behavior.

Although much of the theory that I presented is developed in the context of a continuum system, *i.e.* a system in which the effects of the coupling of the underlying lattice on the electronic order is ignored, I also gave a qualitative analysis of the symmetry-breaking effects resulting from the coupling to the lattice. This analysis will be generally correct even though the details of the microscopic band structures were ignored, as they will be reflected in the form of symmetry breaking fields and in their coupling constants. I expect that the discussion of the continuum (isotropic) theory will be applicable if the effects of the coupling to the lattice are comparatively weak (as expected far from van Hove singularities) and at temperatures high compared to the scale of these couplings. Quite surprisingly, although the pinning of the nematic Goldstone mode by the lattice was expected, I found that the smectic collective modes in general remain strongly fluctuating as the QCP is approached and into the smectic phase. This happens provided that the magnitude of the ordering wave vector obeys $Q_S < 2k_F$. Contrary to what happens in the case of the FL-nematic quantum phase transition, in which lattice effects often drive the transition first order, the nematic-smectic transition can naturally be continuous even in the presence of the coupling to the lattice.

I also considered the effects of low-temperature thermal fluctuations, and showed that the signatures of the electronic smectic phase can be detected through heat-capacity measurements as subleading corrections to FL. In the electronic nematic phase and at the nematic-smectic QCP, the heat capacity is dominated by

nematic fluctuations, which goes as $T^{2/3}$. At the QCP, the smectic mode yields an additional contribution $\sim T$ for $Q_S < 2k_F$, a subleading term $\sim T^{3/2}$ for commensurate CDW with $Q_S = 2k_F$ and $\sim T^{4/3}$ for the case of inflection points. In the electronic smectic phase, the smectic Goldstone mode gives a contribution to the heat capacity of $C \sim T^{3/2}$ in the absence of lattice symmetry breaking effects and T^2 with lattice symmetry breaking effects.

The approach that I followed is semi-phenomenological and it is based on the picture of a Fermi liquid that is coupled to an effective field theory describing the fluctuations of the nematic and smectic (stripe) order parameters. This line of attack can be justified, at the level of mean-field theory, in weakly coupled systems based on the existence of a Fermi liquid for some range of parameters and its subsequent instabilities. Examples of this approach is the work on the FL/electron-nematic quantum phase transition of Oganesyan *et al* [150] in continuum models and of Metzner and coworkers[79, 136, 216, 50] and H.-Y. Kee and coworkers[101, 102] in lattice models. The extension of these works to the electron nematic/stripe phase transition that I discuss here is possible and I have obtained some unpublished results in this direction. However, this quantum phase transition requires that a coupling constant be larger than a critical value, which typically is not small, and hence the reliability of mean-field methods in this regime is at least problematic. This will be discussed in a separate publication.

I have not discussed the realization of these electronic liquid crystal phases, and of the quantum phase transitions I discussed in microscopic models of strongly correlated systems. Nevertheless sufficiently close to a continuous quantum phase transition this approach is likely to give the correct universal behavior. However, the use of theories based on the breakdown of the FL state is problematic in the strong correlation regime. In addition, so far there is no microscopic model in which both nematic and stripe phases are known to occur. The existence of an electron nematic phase in a microscopic model of a strongly correlated system has only been shown for the strong coupling regime of the Emery model of the cuprates in the asymptotically low doping regime[106]. The existence of a metallic stripe phase in the same model for the doping range $x \sim 1/8$ has been suggested by a variational wave function (and hence mean-field in spirit) approach which projects out double occupancies of Cu sites [10, 184]. This suggests that the strongly coupled Emery model may more generally exhibit both nematic and stripe phases in its phase diagram. A number of publications have attempted to describe both stripe and nematic phases in Hubbard, $t - J$, and Emery models using slave-particle methods [215, 141, 214]. However, in spite of their widespread use in the field, slave-particle mean-field theories are notoriously unreliable.

It would be highly desirable to have high quality numerical simulations to address this problem in models of strongly correlated systems. Density matrix renormalization group (DMRG) calculations have provided

strong evidence for stripe correlations in Hubbard-type models on narrow strips (with up to 5 legs) [209, 29]. However, the geometry used in DMRG, which breaks the rotational invariance under 90° rotations of the square lattice explicitly makes it difficult to distinguish a stripe from a nematic phase. The same problem arises in finite-size diagonalizations of small systems. Quantum Monte Carlo simulations are less affected by such geometric limitations but suffer from the notorious fermion sign problem at low temperatures. QMC simulations have indeed shown an increase in nematic fluctuations at low temperatures in Hubbard type models (see a discussion in Ref. [29]) but, as far as I know, not yet in the Emery model.

Chapter 4

Fermi liquid properties of polarized dipolar Fermi systems

4.1 Introduction

Recent experimental advances toward the creation of degenerate fermionic rovibronic ground state polar molecules, such as ^{40}K^{87}Rb [153], and highly magnetic fermionic atoms, such as ^{53}Cr [74, 37], ^{167}Er [132], and ^{161}Dy or ^{163}Dy, present new avenues for realizing states of strongly correlated matter in ultracold atomic and molecular systems. A degenerate dipolar Fermi gas is more strongly coupled and has longer range interactions than other (neutral) atomic systems, and it is therefore reasonable to expect that these systems will exhibit novel and exotic behaviors. Recent theoretical studies have already explored BCS-like superfluidity in these systems (see Ref. [13] and references therein).

I explore the possible occurrence in homogeneously trapped dipolar systems of quantum nematic phases; phenomena heretofore only observed in strongly correlated electronic systems [98, 168, 198]. In a nematic state, which is the simplest example of quantum liquid crystal order [104], the fermionic gas becomes spontaneously anisotropic—without the action of an external field—while maintaining overall homogeneity. Nematic phases in fermionic fluids have been discussed in strongly correlated electronic systems, and have been shown to occur in models based on the breakdown of Fermi liquid (FL) theory at a Pomeranchuk instability [150]. Quantum liquid crystal phases were recently proposed to occur in highly magnetic atomic systems in optical lattices [167] and in population unbalanced Fermi gases [171].

I show in this work that a quantum nematic phase is possible in sufficiently strongly coupled, homogeneously trapped dipolar system. More specifically, I consider e.g., KRb and Dy, in a fixed external polarizing field pointing along the z-axis. Thus, I will not consider the interesting—but more complex—states that may arise in systems with a spin degree of freedom [219]. I consider an infinite and homogeneous 3D system in which the fermionic atoms or molecules interact via the dipolar interaction that, unlike r^{-6} contact interactions, has a long-range falloff $\propto r^{-3}$. In the presence of a polarizing field, the interaction itself becomes anisotropic in real space with a d-wave symmetry; the dipole-dipole interaction is repulsive or attractive depending on the spatial configuration of dipoles. Since the dipole-dipole interaction is explicitly anisotropic,

the Hamiltonian (and ground state) of the uniformly polarized dipolar system must have an explicitly broken rotational invariance, with the polarizing field providing the preferred axis. Nevertheless, the Hamiltonian is invariant under rotations about this fixed axis, and it is this remaining symmetry that is spontaneously broken in the nematic phase.

While dipolar Fermi gases with interactions in the particle-particle channel are well-studied [13, 220, 218, 27], the particle-hole (density) channel is relatively unexplored [140]. In the case of fermionic dipoles aligned by an external field, where the two-body dipole-dipole interaction is $V_d(\vec{r}) = (d^2/r^3)(1 - 3\cos^2\theta_r)$, d is the electric or magnetic dipole moment, and θ_r is the angle of the radial vector of relative position with respect to the z-axis, the explicit broken symmetry of the dipole-dipole interaction causes the coupling of even and odd orbital angular momentum channels [49]. More significantly for quantum liquid crystal physics, I show that an important feature of the dipole-dipole interaction in 3D is the presence of an effective attractive particle-hole interaction in the d-wave angular momentum channels. Such situations are of great interest, since the particle-hole d-wave channel interactions have been shown to trigger a Pomeranchuk instability [163] leading to a nematic phase of the Fermi liquid [150]. However, these phases are difficult to observe and study. In contrast, ultracold dipolar Fermi systems provide clean, experimentally realizable systems whose interactions in the, e.g., $l = 0$ and $l = 2$, angular momentum channels can be comparable by changing external parameters such as the polarizing field, trap aspect ratio, and contact interaction strength.

4.2 Generalized Landau parameters for fully polarized dipolar Fermi systems

I now apply Landau Fermi liquid (FL) theory to explore the particle-hole channel instabilities of a fully polarized dipolar system, and in doing so, reveal the possibility for observing a nematic state in the form of a spontaneous xy-symmetry breaking. The starting point of the Landau FL theory is the existence of a Fermi surface (FS) representing the ground state of the FL in the absence of quasiparticle excitations [18]. In a FL, fermionic quasi-particles have residual interactions in the forward scattering channel parametrized by a set of coupling constants, the Landau parameters of the FL. In a 3D system, such interactions can occur in any angular momentum channel. This standard picture—the Landau theory of the FL—is known to be a valid description for interacting Fermi system such as ^{3}He and most metals [18].

The order parameter of a nematic state is a traceless symmetric tensor [48]. In a 3D interacting Fermi system, such as the dipolar system, I can form a nematic order parameter as a bilinear of the Fermi fields, $Q_{ij} = \frac{1}{k_F^2}\psi^\dagger(\vec{x})\left(\partial_i\partial_j - \frac{1}{3}\nabla^2\delta_{ij}\right)\psi(\vec{x})$, which is both symmetric and traceless [150]. Here, $i, j = x, y, z$ and

$\psi(\vec{x})$ is the second quantized fermion operator at position $\vec{x}$. The 3×3 symmetric tensor Q_{ij} has two independent eigenvalues, Q_1 and Q_2. If $Q_1 = Q_2$, then the nematic state is *uniaxial*; otherwise it is *biaxial*. Since the Hamiltonian of the polarized dipolar system has an explicitly broken rotational invariance (due to the polarizing field), $Q_{ij} \neq 0$ in a uniaxial state. In this case, the FS of the gas is not spherically symmetric but must instead have (at least) a uniaxial distortion: the FS is an ellipsoid oriented along the direction of polarization. In a uniformly polarized dipolar system, polarization effects enter only through the anisotropy of the resulting interaction. Hence, the uniaxial distortion of the FS must be a (generally monotonic) function of the polarization. Indeed, Hartree-Fock calculations [140]—accurate in the weak coupling regime—have uncovered this uniaxial FS distortion of a polarized dipolar system.

Since the FS distortions are described by particle-hole condensation in specific angular momentum channels, the general tensor order parameter Q_{ij} can be recast in terms of its angular momentum components $u_{\ell,m}$:

$$u_{\ell,m} = \frac{1}{V} \sum_{\mathbf{k}} Y_{\ell,m}(\hat{\mathbf{k}}) \langle c^\dagger_{\mathbf{k}} c_{\mathbf{k}} \rangle, \tag{4.1}$$

where $c_{\mathbf{k}}$ is the Fourier transform of the Fermi field $\psi(\mathbf{x})$, $\ell > 0$ and $|m| \leq \ell$; $Y_{\ell,m}(\hat{\mathbf{k}})$ are the familiar spherical harmonics. Each order parameter $u_{\ell,m}$ measures a distortion mode of the Fermi surface. Among them, $u_{2,0}$ and $u_{2,2} = u^*_{2,-2}$ are of main interest, as they are order parameters for a uniaxial and biaxial nematic phase, respectively: $|u_{2,0}| \propto (Q_1 + Q_2)/2$ and $|u_{2,2}| \propto |Q_1 - Q_2|$.

Unlike the uniaxial state, which is present in a uniformly polarized dipolar system for all polarizing fields, the biaxial state is accessible only for fields of sufficient magnitude. Whether or not this phase exists in a given dipolar gas depends sensitively on the particular Landau parameters, which is reliably calculated numerically (by intensive quantum Monte Carlo simulations) or analytically in the weak dipole limit. The latter is defined by the condition that the dimensionless coupling constant $\lambda = d^2 n/\epsilon_F$ is small, where n is the particle density and ϵ_F is the Fermi energy. In current ultracold atomic and molecular gas experiments, densities are small $n \sim 10^{12}$ cm^{-3} compared to condensed matter, with temperatures limited to $T \gtrsim 0.1\, T_F$, where T_F is the Fermi temperature; i.e., $\epsilon_F = k_B T_F$. Our mean field analysis predicts that a biaxial phase may arise in dipolar systems for $\lambda \gtrsim 1$.

Consider a uniformly polarized dipolar system described by the Hamiltonian:

$$\hat{\mathbf{H}} = \sum_{\mathbf{k}} \epsilon_{\mathbf{k}} c^\dagger_{\mathbf{k}} c_{\mathbf{k}} + \frac{1}{2} \sum_{\mathbf{k},\mathbf{k}',\mathbf{q}} f(\mathbf{q})\, c^\dagger_{\mathbf{k}-\mathbf{q}} c_{\mathbf{k}} c^\dagger_{\mathbf{k}'+\mathbf{q}} c_{\mathbf{k}'}, \tag{4.2}$$

where

$$f(\mathbf{q}) = \frac{4\pi d^2}{3}(3\cos^2\theta_{\mathbf{q}} - 1) \tag{4.3}$$

is the dipole-dipole interaction in momentum space and $\theta_{\mathbf{q}}$ is the angle between $\mathbf{q}$ and $\hat{\mathbf{z}}$. Within the mean field (Hartree-Fock) approach, the Hartree term ($\mathbf{q} = 0$) does not contribute, since the average of $f(\mathbf{q})$ over a 4π solid angle is zero. The Fock term ($\mathbf{q} = \mathbf{k} - \mathbf{k}'$) can be expanded into angular momentum channels once the magnitudes of $\mathbf{k}$ and $\mathbf{k}'$ are set to the Fermi wave vector k_F (a good approximation in the low energy theory of a Landau FL):

$$f(\mathbf{k} - \mathbf{k}') = -\sum_{\ell,m;\ell',m'} f_{\ell,m;\ell',m'}(k_F, k_F^{'}) Y^*_{\ell,m}(\hat{\mathbf{k}}) Y_{\ell',m'}(\hat{\mathbf{k}}'). \tag{4.4}$$

The minus sign arises from its origin in the Fock term. The dimensionless coupling constants of this expansion, $F_{\ell,m;\ell',m'} = F_{\ell',m';\ell,m} = N(0) f_{\ell,m;\ell',m'}$ are the *generalized* Landau parameters, where $N(0)$ is the density of states at the FS. Because the rotational symmetry is broken by the polarization, Landau parameters $F_{\ell,m;\ell',m'}$ that mix different angular momentum channels enter in the Hamiltonian. For the dipole-dipole interaction of Eq. (4.3), the non-vanishing Landau parameters are

$$F_{\ell,m;\ell,m} = (-1)^m \frac{6\pi(\ell^2 + \ell - 3m^2)}{\ell(4\ell^3 + 8\ell^2 + \ell - 3)}\lambda, \text{ and} \tag{4.5}$$

$$F_{\ell+2,m;\ell,m} = (-1)^{m+1} \frac{3\pi}{2\ell^3 + 9\ell^2 + 13\ell + 6}\lambda \sqrt{\frac{[(\ell+1)^2 - m^2][(\ell+2)^2 - m^2]}{4\ell^2 + 12\ell + 5}}, \tag{4.6}$$

where $\lambda = nd^2/\epsilon_F$ is the dimensionless coupling constant. More generally, the $F_{\ell,m;\ell',m'}$ will be renormalized by interactions beyond the dipole-dipole interaction, such as the contact interaction, but rotational symmetry and space-inversion (or time-reversal) symmetry of the system enforce the selection rules $m = m'$ and $\ell - \ell' =$ even integers.

4.3 Uniaxial phase

The standard mean-field decoupling of the 4-fermion interaction using Eqn (4.4). The $f_{k,k'}$ are constants. This is exact only for $|k| = |k'|$

$$\hat{H}_{MF} = \sum_{\mathbf{k}} \left[\epsilon^0_{\mathbf{k}} + \delta\epsilon_{\mathbf{k}}\right] n_{\mathbf{k}} - \frac{V}{2} \sum_{n,m} f_{l,m;\, l',m'} u^*_{l,m} u_{l'm'}.$$

Where

$$\delta\epsilon_{\mathbf{k}} = \frac{1}{2} \sum_{l,m;\, l',m'} f_{l,m;\, l',m'} u^*_{l,m} Y_{l',m'} + c.c. \tag{4.7}$$

$$f(\mathbf{k},\mathbf{k}') = \sum_{l,m;l'm'} f_{l,m;\, l',m'}(k_F, k'_F) Y^*_{l,m}(\hat{\mathbf{k}}) Y_{l',m'}(\hat{\mathbf{k}}') \tag{4.8}$$

I called the coefficients defined $f_{l,m;\, l',m'}(k_F, k'_F)$, generalized Landau parameters. Note that due the anisotropic nature of the dipolar interaction these Landau parameters depend on the quantum number m and m' of the interacting particles. In particular note that

$$\begin{aligned} f_{20;00} &= -11.76 d^2 \\ f_{20;20} &= 7.51 d^2 \end{aligned}$$

$\epsilon_{\mathbf{k}} = \epsilon^0_{\mathbf{k}} + \delta\epsilon_{\mathbf{k}}$. In [166], a general central interaction potential is studied and the single particle dispersion is taken as a variational parameter which gives renormalizations to v^0_F(effective mass) at the undistorted FS such that Pomeranchuk instability in the $l = 1$ channel in prohibited, as it should, in a galilean invariant system. In our approach the Landau parameters are given and such a condition is recovered from the observation that the Landau parameter with $l = 1, 3, 5, .., m = 0$ are all coupled and positive. If a Pomeranchuck type of analysis is performed on a spherical FS I indeed find that because of the coupling of all channels to the $l = 1$ channel, none of them can become unstable because distortions are linear combinations of all $l = odd$ channels and would break rotational symmetry. I have verified this for the first 2 odd coupled channels.

To gain insight of the effect of the coupling between channels due to the dipolar interaction I first consider the lowest two coupled channels. The uncoupled version of this problem on a lattice was studied in Ref [216]. The interaction matrix has the form

$$\mathbf{F} = \begin{pmatrix} a & g \\ g & f \end{pmatrix} \tag{4.9}$$

where $g = -11.76\, d^2$, $f = 7.51\, d^2$. and hence the density $u_{00}/n \equiv (\sqrt{4\pi}) = \bar{u}_{00}$ =fixed and the $l = 2, m = 0$ density moment $u_{20} = (1/V) \sum_{\mathbf{k}} Y_{2,0}(\hat{\mathbf{k}}) \langle c^\dagger_{\mathbf{k}} c_{\mathbf{k}} \rangle$ are coupled. The quantity a is a parametrization of the hard core repulsion between dipoles and is set to zero at the end of calculation. The Hamiltonian is then Gaussian and yield the free energy density

$$\omega[u_{00}, u_{20}, \mu] \quad = \quad -\frac{T}{V} \sum_{\mathbf{k}} \log \left(1 + e^{-(\epsilon_{\mathbf{k}} - \mu)/T} \right) - \frac{1}{2} f_{00;00}\, u^2_{00} - f_{00;20}\, u_{00} u_{20} - \frac{1}{2} f_{20;20}\, u^2_{20} \tag{4.10}$$

Where the order parameters u_{lm} have to be calculated self-consistently since they enter the definition of $\epsilon_{\mathbf{k}}$ which depends on the value of the order parameters, Eqn. 4.7. The equilibrium configuration minimizes this free energy with respect to u_{20}. If the density is constant, there is a compromise between the 2nd term and 3rd term which favor and dis-favor a non-zero value of u_{20} respectively. Hence, in general, $u_{20} \neq 0$ for any finite value of the dipolar interaction g, d. This is because the dipolar interaction has a preferred direction of orientation 'built in'. I confirmed that to first order in perturbation theory in λ the self energy is, appendix B,

$$\Sigma(\mathbf{k}) \sim P_2(\cos\theta_{\mathbf{k}}) \tag{4.11}$$

This perturbative calculation gives, to this 1st order, no contribution to the total energy. Self-consistency is required. This means that the state with a $u_{20} \neq 0$ has the same energy as the system with undistorted Fermi surface, an indication of explicit broken symmetry.

I numerically confirmed the above conclusions solving for the stationary conditions of ω given by

$$\begin{aligned} \frac{\partial \omega}{\partial u_{20}} &= 0 \\ \frac{\partial \omega}{\partial u_{00}} &= 0 \\ \frac{\partial \omega}{\partial \mu} &= -n \end{aligned}$$

There is an extra condition I have to take into account at fixed density: $\partial\omega/\partial\mu = -n$. Explicit calculation

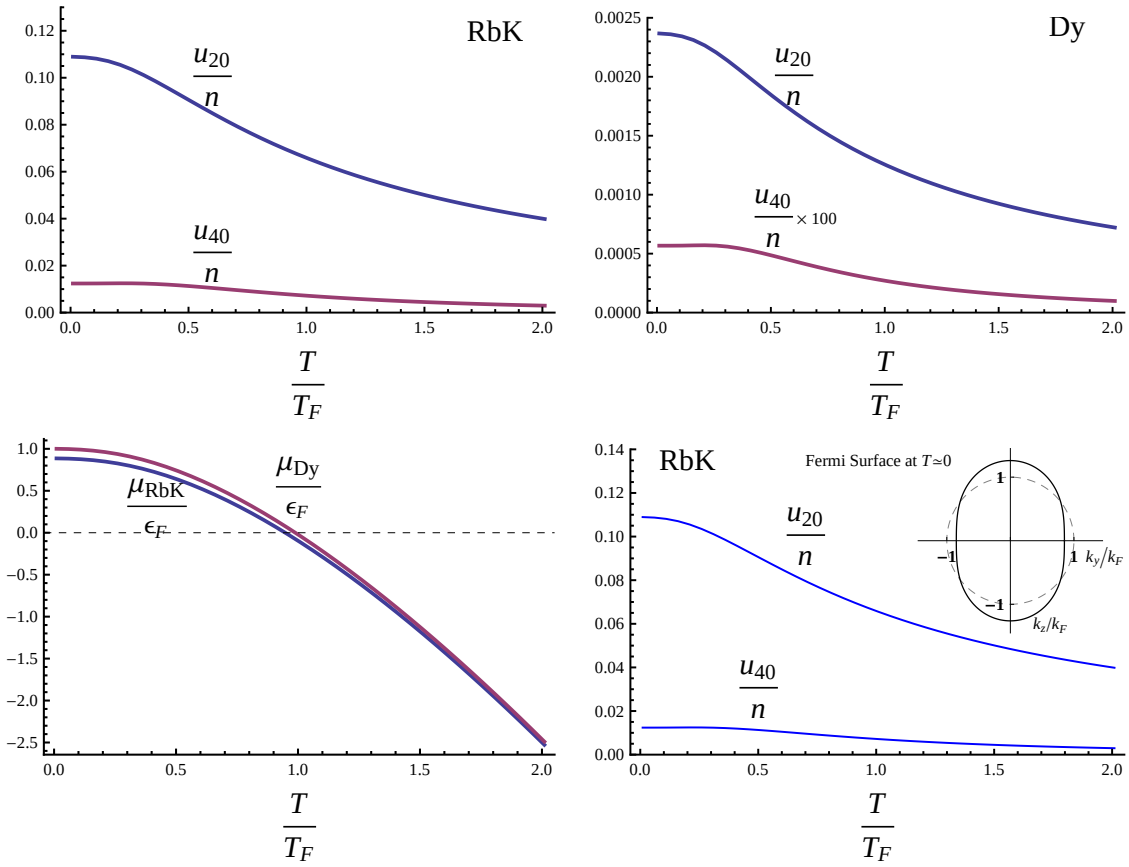

Figure 4.1: u_{20}/n, u_{40}/n and chemical potential vs temperature for fixed density. I chose as examples RbK and ^{163}Dy at $n = 10^{13} cm^{-3}$ which gives $\lambda_{Dy} \sim 0.006$ and $\lambda_{RbK} \sim 0.35$.

shows that if the matrix **F** is non-singular the solutions are unique and given at fixed density by

$$\begin{aligned} u_{00} &= \frac{1}{V}\sum_{\mathbf{k}} Y_{00}(\hat{\mathbf{k}}) f(\epsilon_{\mathbf{k}} - \mu) \\ u_{20} &= \frac{1}{V}\sum_{\mathbf{k}} Y_{20}(\hat{\mathbf{k}}) f(\epsilon_{\mathbf{k}} - \mu) \\ u_{40} &= \frac{1}{V}\sum_{\mathbf{k}} Y_{40}(\hat{\mathbf{k}}) f(\epsilon_{\mathbf{k}} - \mu) \end{aligned} \tag{4.12}$$

for the two unknowns $u_{20},\ u_{40}$ and μ.

$$\lambda = \frac{nd^2}{\epsilon_F} \tag{4.13}$$

$$n = 10^{13} cm^{-3} \tag{4.14}$$

$$\lambda_{Dy} \sim 0.006 \tag{4.15}$$

$$\lambda_{RbK} \sim 0.35. \tag{4.16}$$

I write the above equations in dimensionless form using the length scale given by the density. The question arises as to what is more meaningful as a measure of the dipolar strength. When the FS is spherical at $T = 0$ it is obviously nd^2/ϵ_F but at $T > 0$ ϵ_F is not well defined, $\mu(T)$ is the meaningful quantity, with $\mu(T = 0) = \epsilon_F$. The question is: should I use nd^2/μ?. This is reasonable because μ also changes as a function of the order parameter, $\mu(T, u_{20}, u_{40}, \cdots)$ and, as is well known, the thermodynamic chemical potential has always a well defined meaning(the energy cost to put an extra particle into the system) even for strongly interacting Fermi systems. Yet, I choose instead the density as the fundamental quantity and construct an energy scale based on that. First I define the "Fermi wave vector", k_F of an isotropic systems with the same density n.

$$n = \frac{k_F^2}{6\pi^2}$$

In atomic physics it is called "nominal" k_F. This defines an energy scale("Fermi energy")

$$\epsilon_F = \frac{\hbar^2 k_F^2}{2m}$$
$$T_F = \frac{\epsilon_F}{k_B}$$

I measure the dipolar coupling using the ratio nd^2/ϵ_F or according to the above definition

$$\lambda = n^{1/3} \frac{md^2}{\hbar^2} \frac{2}{(6\pi^2)^{2/3}} = n^{1/3} a_d \frac{2}{(6\pi^2)^{2/3}} = C_{dd} \frac{2}{(6\pi^2)^{2/3}}$$

where $a_d = md^2/\hbar^2$ is a characteristic length scale of the given dipole interaction. For a polar molecule which have permanent dipole moment this scale is a characteristic of its molecular structure. C_{dd} is also a measure of dipolar interaction used in the literature [189, 140]. Using these scales I write in dimensionless

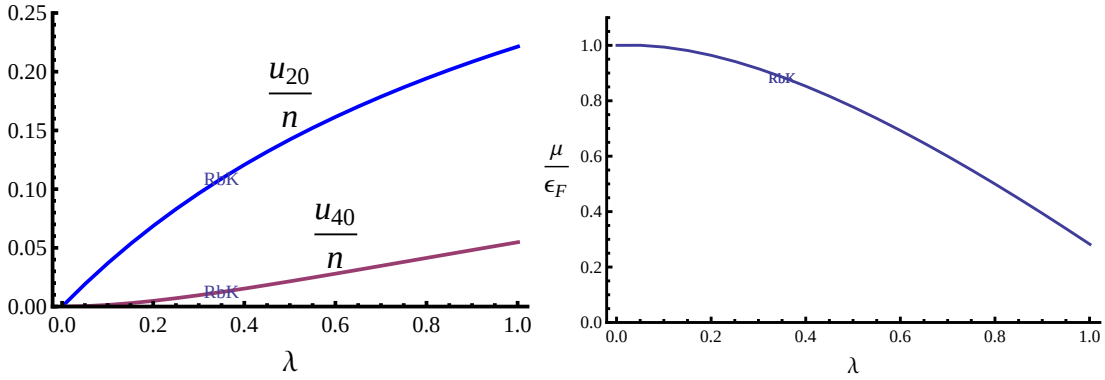

Figure 4.2: u_{20}/n, u_{40}/n and chemical potential μ/ϵ_F vs $\lambda = \frac{n^{1/3}md^2}{\hbar^2}(\frac{2}{(6\pi^2)^{2/3}})$ at $T/T_F = 0.01$. For Rbk at fixed density $n = 10^{13}cm^{-3}$ I have $\lambda_{RbK} \sim 0.35$. μ/ϵ_F decreases monotonically as a function of the dipolar interaction.

units

$$\begin{aligned}
\bar{u}_{00} &\equiv \frac{u_{00}}{n} = 6\pi^2 \int \frac{d^3\bar{k}}{(2\pi)^3} Y_{00}(\hat{\bar{\mathbf{k}}}) f\left(\frac{\bar{\epsilon}_{\bar{\mathbf{k}}} - \bar{\mu}}{\bar{T}}\right) \\
\bar{u}_{20} &\equiv \frac{u_{20}}{n} = 6\pi^2 \int \frac{d^3\bar{k}}{(2\pi)^3} Y_{20}(\hat{\bar{\mathbf{k}}}) f\left(\frac{\bar{\epsilon}_{\bar{\mathbf{k}}} - \bar{\mu}}{\bar{T}}\right) \\
\bar{u}_{40} &\equiv \frac{u_{40}}{n} = 6\pi^2 \int \frac{d^3\bar{k}}{(2\pi)^3} Y_{40}(\hat{\bar{\mathbf{k}}}) f\left(\frac{\bar{\epsilon}_{\bar{\mathbf{k}}} - \bar{\mu}}{\bar{T}}\right)
\end{aligned} \tag{4.17}$$

By definition $u_{00} = (1/\sqrt{4\pi})n$ where $n = (1/V)\sum_{\mathbf{k}} f(\epsilon_{\mathbf{k}} - \mu)$ is the density hence, $\bar{u}_{00} = 1/\sqrt{4\pi}$. n is externally specified independent parameter. Hence the ratio u_{00}/n is fixed. The bar in top of quantities means they are measured with respect to ϵ_F, k_F or T_F., e.g.,

$$\bar{\epsilon}_{\mathbf{k}} = (\frac{k}{k_0})^2 + \bar{g}\frac{d^2}{\epsilon_0} Y_{00}(\hat{\mathbf{k}})\bar{u}_{20} n = \bar{k}^2 + \bar{g}\lambda_0 Y_{00}(\hat{\mathbf{k}})\bar{u}_{20}$$

Recall that only at T=0 I can speak of a Fermi energy, since $\mu(T = 0) = \epsilon_F$. In general however that chemical potential decreases with T as in the ideal Fermi gas. This can be confusing since atomics physicist usually speak of Fermi energy. They mean $\mu(T)$. For $k_B T < \mu(T)$ I have $\mu(T) \approx \mu(T = 0) = \epsilon_F$ In Fig. 4.2 I show the dependence of u_{20} and u_{40} on the dipolar strength. For a molecule Dy and RbK at a density of $10^{13}cm^{-3}$ I have $\lambda \sim .35$ for RbK and $\lambda \sim .006$ for ^{163}Dy. In Fig. 4.1 I use parameters relevant to future experiments on dipolar Fermi gases systems. I found a variation of u_{20} vs T which is quadratic at small temperatures. This behavior is characteristic of all mean field theories, see Fig. 4.1, and comes from the

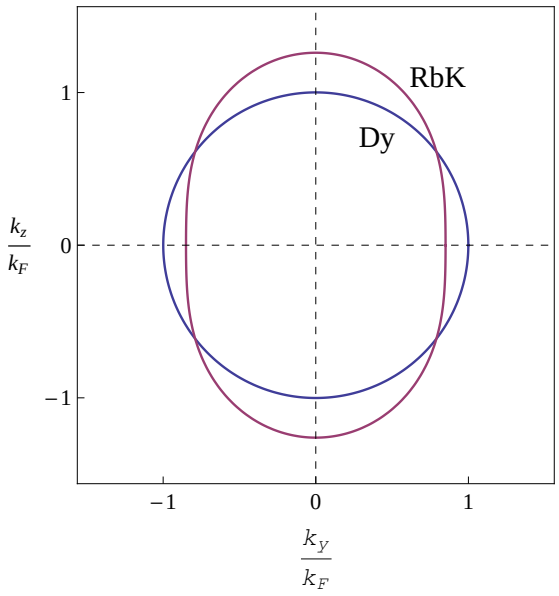

Figure 4.3: Cross section of the FS for Dy and RbK at density $10^{13}cm^{-3}$ where $\lambda_{Dy} = .006$ and $\lambda_{Dy} = .35$. The FS is determined by the k wave vectors satisfying: $\vec{k}/k_F = \sqrt{\mu - \delta\epsilon_{\vec{k}}}$. The temperature was $T/T_F = 0.01$.

gapless fermionic excitations close to the FS, as in standard Fermi liquid theory. As Temperature is increased u_{20} decreases. This is the expected behavior since at higher energies particles redistribute accordingly. The order parameters u_{20} and u_{40} does not vanish with increasing temperature. This is reminiscent of the behavior of the order parameter in a Heisenberg ferromagnetic in an external magnetic which explicitly breaks the rotational invariance of the system. The order parameter decreases monotonically and smoothly but it does not go to zero due to explicit present of the external field. Here, the fixed density acts as and external field due to the mixing all $l = even$ channels. To include $Y_{4,0}$ I need to solve self consistently, beside the above equations, $\bar{u}_{40} = 6\pi^2 \sum Y_{4,0} f((\bar{\epsilon}_k - \bar{\mu})/\bar{T})$. If λ is small $u_{40} \ll u_{20}$, Fig. 4.2. As the interaction increases u_{40} remains smaller than u_{20}, see Fig. 4.3.

4.4 Why does the Fermi surface deforms in fully polarized dipolar Fermi systems?

It is useful to have an intuitive picture that captures the essential physical elements of FS distortions and it is easy to remember. FS deformations due to dipole-dipole interactions can be explained at different levels of sophistication: a) by self-energy calculations, see appendix B. b) by appealing to the existence of an

"orbital source" which acts on the spin the degrees of freedom, see chapter 6. c) by the symmetry of the bare interaction which is invariant under $SO(2)$ rotations about the polarization axis. This argument shows that elliptically distorted FS are consistent with the symmetries of the base interaction. It however, does not tells whether the FS is prolate or oblate. d) by simple kinematics of a particle in an anisotropic potential plus Pauli principle. Here I focus on the last one.

Consider two particles allowed to move in one dimension, say, along x interacting with a position-dependent potential energy $U_x = d^2/r^3$. This mimics the interactions of two polarized dipoles in a plane perpendicular to the polarization axis. The total energy of a single particle, kinetic plus potential, is given by $\hbar^2 k_x^2/2m + d^2/r^3$. Now consider a Fermi gas of these particles. The Pauli principle prevents the collapse of such gas. I can give order of magnitude estimates of the kinetic and potential energy of a single particle in the gas. First note that on average, the separation between particles is $n^{-1/3}$ and hence $\left\langle r^{-3}\right\rangle = n$, the three dimensional density. Hence, on average, $\hbar^2 \left\langle k_x^2\right\rangle /2m + nd^2 = E$. Similarly if I consider a particle subject to move along z with the *same* total energy and a potential $U_z = -2d^2/r^3$. I obtain: $\hbar^2 \left\langle k_z^2\right\rangle /2m - 2nd^2 = E$. As I can be seen, particles moving along z have higher kinetic energy, on average, than those moving along x, i.e., $\left\langle k_z^2\right\rangle > \left\langle k_x^2\right\rangle$; simply because they feel lower, in fact negative, potential energy. Intuitively, particles along z go "down the hill" ($U_z = -2d^2/r^3$) while particles along x go "up the hill"($U_x = d^2/r^3$). In a three dimensional many-body Fermi system this means that the contours of constant energy in momentum space, i.e., the Fermi wave vector must be larger along z than along x. Subtracting the equations above I obtain

$$E_{Fz} - E_{Fx} \quad \sim \quad 3nd^2. \tag{4.18}$$

The difference in the Fermi energies, $\hbar^2 \left\langle k_{z,x}^2\right\rangle /2m$, along the z and x directions is proportional to the dipolar energy per particle. In a translational invariant system, $\mathbf{k}$ is a "good" quantum number. The FS, which concerns only with this quantum number and defined as the highest occupied energy level in $\mathbf{k}$-space, is usually decoupled from other good quantum numbers such as the quantum spin states. This is because, in many practical applications, the spin of particles is also, to high accuracy, a good quantum number. In the presence of dipole-dipole interactions I have shown that the spin state of the particles is not independent of the momentum $\mathbf{k}$- quantum number.

4.5 Biaxial phase

I now demonstrate the existence of a phase transition to a biaxial nematic state above a critical value of the coupling constant λ_c. The procedure consists of expanding the free energy, Eqn. 4.10, in $u_{2\pm 2}$ order

parameters and λ_c in perturbation theory. Theory is strictly valid only for $\lambda_c << 1$ and $u_{2\pm2} \to 0$. A caveat must be mentioned: a self-consistent variational calculation in the local density approximation does not find the biaxial state, see appendix C. Also, such a phase is not found in a numerical study as in section 4.3 by adding the self-consistent equations for $u_{2\pm2}$ order parameters in mean field theory. These methods, however, are valid only in the weak coupling regime. The biaxial phase is therefore not ruled out and its interesting properties, such as non-Fermi liquid behavior, merit its study.

The leading instability to the FS occurs in the $u_{2,\pm2}$ channels, which possess free-energy densities of

$$\frac{F}{V} = \Delta|u_{2,2}|^2 + g|u_{2,2}|^4 + \cdots , \tag{4.19}$$

and is independent of the phase φ_2 as expected by the xy azimuthal symmetry. In a small λ expansion and for $T \ll T_F$, the coefficients Δ and g are

$$\Delta = \frac{\sqrt{2}\pi^3\hbar^3}{7m^{3/2}\sqrt{\epsilon_F}}\lambda\left[1 - \frac{7\pi\lambda}{24}\left(1 - \frac{\pi^2T^2}{24T_F^2}\right)\right], \text{ and} \tag{4.20}$$

$$g = \frac{761\pi^{10}\hbar^9}{254592\sqrt{2}m^{9/2}\epsilon_F^{7/2}}\left(1 + \frac{1571\pi^2T^2}{3044T_F^2}\right)\lambda^4, \tag{4.21}$$

where m is the (effective) mass of the fermions. I only include the leading order contributions to Δ and neglect quantitatively important effects due to, e.g., mixing between different angular momentum channels such as $(2,0)$ and $(2,2)$. To go beyond the present order of approximation requires either extensive numerical computations or the extrapolation of a longer series expansion (e.g., by Padé approximants).

The sign of Δ dictates two different phases. For $\Delta > 0$, the FL phase with an uniaxial distortion ($u_{2,0}$) is stable, and $u_{2,\pm2} = 0$. For $\Delta < 0$ the system is in a biaxial nematic phase, with $|u_{2,2}| = \sqrt{\frac{|\Delta|}{2g}}$. For $\lambda < \lambda_c(T)$, $\Delta > 0$, and the uniaxial nematic phase discussed above is stable. For $\lambda > \lambda_c(T)$ (stronger dipole-dipole interaction), the free energy of Eq. (4.19) predicts a biaxial phase. The uniaxial-biaxial phase boundary, is $T/T_F = (2\sqrt{6}/\pi)\sqrt{1 - \lambda_c/\lambda}$, where $\lambda_c \simeq 24/7\pi$ and $T = 0$ is the QCP.

The biaxial state manifests as a FS distortion along two orthogonal axes, with the in-plane distortion given by $|u_{2,2}|$ and it spontaneously breaks the $SO(2)$ rotational symmetry of the system (up to in-plane rotations by π). Thus, the mean-field-theory description of the uniaxial-biaxial thermal phase transition does not give the correct critical behavior in 3D, which is in the universality class of the 3D classical XY model [34]. There is, however, one caveat for the present situation. In this nematic state, as in all nematics, the broken symmetry is not internal but the symmetry of spatial rotation [148] with a fixed axis. Unlike the classical XY model—which involves an internal symmetry—the topological defects of this biaxial phase are

disclination lines that cannot form closed loops. Although this effect does not change the critical behavior in 3D, it does affect the behavior of the biaxial state.

4.6 Collective modes and final remarks

The uniaxial phase is essentially a FL state with well defined quasiparticles and an explicit static spatial anisotropy. The Fermi velocity and the speed of (zero) sound vary along the "meridians" of the FS, as can be determined directly from the uniaxial distortion.

As the phase transition to the biaxial state is approached, much as in the 2D nematic state [150], the in-plane quadrupolar collective modes become gapless and overdamped, but only when propagating in the basal xy-plane. This becomes a Goldstone mode in the biaxial phase but remains gapped when propagating off-plane. This behavior is expected since this biaxial state develops in the presence of an external symmetry breaking field: the only spontaneously broken symmetry occurs in the rotations about the direction of polarization. In contrast, a full biaxial nematic should have two gapless Goldstone modes as it has two spontaneously broken continuous symmetries [48].

Beyond employing destructive density measurements via light absorption to measure FS distortions, I suggest the use of polarized light scattering [48] to detect the collective behavior of dipolar systems, since the nematic state behaves as a birefringent, anisotropic medium for light propagation. While this is a conceptually natural and direct way to access the collective mode spectrum of the nematic phase, experimentally it may be challenging to perform without destroying the nematic state. In particular, only small scattering signals may be present due to the need for limiting the atomic excited state population while interrogating the small trap population. Previous work has explored the amenability of Bragg scattering for structure factor measurements (see Ref. [201] and citations within),

Nematic Fermi fluids—in the absence of a background lattice or at quantum criticality—are a striking example of a "non-Fermi liquid," in the sense that the quasiparticles are generally broad and poorly defined [150, 136]. However, in the case of this biaxial state, the quasiparticles become broad and non-Fermi liquid-like only when they propagate in-plane due to the polarizing field. An exciting issue is the possibility for realizing a true biaxial nematic which would exhibit exotic defects known as non-Abelian disclination lines [161]. Such defects involve twisting polarization and have skyrmionic structure.

In the context of a dipolar system, a biaxial necessarily requires the polarization to be regarded as an order parameter, i.e., ferromagnetism. Thus, the biaxial phase of a dipolar system is more complex than in conventional liquid crystals. In the absence of a ferromagnetic phase of 3D dipolar systems, a

true biaxial phase may appear as a metastable state obtained by turning off the external polarization field. Homogeneously trapped dipolar systems are thus a natural setting to investigate the possible existence of quantum liquid crystal phases in Fermi fluids and will provide a fertile ground for explorations in non-Fermi liquid physics.

Chapter 5

Ferronematic phase

5.1 Introduction

Cold dipolar Fermi gases have attracted much attention due to the novel anisotropic and long-range character of dipole-dipole interactions. Recent studies of many-body effects predicted an elongated Fermi surface (FS) in a one-component fully polarized Fermi gas with dipolar interactions along the polarization direction established by an external field[140, 189]. A biaxial state with a critical value of the effective coupling constant $\lambda_d = n\mu^2/\epsilon_F$ was proposed in Ref. [68] (μ is the dipole moment of the fermion, n is the total density and ϵ_F is the Fermi energy of the free Fermi gas at the same density). It was found[68] that the system will exhibit violations of the Landau theory of the Fermi liquid both at quantum criticality and in the biaxial phase. More generally, understanding anisotropic non-Fermi liquid phases of cold atomic systems may shed light into the quantum liquid crystal phases in strongly correlated systems and high T_c superconductors [104, 150, 193].

The question I want to address here is whether a cold spin-$1/2$ Fermi gas with long range dipolar interactions can become spontaneously polarized and what is the nature of the broken symmetry state. The theory I present here is a generalization of the theory of the Stoner (ferromagnetic) transition in metals to take into account the effects of the long range and anisotropic dipolar interaction. As I will show below, much as in the theory of Stoner ferromagnetism, the polarized state can only occur for sufficiently large values of the magnetic dipole moment and/or of the spin-flip scattering rate. However, unlike what happens in Stoner ferromagnetism, as a result of the structure of the dipolar interactions, the resulting polarized state is also spatially anisotropic, a *ferro-nematic* state.

The *classical* version of this problem has been considered in mixtures of ferromagnetic particles with nematic liquid crystals[25], and in dipolar colloidal fluids and ferrofluids[185]. Classical dipolar fluids have complex phase diagrams, typically featuring inhomogeneous phases with complex spacial structures. Much less is known about their quantum counterparts. In the case of simple quantum fluids, such as ^{3}He, the dipolar interaction plays a very small role compared to the short-range exchange interaction[61]. In the

context of ultracold gases, a number of atomic and molecular systems with strong dipolar interactions, such as Dysprosium, have been the focus of recent experiments.

5.2 Model Hamiltonian

Consider a restricted Hilbert space of two hyperfine states, called 1 ("spin up") and 2 ("spin down"), of a point-like magnetic atom of mass m and magnetic moment, $\mathbf{M}$, with components $M_i = \mu\sigma^i$, where $i = 1, 2, 3$ and σ^i are the usual spin-1/2 Pauli matrices. In our notation the factor of $\hbar/2$ is absorbed in the definition of μ. The Hamiltonian is

$$\begin{aligned} \hat{H} &= \int d^3x \psi^\dagger_\alpha(\mathbf{x}) \left(-\frac{\hbar^2\nabla^2}{2m}\right) \psi_\alpha(\mathbf{x}) \\ &+\frac{1}{2}\int d^3x\ d^3x \psi^\dagger_\alpha(\mathbf{x})\psi^\dagger_\beta(\mathbf{x}')U_0(\mathbf{x},\mathbf{x}')_{\alpha\alpha';\beta\beta'}\psi_{\beta'}(\mathbf{x}')\psi_{\alpha'}(\mathbf{x}) \end{aligned} \tag{5.1}$$

where the fields $\psi_\alpha(\mathbf{x})$ destroy fermions on spin state with z-component $\alpha = 1, 2$ at position $\mathbf{x}$. I consider the model interaction is of the form

$$U_0(\mathbf{x},\mathbf{x}')_{\alpha\alpha';\beta\beta'} = \frac{\mu^2}{r^3}\sigma^i_{\alpha\alpha'}(\delta_{ij} - 3\hat{\mathbf{r}}_i\hat{\mathbf{r}}_j)\sigma^j_{\beta\beta'} + g\,\delta_{\alpha\alpha'}\delta_{\beta\beta'}\delta(\mathbf{r}) \tag{5.2}$$

where $\mathbf{r} \equiv (\mathbf{x} - \mathbf{x}')/|\mathbf{x} - \mathbf{x}'|$ and $\hat{\mathbf{r}}$ is a unit vector in the direction of $\mathbf{r}$. The last term in Eq.(5.2) represents the short-range isotropic interactions. It only affects the spin-triplet channel and I denote by g the associated coupling constant. The Fourier transform of the bare two body interaction is $(4\pi\mu^2/3)\sigma^i_{\alpha\alpha'}(3\hat{\mathbf{q}}_i\hat{\mathbf{q}}_j - \delta_{ij})\sigma^j_{\beta\beta'} + g\delta_{\alpha\alpha'}\delta_{\beta\beta'}$. The Hamiltonian is invariant under *simultaneous* $SU(2)$ transformations in spin space and $SO(3)$ rotations in real space.

The ferro-nematic state breaks simultaneously the rotational invariance in spin space and in real space of the Hamiltonian, and its order parameters reflect this pattern of symmetry breaking. The order parameters are: a) the local magnetization vector M_a $(a = x, y, z)$ that measures the spin polarization, b) the nematic order parameter, a 3×3 symmetric traceless matrix, Q_{ij} $(i, j = x, y, z)$ that measures the breaking of rotational invariance in space, and c) the generalized "nematic-spin-nematic" order parameter Q^{ab}_{ij}, a tensor symmetric and traceless on the spatial $(i, j = x, y, z)$ and spin $(a, b = x, y, z)$ components, that measures the breaking of both symmetries [3]. General order parameters of the latter (nematic-spin-nematic) type were considered by Wu *et. al.* [212] who gave a detailed description in 2D systems and partially in 3D systems. The ferro-nematic state has an unbroken uniaxial symmetry in real space. It is a 3D generalization of the quadrupolar α of Ref.[212].

An intuitive way to describe these phases in a Fermi system is in terms of spontaneously deformed Fermi surfaces (FS)[150, 212, 68]. A ferromagnetic state is isotropic in real space and has a spherical FS of unequal size for both spin polarizations. The nematic phase is isotropic in spin space, and its FS has a uniaxial distortion in real space, with the up and down spin FS being identical in shape and size. For small values of the order parameter, the distorted FS are ellipsoids with an eccentricity determined by the magnitude of the order parameter. Due to the anisotropy of the dipolar interaction, a ferromagnetism causes the FS to distort, thus driving the system into an uniaxial nematic state. Since the state is ferromagnetic, the up (down) FS is a prolate(oblate) revolution ellipsoid. Both FS are collinear, and have unequal distortion and volume. Hence, the nematic-spin-nematic order parameter Q_{ij}^{ab} has a finite value. I find that all three order orders are present even for arbitrary small values of the dipolar coupling, where the ferromagnetic is the strongest, the nematic intermediate, and the nematic-spin-nematic the weakest.

5.3 Ferronematic ansatz and phase diagram

I make a variational ansatz of the wave function of the form of a Slater determinant describing a state in which the spin up and down Fermi surfaces are spontaneously deformed away from their non-interacting spherical shape, much as in the Hartree-Fock description of the nematic Fermi fluid[150]. Since I am interested in magnetism I allow for the volume of the up and down Fermi surfaces to change as well. This results in a Thomas-Fermi-like distribution function of fermions in momentum space with 4 variational parameters, k_{F1}, k_{F2} α_1 and α_2. I keep the total particle density $n = n_1 + n_2$ fixed,[140, 189]

$$n_{\sigma\mathbf{k}} = \Theta\Big(k_{F\sigma}^2 - \alpha_\sigma^{-1}(k_x^2 + k_y^2) - \alpha_\sigma^2 k_z^2\Big) \tag{5.3}$$

where $\Theta(x)$ is the step function and $\sigma = 1, 2$. If $\alpha = 1$ the FS of are spheres. It has the property that $V^{-1}\sum_{\mathbf{k}} n_{\sigma\mathbf{k}} = k_{F\sigma}^3/(6\pi^2) \equiv n_\sigma$, *i.e.* the total density does not depend on the distortion parameters, α_σ. Computing the energy in Hartree-Fock I obtain an expression for the ground state energy density in terms of the distribution functions of spin up and down particles $n_{\sigma,\mathbf{k}} = \langle c_{\sigma\mathbf{k}}^\dagger c_{\sigma\mathbf{k}}\rangle$, and $\sum_{\mathbf{k}} n_{\sigma,\mathbf{k}} = N_\sigma$,

$$\mathcal{E}_{int} \;\; = \;\; g\, n_1 n_2 + \frac{2\pi\mu^2}{3V^2}\sum_{\mathbf{k},\mathbf{k}'}(1 - 3\cos^2\theta_{\mathbf{k}-\mathbf{k}'})\big(n_{1\mathbf{k}'}n_{1\mathbf{k}} - 2n_{1\mathbf{k}'}n_{2\mathbf{k}} + n_{2\mathbf{k}'}n_{2\mathbf{k}}\big) \tag{5.4}$$

Computing the integrals I obtain the total energy *density* given by $\mathcal{E} = \mathcal{E}_{kin} + \mathcal{E}_{int}$ where

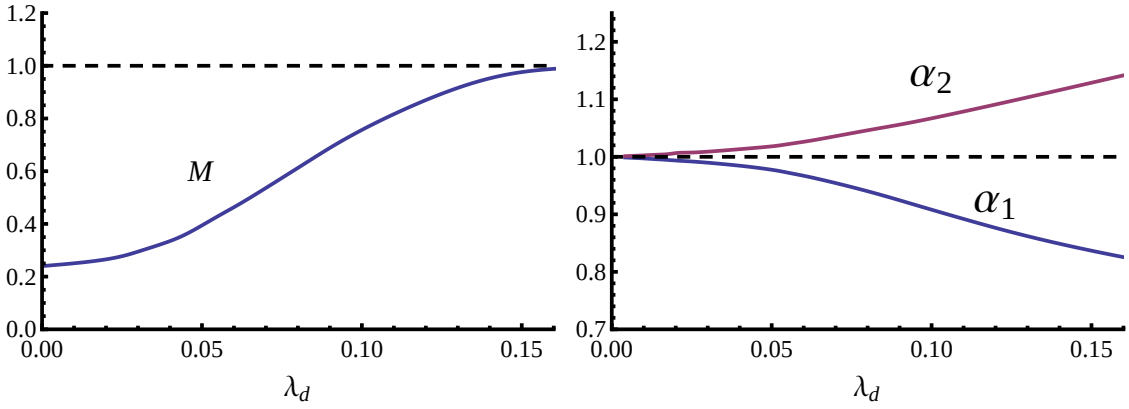

(a) Magnetization (b) FS distortions

Figure 5.1: Magnetization M and Fermi surface distortion parameters α_1 and α_2 vs the dimensionless dipolar coupling λ_d for an s-wave coupling $\lambda_s = 1.34$.

$$\begin{aligned}
\mathcal{E}_{kin} &= \frac{C_1\hbar^2}{3m}\left[n_1^{5/3}\left(2\alpha_1+\frac{1}{\alpha_1^2}\right)+n_2^{5/3}\left(2\alpha_2+\frac{1}{\alpha_2^2}\right)\right] \\
\mathcal{E}_{int} &= gn_1n_2-\frac{\pi\mu^2}{3}\left[n_1^2I(\alpha_1)-2n_1n_2\,I(\alpha_1,\alpha_2,M)+n_2^2I(\alpha_2)\right]
\end{aligned} \tag{5.5}$$

where $C_1 = (3/10)(6\pi^2)^{2/3}$, and $I(\alpha_1,\alpha_2,M)$ and $I(\alpha) = I(\alpha,\alpha,M)$ are given by

$$\begin{aligned}
I(\alpha_1,\alpha_2,M) &\equiv \frac{9}{8\pi^2}\int d^3k_1d^3k_2\,\Theta\left(1-\alpha_1^{-1}(k_{1x}^2+k_{1y}^2)-\alpha_1^2k_{1z}^2\right) \\
&\times\ \Theta\left(1-\alpha_2^{-1}(k_{2x}^2+k_{2y}^2)-\alpha_2^2k_{2z}^2\right)\left(3\cos^2\theta_{r\mathbf{k}_1-\mathbf{k}_2}-1\right) \\
I(\alpha) &= -2-\frac{6}{\alpha^3-1}-\frac{3\arccos\alpha^{3/2}}{(\alpha^{-1}-\alpha^2)^{3/2}}
\end{aligned} \tag{5.6}$$

where $M \equiv (n_1-n_2)/n$. Using that n_1 and n_2 are given by $n_1 = n(1+M)/2$, $n_2 = n(1-M)/2$, and that the ratio of the undistorted Fermi surface volumes is $r^3 = k_{F1}^3/k_{F2}^3 = (1+M)/(1-M)$, the total energy $\mathcal{E}$ becomes

$$\begin{aligned}
\frac{\mathcal{E}}{\mathcal{E}_0} &= \frac{1}{6}\left[(1+M)^{5/3}\left(2\alpha_1+\frac{1}{\alpha_1^2}\right)+(1-M)^{5/3}\left(2\alpha_2+\frac{1}{\alpha_2^2}\right)\right] \\
&\quad -\frac{5\pi}{36}\lambda_d\left[(1+M)^2I(\alpha_1)-2(1-M^2)I(\alpha_1,\alpha_2,M)+(1-M)^2I(\alpha_2)\right] \\
&\quad +\frac{5}{12}\lambda_s(1-M^2)
\end{aligned} \tag{5.7}$$

where $\mathcal{E}_0 = (2C_1\hbar^2n^{5/3})/(2^{5/3}m)$. Numerically minimizing the energy I obtain the phase diagram in the parameters λ_s and λ_d of Fig. 5.3. The phase diagram shown in Fig. 5.3 exhibits a ferro-nematic phase and a paramagnetic phase, separated by a phase boundary consisting of a line of 1st order transitions that

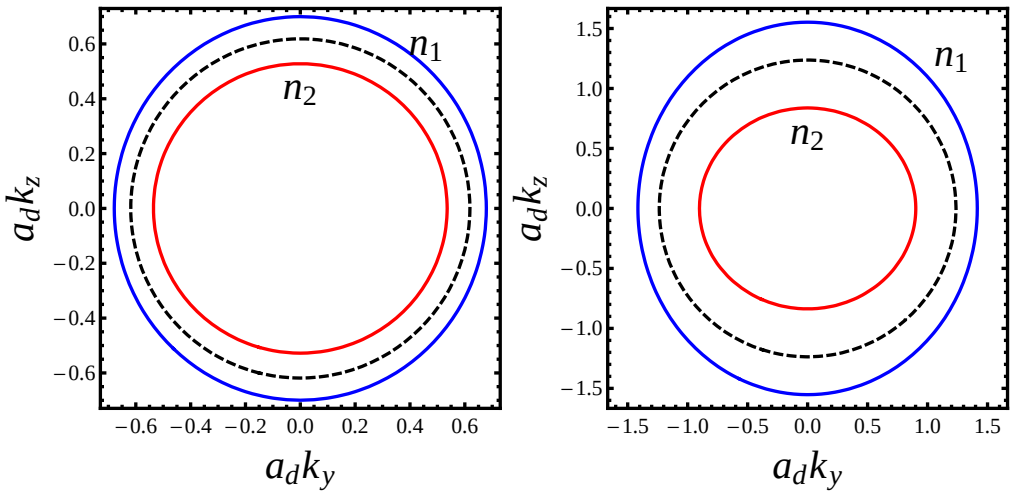

(a) $\lambda_s = 1.34$, $\lambda_d = 0.04$

(b) $\lambda_s = 1.34$, $\lambda_d = 0.08$

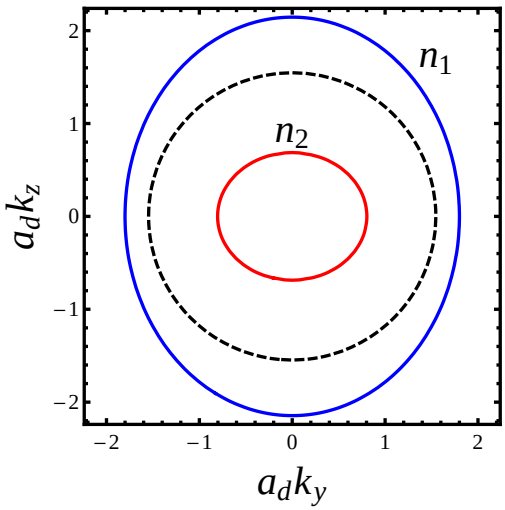

(c) $\lambda_s = 1.37$, $\lambda_d = 0.10$

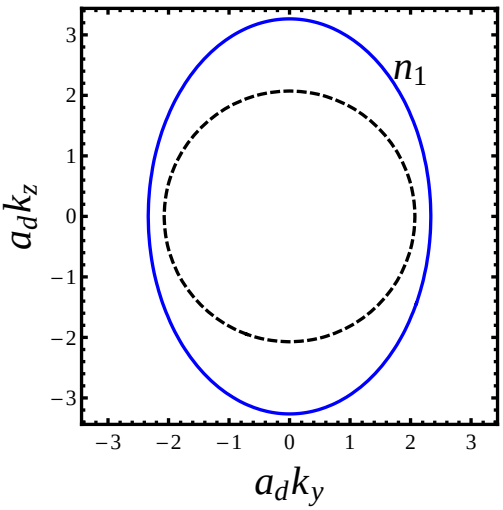

(d) $\lambda_s = 1.37$, $\lambda_d = 0.14$

Figure 5.2: a-d: Spin up and down FS, labeled by n_1 and n_2, for several values of λ_s and λ_d and fixed particle density n. $a_d = m\mu^2/\hbar^2$ is the dipole-dipole interaction length scale. Dashed lines: Free fermion FS.

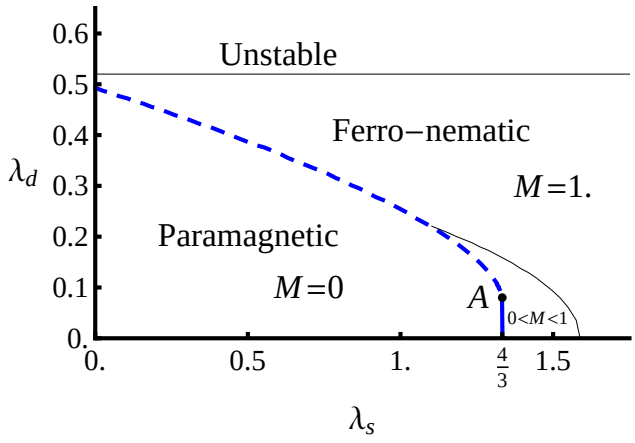

Figure 5.3: Phase diagram as a function of $\lambda_s = gn/\epsilon_F$ and $\lambda_d = n\mu^2/\epsilon_F$. It has a paramagnetic phase ($M = 0$), and a ferro-nematic phase with partial ($0 < M < 1$) and full polarization ($M = 1$). The phase boundary has a line of 1st order phase transitions (dashed) which turns into a line of continuous phase transitions (full) at the tricritical point A.

meets a line of continuous transitions at a tricritical point (labeled by A.) As expected the ferro-nematic state becomes more accessible as the s-wave coupling increases. This phase is fully polarized ($M = 1$) for much of the phase diagram, except for a small region where the polarization is partial, $0 < M < 1$. In the ferro-nematic phase with partial polarization the up and down Fermi surfaces are unequally distorted, while in the fully polarized regime only one distorted up FS exists. The conventional Stoner transition occurs at $\lambda_d = 0$ and $\lambda_s = 4/3$, where the up and down FS become distorted even for arbitrarily small values of the dipolar coupling (see Fig. 5.1.) From the structure of the the free energy for small values of $Q_1 = \alpha_1 - 1$, $Q_2 = \alpha_2 - 1$ and M (valid in the vicinity of the continuous transition) It can be seen that the dipolar interaction leads to a leading term of the form $M(Q_1 - Q_2)$, which is invariant under $1 \leftrightarrow 2$. Since the ferromagnetic state is already favored by the contact term, this term also favors $Q_1 < 0$ and $Q_2 > 0$.

In the ferro-nematic phase the $SU(2)$ spin symmetry of the Hamiltonian is broken down to the residual $U(1) \cong SO(2)$ invariance of this uniaxial state. The equilibrium FS of the up and down spin components are shown in Fig. 5.2 for several values of of the coupling constants. Both FS's are invariant under $SO(2)$ rigid rotations about $\mathbf{M} = M\hat{\mathbf{e}}_z$.

5.4 An intuitive picture

Prolate and oblate FS can be explained in several ways. The simplest is to consider single particle energy levels. In mean field theory one can think of the average local magnetic field produced by the rest of the particles. Because of its vectorial nature, spins up modify their single particle energy levels as explained in

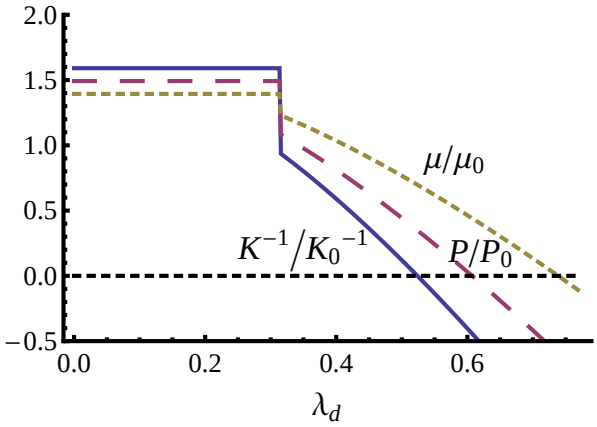

Figure 5.4: Pressure (broken), bulk compressibility (full) and chemical potential (dashed) (normalized to their values at the non-interacting Fermi gas) vs the dimensionless dipolar coupling λ_d, for $\lambda_s = 0.8$. The discontinuity in the thermodynamic quantities signals a 1st order phase transition from the paramagnetic state to the Ferro-nematic state. The gas becomes formally unstable to collapse when $K^{-1}/K_0^{-1} < 0$ at $\lambda_d \simeq 0.52$.

section 4.4. In particular, due to anisotropy on the potential energy the majority spin FS elongates along the net polarization of the system. Spins down, however, "see"the inverted field and hence have the sign switched. This leads to oblate FS. Note also that the bare two-body dipolar interaction changes sign if one flips one of the interacting spins. One crucial fact is left out: dipole-dipole interaction can flip spin of one of the two interacting particles, see chapter 6. I will show that these correlation effects cause the spin to become linear combination of eigenstates of σ^z and hence one can no longer define FS for the each eigenstate independently.

5.5 Pressure, bulk modulus and chemical potential

The total energy, the equilibrium values of the FS distortions and the magnetization are functions of the particle density $n = N/V$. The pressure $P = -(\partial E/\partial V)_N$, chemical potential $\mu = (\partial E/\partial N)_V$ and the compressibility $K^{-1} = n(\partial P/\partial n)$ can be computed straightforwardly with these equations. The characteristic behavior on the pressure chemical potential and inverse compressibility is monotonically decreasing as the dipolar coupling increases, see Fig. 5.4. The compressibility becomes negative at a critical dipolar coupling $\lambda_d^c \simeq 0.52$ (as in the case of the fully polarized dipolar Fermi gas[189, 4]) where it becomes formally unstable to collapse. In current experiments on cold atoms it is possible to prepare a two-component Fermi gas out of the hyperfine manifold of the atom. One can imagine, a two-component dipolar Fermi gas made out of, say, the hyperfine manifold of strongly magnetic atom such as Dy. With a density of

10^{13}cm^{-3}, I find $\lambda_{d,^{163}Dy} \simeq 0.01$. The recent experimental observation of itinerant (Stoner) ferromagnetism in ultracold gases of ^{6}Li atoms[96] opens the possibility to detect the ferronematic state in the laboratory possibly by tuning the s-wave scattering amplitude. Depending on the strength of the dipole moment and of the s-wave coupling, the FS for the two components may differ considerably from the spherical shape, and free expansion experiments may be able to provide signatures of this state. Ferromagnetism in cold dilute systems interacting only by s-wave contact pseudo-potential has been difficult to observe as the spin states of fermions are conserved separately on the time scales of the experiments[54]. However, a ferronematic state which may also exhibit other anisotropic and inhomogeneous phases could be set up experimentally in systems with a population imbalance of hyperfine states. Since the difference in energy between hyperfine levels is large compared to the dipole energies we expect the spins to be long-lived on time scales of the experiment. However there will be a small Zeeman field due to the difference in particle number with distinct spin projections; I am currently studying the effects of this field.

In actual experiments the trap potential maybe weakly anisotropic anisotropic. We now estimate the order of magnitude energy due to trap anisotropy and compared to the average order of magnitude estimate of dipole-dipole energy. If the former is smaller we expect effects of dipole anisotropy to play a small role. From this we derive an estimate of the maximum trap anisotropy. The anisotropic trap potential can be written in the form

$$U_{trap}(r) = \frac{1}{2}m\omega^2(\kappa\rho + \frac{z^2}{\kappa^2})$$

where κ is a measure of the trap anisotropy and we defined it as $\kappa = (\omega_\rho/\omega_z)^{2/3}$. $\kappa = 1$ means the trap is a perfectly spherical. We defined $\omega = (\omega_\rho^2\omega_z)^{1/3}$ as the geometric mean of the anisotropic trap frequencies. In order or magnitude estimates we set the lengths to the characteristic length scale of the trap $R = (\hbar/m\omega)^{1/2}$ then

$$E_{trap} = \frac{1}{2}m\omega^2(\kappa\rho + \frac{z^2}{\kappa^2}) \sim \hbar\omega(\kappa + \frac{1}{\kappa^2})$$

We want the energy due to *anisotropy* to be small compared to the energy due dipole-dipole interaction which is $E_{dipole} \sim n\mu^2$, i.e.

$$\hbar\omega(\kappa + \frac{1}{\kappa^2}) - 2\hbar\omega < n\mu^2 \tag{5.8}$$

note that if $\kappa = 1$, the left-hand side vanishes which just means that the energy due to *anisotropy* is zero(

of course, the energy of due to the trap is still there). In experiments it is possible to archive $n\mu^2/\hbar\omega \sim 1$ or even higher. This was discussed by Sogo and Miyakawa[140, 189] for the one-component dipolar Fermi gas. Moreover the phases that we are interested happened around the strongly interacting regime. Assuming that this order of magnitude number we obtain $\kappa \approx 3$. This means that the maximum anisotropy is

$$\omega_\rho/\omega_z \approx 5 \tag{5.9}$$

Real experimental anisotropies are much smaller and hence the dipole-dipole effects are robust against possible trap anisotropies. However, this argument is pure energetics and other surface effects at the boundaries may play a role due to the long-range nature of the dipolar interaction. This effects are currently being investigated. It is likely that the anisotropy acts as a weak symmetry breaking field, that orients the ferronematic order.

In this work I have shown the existence a new phase of matter, the ferro-nematic Fermi fluid, a ground state of a dipolar Fermi gas with short range interactions with a spontaneous magnetization and long range orientational order. In this state the up and down FS manifolds have unequal shapes and volumes. Since rotational invariance in real space and in spin space is simultaneously spontaneously broken in this state, it supports a rich spectrum of Goldstone excitations. As a result the fluid is an optically anisotropic medium whose effects that may be detected by light scattering experiments.

Chapter 6

Imbalanced Fermi systems with magnetic dipolar interactions

6.1 Introduction

Here I study the magnetic structure of the ground state of an itinerant Fermi system of spin-1/2 particles with dipolar interactions in a partially polarized state. I determine the distribution of quasiparticle spins states. The spin quantization axis is not along the spin magnetization axis but develops instead "spin textures" in momentum space. I computed the shape of the Fermi surfaces, and the effective magnetic moment of the quasiparticles, at zero temperature and weak coupling. I discuss realizations of this state with ultracold magnetic atoms.

Interest in dipole-dipole interactions arise due to the long range and anisotropic nature of dipolar forces. If the dipolar Fermi gas is fully polarized the anisotropic form of the interactions leads to a distortion of the Fermi surface (FS) [140] and to a mixing of the collective excitations due to the structure of the Fermi liquid parameters.[68] Although this system can be described in terms of the standard Landau theory of the Fermi liquid[18] important changes are needed to account for the effects of the dipolar forces.[68, 174, 36, 122] Recent theoretical work has revealed that gases of dipolar Fermi atomic systems can exhibit interesting and unconventional properties, including novel ordered quantum liquid crystal states, such as biaxial nematic and ferronematic phases[68, 67]. Quantum liquid crystal phases have been conjectured to play an important role in the physics of strongly correlated systems and high T_c superconductors.[104] Recent experimental progress in trapping strongly magnetic dipolar Fermi gases in magnetic traps opens the way to simulate these interesting physical systems in the laboratory.[125]

Dipolar Fermi systems where spin degrees of freedom are allowed to play a dynamical role [68, 187, 212] are much less studied. Magnetic dipole-dipole interactions, unlike electric dipole-dipole interactions, conserve total angular momentum, spin + orbital ($\mathbf{J} = \mathbf{L} + \mathbf{S}$),[160], and hence mix the spin and orbital degrees of freedom. Interactions in dense nuclear matter with non-central forces are similar. In fact, many of the above effects have been studied theoretically in the nuclear physics literature.[152] and references therein.

In this work I consider, in perturbation theory, the effects of *magnetic* dipolar forces on a spin-1/2 Fermi

system with a population imbalance of particles originally in eigenstates of σ^z(z-Pauli matrix), corresponding to a partially polarized ferronematic state.[68]. To 1st order in the interaction, the quantization axis is not along $\hat{\mathbf{z}}$ and hence spin textures in *momentum space* develop. Such a system can be simulated experimentally with two hyperfine levels of a strong fermionic magnetic atom such as Dy^{163} in an optical trap.[125]. I define the dipolar interaction parameter as $\lambda = \bar{n}\mu_0^2/\bar{\epsilon}_F$, where μ_0 is the magnetic moment of particles, $\bar{n} = \bar{k}_F^3/(3\pi^2)$ and $\bar{k}_F$ is defined by the average chemical potential $\bar{\mu} = (\mu_1 + \mu_2)/2 = \bar{\epsilon}_F = \hbar^2\bar{k}_F^2/2m$. Our calculations are to first order in λ, but the physical principles I describe are quite general. I do not consider here important questions such as pairing effects, collapse instabilities[65], temperature or optical trap effects. The physics I describe does not rely on trap parameters; such effects can taken into account using Thomas-Fermi functionals.[173]. Collapse instabilities will be considered in a future work; Collapse instabilities require a finite dipolar coupling strength[67] whereas the phenomena I study occurs for infinitesimal dipolar couplings.

Before presenting the details I summarize the physical picture that emerges as follows. A fixed population difference of particles in the eigenstates of σ^z acts, for static effects, as a uniform external magnetic field along $\hat{\mathbf{z}}$. Then the interaction conserves conserves the z-projection of the total angular momentum $J_z = L_z + S_z$. $\hat{\mathbf{z}}$ is the unperturbed spin quantization axis. Recall that $L = 2$ for the dipole-dipole interaction[160] and that, unlike contact, Coulomb or exchange interactions, it can flip the spin of one of the two interacting particles, the angular momentum being taken from the orbital degrees of freedom. In a many-body single-particle picture, this means that the mean field acting on the quasiparticle is not a scalar but a $\mathbf{k}$-dependent vector field, i.e., a "magnetic" field, which necessarily is not along $\hat{\mathbf{z}}$. Intuitively, consider a Bloch sphere on which a spin-1/2 is pictorially represented, Fig. 6.1; An external magnetic field is applied and is at a Θ angle with respect to the spin. Measurement of the spin state of the particle will yield $|\uparrow\rangle$ with probability $\cos^2\Theta/2$ or $|\downarrow\rangle$ with probability $\sin^2\Theta/2$. The two-body dipole-dipole interaction can mimic just this behavior, namely, one of the two spins can be flipped, the missing angular momentum being borrowed from the orbital angular momentum. This is confirmed by calculation of the single particle energy Eqn. 6.5 Since the spin quantization axis is not parallel to the polarization direction $\hat{\mathbf{z}}$, the $\mathbf{k}$-dependent spin state of particles becomes a linear combinations of eigenstates of σ^z, i.e., the spins tilts. Interestingly, neither the tilting angle nor the momentum distribution of the quasiparticles are isotropic in momentum space, and vary with direction as $\sim |Y_{2\pm1}(\hat{\mathbf{k}})|$ and $Y_{20}(\hat{\mathbf{k}})$ respectively because of the spin-orbit coupling. This can be described in perturbation theory as arising from two processes: a) $|\uparrow\rangle \to |\uparrow\rangle$ (no spin flip), with $\Delta L_z = 0$; since I consider particles with no internal structure, the orbital distribution of quasiparticles acquires a correction to its spherical shape of the form $Y_{20}(\hat{\mathbf{k}})$. b) $|\uparrow\rangle \to |\downarrow\rangle$ (spin flip) with $\Delta L_z = \mp 1$,

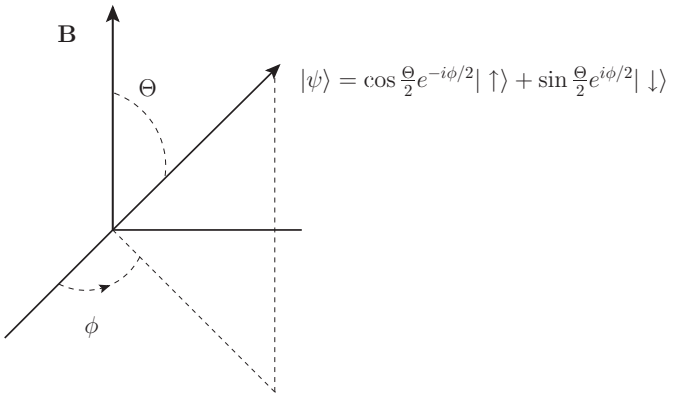

Figure 6.1: Spin-1/2 in an external magnetic field and analogy with an external molecular field due to dipole-dipole interaction.

the quasiparticle self-energy gets a correction of the form $|Y_{2,\pm1}(\hat{\mathbf{k}})|$. Therefore the self-energy now has an off-diagonal momentum-dependent component. These changes in the structure of the self-energy lead to qualitative modifications to the quasiparticle distribution functions and of the Fermi surface. In particular *it is no longer possible to define separate Fermi surfaces for up and down fermions independently.*

If and only if one were to ignore spin-flip processes the corrections from the $\Delta L_z = 0$ process are such that the majority-spin FS is elongated while the minority FS compressed along $\hat{\mathbf{z}}$. The reason being that the orbital degrees of freedom act as a "source field" on the spin degrees. As an illustration consider the work on Ref. [67], were I showed there is a coupling between the density, u_{00}, $(L = 0)$ and elliptical FS distortions, u_{20}, $(L = 2)$ of the form, $-u_{00}u_{20}$, in the the free energy. The fixed density acts as an external field with $L = 0$ symmetry under rotations. Hence the system always minimizes its energy by choosing non-zero (nematic-like) distortions. This is the physics behind the FS distortions in fully polarized dipolar Fermi gases. Another example: an external magnetic field, h_{ext}, along $\hat{\mathbf{z}}$ couples to the spins as $-\sigma^z h_{ext}$. It gives a negative energy correction to the single particle energies of the spins up while a positive correction to spins down. The physics here is similar. Due to spin-orbit mixing, an "orbital field" couples to the spins as, $-\sigma^z(\mu_r + Y_{20}(\hat{\mathbf{k}}))$. The chemical potential difference is acting as external magnetic field. This leads to anisotropic corrections of the form, $-Y_{20}(\hat{\mathbf{k}})$, to the single quasiparticle energies of spins "up"; elongating their FS along $\hat{\mathbf{z}}$. Spins "down" obtain corrections of the form, $Y_{20}(\hat{\mathbf{k}})$, compressing their FS along $\hat{\mathbf{z}}$. The quotation marks are explained bellow. This is the basic physics behind the ferronematic phase of Ref. [68].

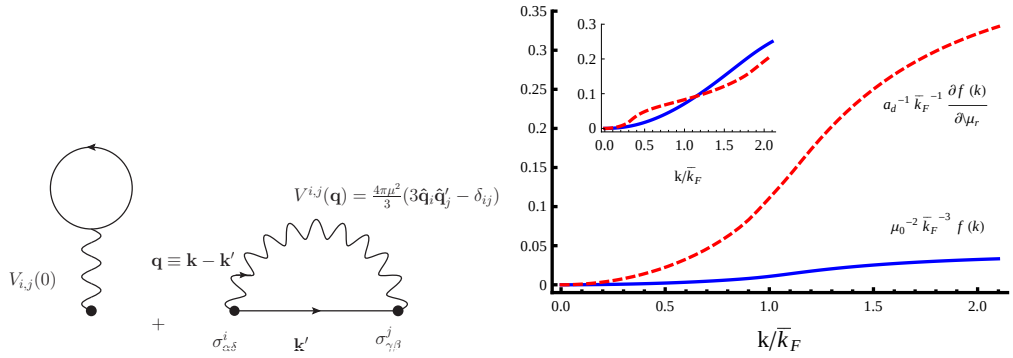

Figure 6.2: (left)First order terms in the expansion of the self-energy in power of the dipole interaction. The 1st, Hartree, term vanishes for a uniform system. (right) form of Eqn. 6.4.

6.2 Quasiparticle energy

In the presence of dipole-dipole interactions I can guess the form of the self energy by symmetry arguments. I thus require that the quasiparticle self energy be invariant under simultaneous rotations of the effective magnetic field and the quasiparticle momentum, which leads to an expression of the form

$$\Sigma^{ij}(\mathbf{k}) = \Sigma_0(k)\delta_{ij} + \frac{\Sigma_T(k)}{2}(3\hat{\mathbf{k}}_i\hat{\mathbf{k}}_j - \delta_{ij}) \tag{6.1}$$

where $i = x, y, z$ is the direction of the effective magnetic field and $j = x, y, z$ is the direction of the spin polarization. The form of this expression is valid to all orders in perturbation theory. Without loss of generality, I consider a microscopy Hamiltonian with a population imbalance of particles in eigenstates of σ^z, *i.e.* I will assume a fixed polarization. The interaction Hamiltonian is

$$\hat{H}_{int} = \frac{1}{2V}\sum_{\mathbf{q}} \hat{S}^i(\mathbf{q})V_{ij}(\mathbf{q})\hat{S}^j(-\mathbf{q}) \tag{6.2}$$

The dipole-dipole interaction is given by $V_{ij}(\mathbf{q}) = (4\pi\mu_0^2/3)(3\hat{\mathbf{q}}_i\hat{\mathbf{q}}_j - \delta_{ij})$ where $\hat{\mathbf{q}}$ is the unit vector in the direction of $\mathbf{q}$, $\mu_0 \equiv \gamma\hbar/2$ is the bare magnetic moment of particles and γ the gyromagnetic ratio, e.g., for electron spins, $\gamma = 2\mu_B$. Repeated indexes are to be summed over. $\hat{S}^i(\mathbf{q}) = \sum_{\mathbf{k}} c^\dagger_{\mathbf{k}+\mathbf{q},\alpha}\sigma^i_{\alpha\beta}c_{\mathbf{k},\beta}$ is the spin density in momentum space. σ^i are Pauli matrices and α, β are spin indexes that label the eigenstates of σ^z. To first order, Fig. 6.2, the self energy is given by,

$$\begin{aligned}\hbar\Sigma_{\alpha\beta}(\mathbf{k}) &= -\int \frac{d^3k'}{(2\pi)^3}\frac{1}{\hbar\beta}\sum_{n'} e^{i\omega_{n'}0^+}G^0_{\delta\gamma}(\mathbf{k}', i\omega_{n'})V_{ij}(\mathbf{k}-\mathbf{k}')\sigma^i_{\alpha\delta}\sigma^j_{\gamma\beta} \\ &= \Sigma^{zi}(\mathbf{k})\sigma^i_{\alpha\beta},\end{aligned} \tag{6.3}$$

where $\Sigma^{zi}(\mathbf{k}) = -f(k)(3\hat{\mathbf{k}}_i\hat{\mathbf{k}}_z - \delta_{i,z})$. In the last line I have expanded in Pauli matrices. Details of the calculation can be found is appendix B.2 The Hartree term vanishes for the uniform system I are considering. As can be seen, $\Sigma_0 = 0$ and $\Sigma_T = -2f(k)$. I assume a fixed population imbalance of particles in the two eigenstates of σ^z, by introducing two chemical potentials μ_1 and μ_2. $G^0_{\alpha\beta}(\mathbf{k}, i\omega_n) = \delta_{\alpha\beta}/(i\omega_n - \xi_{\mathbf{k}\alpha})$ is the free temperature Green function, where $\hbar\xi_{\mathbf{k}\alpha} = \epsilon^0_{\mathbf{k}} - \mu_\alpha$ is the bare single particle dispersion relation and $\epsilon^0_{\mathbf{k}} = \hbar^2k^2/2m$. $f(k)$ is a smooth monotonic function of the magnitude of the wave vector:

$$f(k) \quad = \quad \frac{2\mu_0^2}{\pi}\int_0^\infty k'^2 dk' \int_0^\infty \frac{dr}{r} j_2(kr)j_0(k'r)\left[n_F(\epsilon^0_{\mathbf{k}'} - \mu_r) - n_F(\epsilon^0_{\mathbf{k}'} + \mu_r)\right] \tag{6.4}$$

where $n_F(x) = \{\exp(\hbar\beta(x - \bar{\mu})) + 1\}^{-1}$ is the Fermi function, $\bar{\mu} = (\mu_1 + \mu_2)/2$ is the average chemical potential, and $\mu_r = (\mu_1 - \mu_2)/2$. The self energy vanishes for an equal number of quasiparticles in each eigenstate of σ^z.

A few comments are in order. The diagonal matrix elements of the self-energy, proportional to $\pm(3\cos^2\theta_{\mathbf{k}} - 1)$, give anisotropic re normalizations to the single particle energies, which lead to distortions of the FS for the "up" and "down" FS's as in the ferronematic phase of Ref. [68]. The non-diagonal elements of the self energy come from spin-½ particles flipping spin. As I now show, spin-flip processes due to dipole-dipole interaction cause the spins to tilt and the structure of the state becomes richer. The forms, $\Sigma_{12} \sim Y_{2,-1}$, and $\Sigma_{21} \sim Y_{2,1}$ of the non-diagonal matrix elements are expected since the magnetic dipole-dipole interaction conserves $J_z = L_z + S_z$. Then, $S_z = \pm 1$ implies $L_z = \mp 1$.

Therefore the energy of the quasiparticle of a dipolar Fermi gas, has a *tensor* structure[18]: $\hbar\xi_{\mathbf{k}\alpha}\delta_{\alpha\beta} + \hbar\Sigma_{\alpha\beta}(\mathbf{k}) \equiv (\epsilon_{\mathbf{k}})_{\alpha\beta} - \bar{\mu}\delta_{\alpha\beta}$, much *as if* the quasiparticle interacted with an effective magnetic field,

$$(\epsilon_{\mathbf{k}})_{\alpha\beta} \equiv \epsilon^0_{\mathbf{k}}\delta_{\alpha\beta} + \epsilon^i_{\mathbf{k}}\,\sigma^i_{\alpha\beta}, \tag{6.5}$$

where the effective magnetic field is given by $\epsilon^i_{\mathbf{k}} = \mu_0 h^i_{\mathbf{k}}$. This $\mathbf{k}$-dependent field has a contribution from the external field long $\hat{\mathbf{z}}$ (i.e., μ_r) and a molecular contribution due to interactions with other particles, which is *not* along $\hat{\mathbf{z}}$, see Fig. 6.3.

6.3 Quasiparticle magnetic moment

In a small field, the effective magnetic moment of the quasiparticle is

$$\mu_{ij}(\mathbf{k}) \equiv -\frac{\partial\epsilon^i_{\mathbf{k}}}{\partial h^j_{ext}} = -\mu_0\frac{\partial\epsilon^i_{\mathbf{k}}}{\partial\mu^j_r}. \tag{6.6}$$

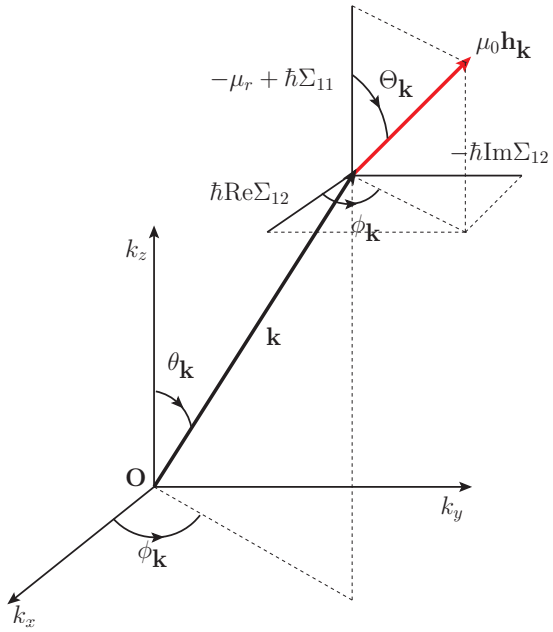

Figure 6.3: Effective magnetic field, (red arrow), at point $\mathbf{k}$ in momentum space. The spin quantization axis is tilted with respect to $\hat{\mathbf{z}}$ because the self energy for dipolar interactions have non vanishing off-diagonal matrix elements, $\Sigma_{12}(\mathbf{k})$, Eqn. 6.3.

Where I defined the external field by $\mu_0 h^z_{ext} = \mu_r$.

The magnetic moment carried by the Hartree-Fock quasiparticles is not the bare magnetic moment μ_0. In fact, when dipole-dipole interactions are present I can guess the form of the magnetic moment carried by the quasiparticle by symmetry arguments.[152]. I require that the magnetic moment be invariant under simultaneous rotations of the magnetic field and the momentum of the quasiparticle, i.e.,

$$\mu_{ij}(\mathbf{k}) = \mu\delta_{ij} + \frac{\mu_T}{2}(3\hat{\mathbf{k}}_i\hat{\mathbf{k}}_j - \delta_{ij}) \tag{6.7}$$

where I find $\mu = \mu_0$ and $\mu_T = 2\mu_0(\partial f(k)/\partial\mu_r)$. $f(k)$ is given by Eqn. 6.4. For the values used in Fig. 6.4 I find $\mu_T/\mu \sim 0.3$ at the outer FS. For small dipolar couplings, where our microscopic calculations are accurate, the occupied states in momentum space lie outside the singularities see Fig. 6.4. The line singularity is a ring in the k_x,k_y-plane with radius, k_0, given by $\mu_r = f(k_0)$. This wave vector, $k_0 \sim (\mu_r/\mu_0^2)^{1/3}$, is perpendicular to the unperturbed polarization axis, and naturally introduces a length scale, $1/k_0$. In the regime were our calculation is valid the length scale is much sorter than the inter-particle distance, $1/k_0 < 1/\max(k_{F1}, k_{F2})$ and hence it is related to microscopic effects not considered by our microscopic dipole-dipole Hamiltonian Eqn 6.2. For strong dipolar couplings, our calculation suggests that the radius of the ring penetrates one or both of the FS's. In this case, the resulting state would acquire a structure similar to the "β phases" of

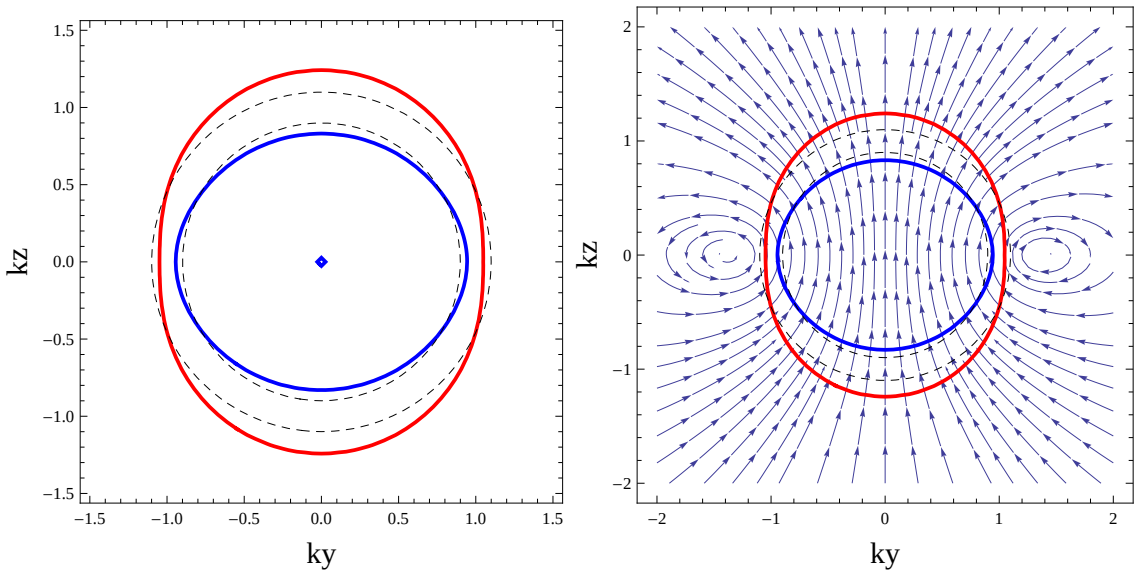

Figure 6.4: 2D cuts of (Left): points in k-space where $E_{\mathbf{k}\pm} = \bar{\mu}$. Dashed lines are FS's of free system: $\epsilon^0_{\mathbf{k}} = \bar{\mu} \pm \mu_r$. (Right): stream lines of magnetic moment field carried by quasiparticles in momentum space, Eqn. 6.7. This field resembles the magnetic field produced by an electric current circulating counterclockwise in a ring placed in the horizontal plane. Values for these plots are $k_{F1} = 1.1$ and $k_{F2} = 0.9$, in units of $\bar{k}_F$, and $\lambda = 0.3 << 1$.

Ref.[212]. Another possibility is for the state to become a spatially modulated "pion-condensed" state of Ref.[5].

6.4 Quasiparticle one-body density matrix

The distribution function of quasiparticles, $(n_{\mathbf{k}})_{\alpha\beta}$, is now a 2×2 matrix in spin space. Dyson equation, $(G^{-1})_{\alpha\beta} = (i\omega_n - \xi_{\mathbf{k}\alpha})\delta_{\alpha\beta} - \Sigma_{\alpha\beta}(\mathbf{k})$, gives a conserving approximation for the Green function. Defining $\hbar\xi_{\mathbf{k}\pm} = E_{\mathbf{k}\pm} - \bar{\mu}$, I obtain

$$\begin{aligned}
G_{11}(\mathbf{k}, i\omega_n) &= \frac{u^2_{\mathbf{k}}}{i\omega_n - \xi_{\mathbf{k}+}} + \frac{v^2_{\mathbf{k}}}{i\omega_n - \xi_{\mathbf{k}-}} \\
G_{22}(\mathbf{k}, i\omega_n) &= \frac{v^2_{\mathbf{k}}}{i\omega_n - \xi_{\mathbf{k}+}} + \frac{u^2_{\mathbf{k}}}{i\omega_n - \xi_{\mathbf{k}-}} \\
G_{12}(\mathbf{k}, i\omega_n) &= u_{\mathbf{k}} v_{\mathbf{k}} e^{-i\phi_{\mathbf{k}}} \left[\frac{1}{i\omega_n - \xi_{\mathbf{k}+}} - \frac{1}{i\omega_n - \xi_{\mathbf{k}-}} \right] \\
G_{21}(\mathbf{k}, i\omega_n) &= u_{\mathbf{k}} v_{\mathbf{k}} e^{i\phi_{\mathbf{k}}} \left[\frac{1}{i\omega_n - \xi_{\mathbf{k}+}} - \frac{1}{i\omega_n - \xi_{\mathbf{k}-}} \right]
\end{aligned}$$

where $E_{\mathbf{k}\pm} = \epsilon^0_{\mathbf{k}} \pm \left[(\hbar\Sigma_{11} - \mu_r)^2 + |\hbar\Sigma_{12}|^2 \right]^{1/2}$ and $u_{\mathbf{k}} = \cos(\Theta_{\mathbf{k}}/2)$ $v_{\mathbf{k}} = \sin(\Theta_{\mathbf{k}}/2)$, and $0 < \Theta_{\mathbf{k}} \leq \pi$ is defined in Fig. 6.3. Note that $u^2_{\mathbf{k}}$ is the probability of up-spin propagation and $v^2_{\mathbf{k}}$ is the probability of

down-spin propagation. The one-body density matrix is given by $(n_{\mathbf{k}})_{\alpha\beta} \equiv \int (d\omega/2\pi) n_F(\omega) \rho_{\alpha\beta}(\mathbf{k},\omega)$, where $\rho_{\alpha\beta}$ is 2×2 matrix of spectral functions. In Hartree-Fock, it consists of two delta functions corresponding to the poles of the Green functions. It is useful to expand the density matrix in Pauli matrices,

$$(n_{\mathbf{k}})_{\alpha\beta} = \bar{n}_{\mathbf{k}}\delta_{\alpha\beta} + \frac{1}{\hbar}\left\langle S^i_{\mathbf{k}}\right\rangle \sigma^i_{\alpha\beta}. \tag{6.8}$$

where $\bar{n}_{\mathbf{k}} \equiv (1/2)\mathrm{tr}[(n_{\mathbf{k}})]$ is the average occupation of state with momentum $\mathbf{k}$, and $\left\langle S^i_{\mathbf{k}}\right\rangle \equiv \hbar\, n^i_{\mathbf{k}} \equiv (\hbar/2)\mathrm{tr}[\sigma^i(n_{\mathbf{k}})]$ is the i-th spin density component. $\left\langle S^i_{\mathbf{k}}\right\rangle$ has a clear physical interpretation: it is a vector field, with polar angles defined in Fig. 6.3, which gives the $\mathbf{k}$-dependent quantum mechanical average of the spin state of the quasiparticle, in general, a superposition of eigenstates of σ^z,

$$\begin{aligned}
\bar{n}_{\mathbf{k}} &= \frac{1}{2}\left[n_F(E_{\mathbf{k}+}) + n_F(E_{\mathbf{k}-})\right] \\
\langle S^x_{\mathbf{k}}\rangle &= \hbar\, u_{\mathbf{k}} v_{\mathbf{k}} \cos\phi_{\mathbf{k}}\ \left[n_F(E_{\mathbf{k}+}) - n_F(E_{\mathbf{k}-})\right] \\
\langle S^y_{\mathbf{k}}\rangle &= \hbar\, u_{\mathbf{k}} v_{\mathbf{k}} \sin\phi_{\mathbf{k}}\ \left[n_F(E_{\mathbf{k}+}) - n_F(E_{\mathbf{k}-})\right] \\
\langle S^z_{\mathbf{k}}\rangle &= \frac{\hbar}{2}(u^2_{\mathbf{k}} - v^2_{\mathbf{k}})\left[n_F(E_{\mathbf{k}+}) - n_F(E_{\mathbf{k}-})\right]
\end{aligned}$$

Since $n^x_{\mathbf{k}} \neq 0$ and $n^y_{\mathbf{k}} \neq 0$, there is a non-zero average probability that the spin is pointing along the xy-plane in the region between the two "FS's", Fig. 6.5. However, $\sum_{\mathbf{k}} \langle S^x_{\mathbf{k}}\rangle = \sum_{\mathbf{k}} \langle S^y_{\mathbf{k}}\rangle = 0$. The net spin magnetization in the z direction is $\sum_{\mathbf{k}} \langle S^z_{\mathbf{k}}\rangle$. The average occupation number of state $\mathbf{k}$ and spin projection along $\hat{\mathbf{z}}$, $n_{\mathbf{k}\uparrow} \equiv \bar{n}_{\mathbf{k}} + n^z_{\mathbf{k}}$ and $n_{\mathbf{k}\downarrow} \equiv \bar{n}_{\mathbf{k}} - n^z_{\mathbf{k}}$, are

$$\begin{aligned}
n_{\mathbf{k},\uparrow} &= u^2_{\mathbf{k}} n_F(E_{\mathbf{k}+}) + v^2_{\mathbf{k}} n_F(E_{\mathbf{k}-}) \\
n_{\mathbf{k},\downarrow} &= v^2_{\mathbf{k}} n_F(E_{\mathbf{k}+}) + u^2_{\mathbf{k}} n_F(E_{\mathbf{k}-})
\end{aligned} \tag{6.9}$$

Fig. 6.5 is a density plot of the occupation probabilities of the average projected z-component of the spin. Note that the average occupation in momentum space is not uniform even at zero temperature. It has sharp discontinuities at positions which agree with the momentum distribution found in Ref. [68] for the ferronematic phase. These discontinuities define elliptically distorted "Fermi surfaces". In particular, note that dipole-dipole interactions cause the spins to tilt predominantly along the diagonals, see also Fig. 6.4, in such a way that measurement of quantum spin state will yield "down" with non-vanishing probability even in regions in momentum space originally occupied only by spins pointing up.

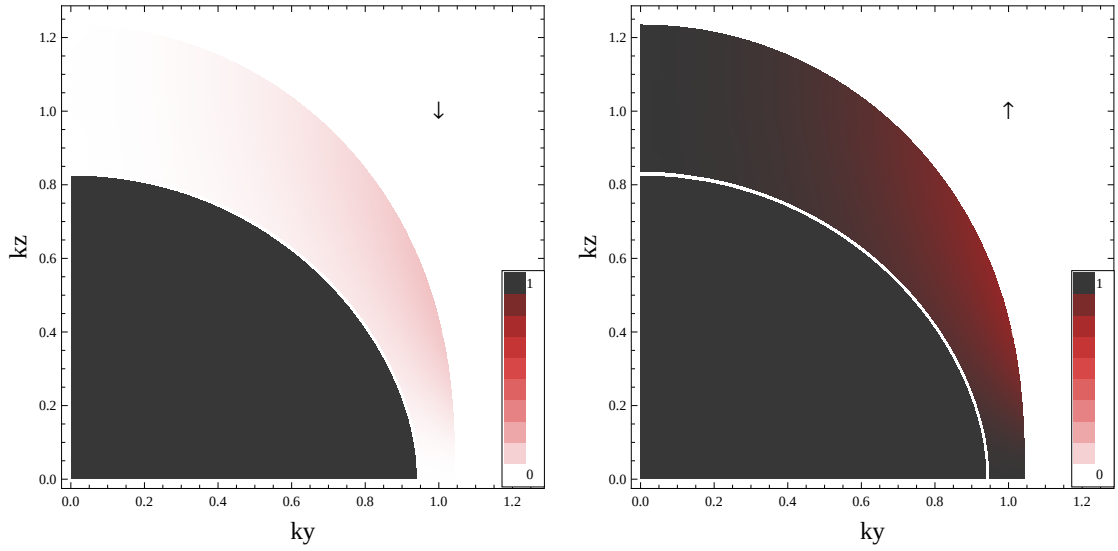

Figure 6.5: Occupation probability of z-projection of spin in momentum space, $n_{\mathbf{k}\uparrow}$(Left) and $n_{\mathbf{k}\downarrow}$(Right), (Eqn. 6.9). Values of for this plot are the same as those of Fig. 6.4.

6.5 Experimental realization

A possible realization of the above physics is in ultracold magnetic atoms in which the "spin" states are two hyperfine states of the atom in an optical trap e.g. of ^{163}Dy which have large magnetic moment. In its ground state the spin, orbital and nuclear angular momentum quantum numbers are $S = 2$, $L = 6$, $I = 5/2$, respectively. The total electronic angular momentum is $J = S + L = 8$ and the total angular momentum of the atoms is $\mathbf{F} = \mathbf{I} + \mathbf{J}$. In the presence of a magnetic field or chemical potential difference the spin Hamiltonian is $H_{spin} = A\mathbf{I} \cdot \mathbf{J} + BJ_z + CI_z$. The 1st term is the hyperfine interaction and is diagonalized in the bases of total angular momentum of the atom $|F, m_F\rangle$ with eigenvalues that depend only on F but not on m_F. The Zeeman terms will split this degeneracy. I propose the use of atoms with $F_1 = F_2 = 11/2$ and projections $m_F = \pm 11/2$. The dipole-dipole interaction have non-zero matrix elements between these hyperfine states and if the Zeeman splitting between the levels is small enough the dipolar interaction will dominate the spin dynamics. This systems will simulate a spin-1/2 system. The dipolar interaction between two atoms of total spin F is $(\mu_0^2/r^3)(\mathbf{F}_1 \cdot \mathbf{F}_2 - 3(\mathbf{F}_1 \cdot \hat{\mathbf{r}})(\mathbf{F}_2 \cdot \hat{\mathbf{r}}))$ and its restriction to the Hilbert space of $|m_{F_1}, m_{F_2}\rangle = |\pm 11/2, \pm 11/2\rangle$ is,

$$\langle \alpha\beta|\hat{\mathbf{U}}_{dip}|\alpha'\beta'\rangle \equiv U_{\alpha\alpha'\beta\beta'}(\mathbf{r}) = \frac{\mu_0\gamma^2}{4\pi r^3} F^i_{\alpha\alpha'}(\delta_{ij} - 3\hat{\mathbf{r}}_i\hat{\mathbf{r}}_j)F^j_{\beta\beta'}$$

Where

$$\mathbf{F^x} = \frac{\sqrt{11}}{2}\begin{pmatrix} 0 & 1 \\ 1 & 0 \end{pmatrix}, \mathbf{F^y} = \frac{\sqrt{11}}{2}\begin{pmatrix} 0 & -i \\ i & 0 \end{pmatrix}, \mathbf{F^z} = \frac{11}{2}\begin{pmatrix} 1 & 0 \\ 0 & -1 \end{pmatrix},$$

γ is the gyromagnetic ratio for the states in question and is defined by $\mathbf{M} = \gamma\mathbf{F}$. For femions the anti-symmetry of the wave function allows only a contact interaction between distinct hyperfine states; i.e., the central part of the interaction does not have the exchange term of the form $\mathbf{F}_1 \cdot \mathbf{F}_2$ that typically appear for bosonic atoms with large spin.[160]. It is also important that the matrix elements connecting these states to all others be much smaller. It is not at all clear that this can be done without much experimental effort specifically since in our case there is also a Zeeman field due to the chemical potential difference.

Another possibility is preparing the systems in two different hyperfine states such as $F = 21/2$ and $F = 11/2$ in an optical trap. We expect the hyperfine splitting to be the dominant energy scale, $\sim$ GHz, and to be much larger than the dipolar energy per particle. In this conditions I expect no spin relaxation on time scales of the experiment. For typical densities, $\bar{n} \sim 10^{13}$ cm^{-3}, for the magnetic atom, ^{163}Dy, the dipolar coupling is $\lambda \sim 0.01$. Hence, the "spin textures" will be hard to detect by conventional techniques. In future experiments these effects could be amplified with the use of electromagnetic fields or with denser clouds and one will obtain images that resemble Fig. 6.5 in time-of-flight experiments.

6.6 Final remarks

I studied the magnetic structure of the ground state of a magnetic dipolar Fermi system of spin-1/2 particles in an imbalanced, partially polarized, state. I determine the distribution of quasiparticle spins states. The k-dependent spin quantization axis is not along the spin magnetization axis but develops instead spin textures in momentum space. I computed the shape of the Fermi surfaces and the effective magnetic moment of the quasiparticles, at zero temperature and weak coupling. In particular I showed that the perturbed wave function has the general form

$$|\Psi\rangle = \prod_{\mathbf{k}<\mathbf{k}_F} \left(u_{\mathbf{k}} c^\dagger_{\mathbf{k},\uparrow} + v_{\mathbf{k}} c^\dagger_{\mathbf{k},\downarrow}\right)|0\rangle$$

with $\mathbf{k}$-dependent coefficients $u_{\mathbf{k}}$ and $v_{\mathbf{k}}$. In a future work this wave function is a good start for a self-consistent calculation of $u_{\mathbf{k}}$ and $v_{\mathbf{k}}$. Note that at each point in momentum space the quantum spin state is in general a linear combination of eigenvectors of σ^z. This just means that the spins tilt. To my acknowledge

this is the first example of a fully quantum, i.e., not semiclasical

Further issues that one might wish to consider within the present framework include the study of the possible quantum phase transition to a modulated state in an imbalanced two component Fermi system at intermediate dipolar couplings. Its existence is expected since the extreme case of strong coupling, where the dipoles reside on a lattice sites, have been shown to be a non-trivial modulated state [126].

Another extension of the present work is the dynamics of collective modes, the interaction matter-light is also interesting as the spin-orbit effects my be amplified. In a similar spirit interactions with a superfluid condensate may amplify the dipole effects as occurs in ^{3}He-A phase.[118].

Appendix A

A.1 Tensor form of the order parameters

In this appendix we rewrite the order parameters in a tensorial form which makes their correct symmetry transformation properties apparent. Much of what is done here follows closely the analysis of the classical case[34].

In 2D, because the rotation group $SO(2)$ group is Abelian, and has only two $1D$ representations with l=2 ($l_z = \pm 2$), it follows that the nematic order parameter $\mathbf{N}$, a 2×2 symmetric traceless tensor, has just two independent components, n_{11} and n_{12}, as shown in Eq. (3.1). The Abelian nature of the $SO(2)$ group enables us to use complex numbers, instead of tensors to represent the action of the group, as shown in Eq. (3.2).

All the formulas we have presented in the main text using the complex order parameter can be translated into the tensor language, which can more naturally be generalized to higher dimensions. Thus, Eq. (3.7) becomes

$$-2\kappa \, \mathrm{tr} \left\{ \mathbf{N}(\vec{r}) \left[\mathbf{D}\mathbf{N}(\vec{r}) \mathbf{N}(\vec{r}) \right] \right\} . \tag{A.1}$$

$\mathbf{D}$ is the rank 2 tensor formed by the outer product of the two-component real vector (∂_x, ∂_y):

$$\mathbf{D} = \begin{pmatrix} \partial_x \\ \partial_y \end{pmatrix} \otimes (\partial_x, \partial_y) , \tag{A.2}$$

In Eq (A.1) the first derivative operator acts on the second $\mathbf{N}$ factor, while the second derivative operator acts on the last $\mathbf{N}$ factor. Here only the traceless part of $\mathbf{D}$, $\mathbf{D} - \mathrm{tr}[\mathbf{D}]\mathbf{I}/2$, gives non-zero contribution to Eq. (A.1). The assignment of derivatives is not unique. But only this term gives a linearly independent contribution to the nematic Goldstone mode. Other assignments either have no contribution, or just give a contribution proportional to this one. Therefore, there is no needs to study other terms.

Similarly, Eq. (3.12) has the tensor form:

$$S_{\rm int} = -2g\int\frac{\mathrm{d}\vec{k}\mathrm{d}\Omega}{(2\pi)^3}\int\frac{\mathrm{d}\vec{q}\mathrm{d}\omega}{(2\pi)^3}\frac{1}{k^2}\mathrm{tr}\left\{\mathbf{N}(\tilde{\mathbf{q}},\omega)\begin{pmatrix}k_x^2 & k_xk_y\\ k_xk_y & k_y^2\end{pmatrix}\right\}$$
$$\times\rho(\vec{k}-\vec{q}/2,\Omega-\omega/2)\rho(-\vec{k}-\vec{q}/2,-\Omega-\omega/2). \tag{A.3}$$

Again, it is easy to check that only the traceless part of the tensor composed by the momenta $\vec{k}$ is needed here, since the trace of that tensor has no contribution. Notice that although there is a factor of $1/k^2$ in our formula, it will not cause divergence, since what we are interested in is a CDW, a state that orders at a finite wave vector $k \sim Q_S$.

Finally, using the fermionic density quadrupole tensor defined in Eq. (3.19), Eq. (3.21) can be written in tensorial form as

$$-g_N\int\mathrm{d}\vec{r}\mathrm{d}t\ \mathrm{tr}[\mathbf{QN}] \tag{A.4}$$

A.2 Quantum critical point for $Q_S < 2k_F$

As discussed in the main text, at the nematic-smectic critical point $Q_S < 2k_F$, the nematic Goldstone mode is the low-energy mode. To obtain its effective low-energy effective action we integrate the high energy mode of the smectic field, Φ. Terms like

$$\langle(\partial_x\Phi^\dagger\Phi)(\Phi^\dagger\partial_x\Phi)\rangle\phi_N\phi_N, \tag{A.5}$$

will generate the leading corrections to the ϕ_N propagator. We evaluate the integral numerically to deduce the kernel for the quadratic fluctuations. To the one-loop level, it is

$$C_1q^2 + iC_2\omega^3|\log(\omega/q^2)|/q^4, \tag{A.6}$$

for $0 < \omega \ll q^2$. The first term C_1q^2 renormalizes the two Frank constant K_1 and K_2, while the second one is subleading compared to the dynamical term of the nematic Goldstone mode, which is proportional to $i|\omega|/q$. This result suggests that the smectic field Φ is an irrelevant perturbation to the nematic Goldstone mode at the nematic-smectic critical point.

Terms of the form

$$\langle \partial_x \Phi^\dagger \phi_N \partial_x \Phi \phi_N \rangle \Phi^\dagger \Phi \tag{A.7}$$

provide leading order corrections to the propagator of the smectic field Φ, and yield a self-energy correction to the field Φ. The loop integral is computed numerically and is well fit by the form

$$\sim C_3 q^2 + i C_4 \omega^{5/4}, \tag{A.8}$$

when $\omega \gg q^3$. The first term renormalizes the constants C_x and C_y defined in Eq. (3.15) and the second one is subleading compared to the dynamical term of the smectic field which is linear in $|\omega|$.

Therefore, these arguments provide strong evidence that the coupling between the nematic Goldstone mode ϕ_N and the smectic order parameter Φ is irrelevant. In the low-energy theory, we can treat in practice ϕ_N and Φ as two separate modes.

A.3 Non-analytic terms of the effective field theory of the electron smectic with $Q_S = 2k_F$

The mean-field Hamiltonian of the smectic phase is

$$\begin{aligned} H_{MF} &= \int \frac{d^2k}{(2\pi)^2} \Big(\epsilon(\vec{k}) \psi^\dagger(\vec{k}) \psi(\vec{k}) + g_S \bar{\Phi} \psi^\dagger(\vec{k} + \vec{Q}_S) \psi(\vec{k}) \\ &\qquad + g_S \bar{\Phi}^* \psi^\dagger(\vec{k} - \vec{Q}_S) \psi(\vec{k}) \Big) + \Delta_S |\bar{\Phi}|^2. \end{aligned} \tag{A.9}$$

The smectic order parameter $\bar{\Phi}$ will act as a periodic background potential in the direction of $\vec{Q}_S$ which will reconstruct the band structure and the FS. For $Q_S = 2k_F$, we will only consider the lowest two bands. By ignoring higher bands, we can diagonalize this mean-field Hamiltonian to get the single particle dispersion relation

$$E_\pm(\vec{k}) = \frac{1}{2} \left(\epsilon(\vec{k}) + \epsilon(\vec{k} + \vec{Q}_S) \right) \pm \sqrt{\frac{1}{4} \left(\epsilon(\vec{k}) - \epsilon(\vec{k} + \vec{Q}_S) \right)^2 + g_S^2 |\bar{\Phi}|^2}. \tag{A.10}$$

Here the + sign is for the upper band and the − sign is for the lower band. The lower band is partially filled by the fermions, but the upper band is empty. So the Landau free energy will be

$$F(|\bar{\Phi}|) = \int_{E_-(\vec{k})<\mu} \frac{d^2k}{(2\pi)^2} E_-(\vec{k}) + \Delta_S |\bar{\Phi}|^2, \tag{A.11}$$

where μ is the chemical potential. By expanding the dispersion relation around the two points marked on Fig. 3.2(b)

$$\epsilon_{1,2}(\vec{q}) = \pm q_y + \frac{\kappa}{2} q_x^2, \tag{A.12}$$

where $\vec{q}$ is measured from the special points marked in Fig. 3.2(b). The Fermi velocities at these two points are just opposite to each other, $v_F = \pm 1$, and the curvatures of the FS have the same value κ at these two points.

By using this approximate dispersion relation, the Landau free energy can be determined as

$$F(|\bar{\Phi}|) = F(0) + r|\bar{\Phi}|^2 + u'|\bar{\Phi}|^{5/2}. \tag{A.13}$$

Here the coefficient of the quadratic term r depends on the high-energy cutoff, which reflects that the Landau free energy depends on the band structure all the way down to the bottom of the band.

On the other hand, u' is universal, as it depends only on the dispersion relation around the two special points,

$$u' = -\frac{\Gamma(-1/4)}{5\pi^{3/2}\Gamma(1/4)} \frac{g_s^{5/2}}{\sqrt{\kappa/2}} \approx 0.049 \frac{g_S^{5/2}}{\sqrt{\kappa/2}}. \tag{A.14}$$

u' diverges in the limit of $\kappa \to 0$, which means terms in lower order, such as $|\bar{\Phi}|^9/4$, will be generated (see below).

Around an inflection point, the dispersion relation is shown in Eq. (3.42). Similar to the calculation above, a term proportional to $|\bar{\Phi}|^{9/4}$ will be found. The coefficient of these term u'' will be

$$u'' = -\frac{2\Gamma(-1/8)}{9\pi^{3/2}\Gamma(3/8)} \frac{g_S^{9/4}}{b^{1/4}} \approx 0.15 \frac{g_S^{9/4}}{b^{1/4}} \tag{A.15}$$

A.4 Goldstone mode in the smectic phase

In the smectic phase, the smectic order parameter obtains an expectation value. We write $\bar{\Phi}$ as

$$\Phi = \bar{\Phi} + \delta\Phi. \tag{A.16}$$

$\bar{\Phi}$ can be considered as a periodic potential background for the fermions. As a result, the fermions will form band structure in the y direction. Define the Bloch states as

$$\psi_n(\vec{k}) = \sum_m T_{n,m}(\vec{k}) e^{im\phi} \psi(\vec{k} + m\vec{Q}_S), \tag{A.17}$$

where $T_{n,m}$ is an orthogonal transfer matrix which depends on the amplitude of the order parameter, and ϕ is the phase of $\bar{\Phi}$. In general, the Bloch wave is related to the plane wave by a unitary transformation. Here, due to the fact that only one harmonic of the CDW with wave vector $\vec{Q}_S$ is considered, after a proper spatial translation, which is a shift of ϕ, it can be simplified to an orthogonal transformation, which enables us to define the orthogonal transfer matrix $T_{n,m}$. The inverse formula can also be written down, since the $T_{n,m}e^{im\phi}$ must be unitary:

$$\psi(\vec{k} + m\vec{Q}_S) = \sum_n T_{n,m}(\vec{k}) e^{-im\phi} \psi_n(\vec{k}). \tag{A.18}$$

Integrating out the fermionic degrees of freedom, the leading term in the power series of the smectic fluctuations $\delta\Phi$ starts from the quadratic order.

$$\begin{aligned} \mathcal{L} \;=\; & -\begin{pmatrix} \delta\Phi^\dagger(\vec{q},\omega) & \delta\Phi(-\vec{q},-\omega) \end{pmatrix} \begin{pmatrix} \Delta_S - \Pi(\vec{Q}_S + \vec{q},\omega) & -\Pi'(\vec{Q}_S + \vec{q},\omega) \\ -\Pi'(-\vec{Q}_S - \vec{q},-\omega) & \Delta_S - \Pi(\vec{Q}_S - \vec{q},-\omega) \end{pmatrix} \\ & \times \begin{pmatrix} \delta\Phi(\vec{q},\omega) \\ \delta\Phi^\dagger(-\vec{q},-\omega) \end{pmatrix}. \end{aligned} \tag{A.19}$$

Notice that $\delta\Phi^\dagger(\vec{q},\omega) \neq \delta\Phi(-\vec{q},-\omega)$, since the field Φ is complex. The continuous translational symmetries have been broken into discrete ones. Therefore, a process which changes the momentum by $n\vec{Q}_S$, where n is an integer, is allowed. This is the reason why we have the terms such as $\delta\Phi^\dagger(\vec{q},\omega)\delta\Phi^\dagger(-\vec{q},-\omega)$.

$\Pi(\vec{Q}_S + \vec{q},\omega)$ in the diagonal terms is the standard fermion bubble integral in the smectic phase but with

momentum close to $\vec{Q}_S$,

$$\Pi(\vec{Q}_S+\vec{q},\omega) = \int\frac{\mathrm{d}\vec{k}_1\mathrm{d}\Omega_1}{(2\pi)^3}\int\frac{\mathrm{d}\vec{k}_2\mathrm{d}\Omega_2}{(2\pi)^3}\Big\langle\psi^\dagger(\vec{k}_1+\vec{Q}_S+\vec{q}/2,\Omega_1+\omega/2)\psi(\vec{k}_1-\vec{q}/2,\Omega_1-\omega/2) \times\psi^\dagger(\vec{k}_2-\vec{q}/2,\Omega_2-\omega/2)\psi(\vec{k}_2+\vec{Q}_S+\vec{q}/2,\Omega_2+\omega/2)\Big\rangle. \tag{A.20}$$

Since the eigenstates are Bloch waves, we need to transfer ψ into ψ_n.

$$\Pi(\vec{Q}_S+\vec{q},\omega) = \sum_{m_1,m_2,n_1,n_2}\int\frac{\mathrm{d}\vec{k}}{(2\pi)^2}T_{n_1,m_1+1}(\vec{k}+\vec{q}/2)T_{n_2,m_1}(\vec{k}-\vec{q}/2) \times T_{n_2,m_2}(\vec{k}-\vec{q}/2)T_{n_1,m_2+1}(\vec{k}+\vec{q}/2)F_{n_1,n_2}(\vec{k},\vec{q},\omega) \tag{A.21}$$

where $F_{n_1,n_2}(\vec{k},\vec{q},\omega)$ describe the scattering between fermions in band n_1 and n_2, which is defined as

$$-\int\frac{\mathrm{d}\Omega}{2\pi}\Big\langle\psi^\dagger_{n_1}\left(\vec{k}+\vec{q}/2,\Omega+\omega/2\right)\psi_{n_1}\left(\vec{k}+\vec{q}/2,\Omega+\omega/2\right)\Big\rangle \times\Big\langle\psi^\dagger_{n_2}\left(\vec{k}-\vec{q}/2,\Omega-\omega/2\right)\psi_{n_2}\left(\vec{k}-\vec{q}/2,\Omega-\omega/2\right)\Big\rangle. \tag{A.22}$$

The off-diagonal $\Pi'(\vec{Q}_S+\vec{q},\omega)$ is very similar to $\Pi(\vec{Q}_S+\vec{q},\omega)$.

$$\Pi'(\vec{Q}_S+\vec{q},\omega) = \int\frac{\mathrm{d}\vec{k}_1\mathrm{d}\Omega_1}{(2\pi)^3}\int\frac{\mathrm{d}\vec{k}_2\mathrm{d}\Omega_2}{(2\pi)^3}\Big\langle\psi^\dagger(\vec{k}_1+\vec{Q}_S+\vec{q}/2,\Omega_1+\omega/2)\psi(\vec{k}_1-\vec{q}/2,\Omega_1-\omega/2) \times\psi^\dagger(\vec{k}_2+\vec{Q}_S-\vec{q}/2,\Omega_2-\omega/2)\psi(\vec{k}_2+\vec{q}/2,\Omega_2+\omega/2)\Big\rangle. \tag{A.23}$$

Again, we need to transfer ψ into ψ_n.

$$\Pi'(\vec{Q}_S+\vec{q},\omega) = e^{-2i\phi}\sum_{m_1,m_2,n_1,n_2}\int\frac{\mathrm{d}\vec{k}}{(2\pi)^2}T_{n_1,m_1+1}(\vec{k}+\vec{q}/2)T_{n_2,m_1}(\vec{k}-\vec{q}/2) \times T_{n_2,m_2+1}(\vec{k}-\vec{q}/2)T_{n_1,m_2}(\vec{k}+\vec{q}/2)F_{n_1,n_2}(\vec{k},\vec{q},\omega) \tag{A.24}$$

To study the low-energy excitations, we need to diagonalize the matrix of Eq. (A.19). Then two eigenmodes appear. In the limit where we take $\omega\to 0$ first, then $q\to 0$, it is easy to see that eigenvalues of these two eigenmodes are $\Pi(\vec{Q}_S,0)+\Delta_S\pm|\Pi'(\vec{Q}_S,0)|$. The equation

$$\Pi(\vec{Q}_S,0)+\Delta_S-\Pi'(\vec{Q}_S,0)=0 \tag{A.25}$$

reproduces the mean-field self-consistent equation which determines $\bar{\Phi}$. Therefore, the mode which takes the

minus sign will be the Goldstone mode and the other is the amplitude mode.

As for the Goldstone mode, the intra-band scattering $F_{n,n}$ and the inter-band scattering F_{n_1,n_2} where $n_1 \neq n_2$, have different contributions. The intra-band scattering have no contribution in the $q \to 0$ limit, because its contribution to $\Pi(\vec{Q}_S, 0)$ and $|\Pi'(\vec{Q}_S, 0)|$ cancels.

When $n_1 = n_2$, term in $\Pi(\vec{Q}_S, 0)$ is

$$\int \sum_{m_1,m_2,n} \frac{\mathrm{d}\vec{k}}{(2\pi)^2} T_{n,m_1+1}(\vec{k}) T_{n,m_1}(\vec{k}) T_{n,m_2}(\vec{k}) T_{n,m_2+1}(\vec{k}) F_n(\vec{k}, 0, 0), \tag{A.26}$$

and term in $\Pi'(\vec{Q}_S, 0)$ is

$$e^{-2i\phi} \int \sum_{m_1,m_2,n} \frac{\mathrm{d}\vec{k}}{(2\pi)^2} T_{n,m_1+1}(\vec{k}) T_{n,m_1}(\vec{k}) T_{n,m_2+1}(\vec{k}) T_{n,m_2}(\vec{k}) F_n(\vec{k}, 0, 0). \tag{A.27}$$

From these two equations, the contributions are canceled for the Goldstone mode.

The inter-band scatterings are gapped, so that we have

$$F_{n_1,n_2}(\vec{k}, 0, 0) = -\frac{n_f\left(E_{n_1}(\vec{k})\right) - n_f\left(E_{n_2}(\vec{k})\right)}{E_{n_1}(\vec{k}) - E_{n_2}(\vec{k})}, \tag{A.28}$$

where $E_n(\vec{k})$ is the eigen-energy of fermions in band n with momentum $\vec{k}$ and n_f is the Fermi distribution function. Summing all the inter-band contributions, the equation $\Pi(\vec{Q}_S, 0) + \Delta_S - \Pi'(\vec{Q}_S, 0) = 0$ reproduces the mean-field self-consistent equation which determines $\bar{\Phi}$ as required by the Ward identity

Now let us study the frequency dependence of the smectic Goldstone mode. It is straight forward to show that the frequency dependence from the inter-band scatterings will start from the order ω^2 because the inter-band scattering has an energy gap.

We expect the intra-band scattering gives a dynamical term $\sim i|\omega|/q$ to Π and Π' since there is no energy gap and the T matrix has no singular points. However, as we just showed, the intra-band scattering contributions to Π and Π' cancels at $q = 0$. Hence, the leading dynamical term is $\sim i|\omega|q$. The Lagrangian density reads

$$\mathcal{L} = g_S^2 |\bar{\Phi}|^2 N_S(0) \left(B(\varphi_q) \frac{\omega^2}{k_F g_S |\bar{\Phi}|} + iA(\varphi_q) \frac{|\omega| q}{k_F g_S |\bar{\Phi}|} - \kappa_S(\varphi_q) q^2 \right) |\phi_\Phi(\vec{q}, \omega)|^2, \tag{A.29}$$

Here $\bar{\Phi}$ is the expectation value of the smectic order parameter and the smectic Goldstone mode ϕ_Φ is defined in Eq. (3.45). φ_q is the angle between $\vec{q}$ and the stripe direction and $N_S(0)$ is the density of states in the smectic phase. $A(\varphi_q)$, $B(\varphi_q)$ and $\kappa_S(\varphi_q)$ are coupling constants that depend on microscopic details and the

direction of $\vec{q}$ which reflects the anisotropic nature of the smectic phase.

This low-energy theory has $z = 1$ which is different from $z = 2$ at the QCP. Notice that the denominator of the first two terms in the above formula contains $|\bar{\Phi}|$, which just means that the $z = 1$ breaks down when on approach the QCP from the smectic side. On the other side, if we notice that there is a coefficient $|\bar{\Phi}|^2$ in the front of the Lagrangian density, the $|\bar{\Phi}|$ in the denominator cause no divergence at small $|\bar{\Phi}|$. In fact, as we can see that the intra-band scattering vanishes as $|\bar{\Phi}|$ goes to 0, which is what one should expected.

It is easy to check that the coefficients of $A(\varphi_q)$ and $B(\varphi_q)$ are dimensionless, while $B(\varphi_q)$ and $\kappa_S(\varphi_q)$ are real. $A(\varphi_q)$ is a real function for most values of φ_q. However, from some special cases, for example Fig. 3.2(d), there will be no FS whose Fermi velocity is close to the y direction. As a result, the particle-hole excitations with momentum close to the x direction will not be damped. Therefore, $A(\varphi_q)$ will be imaginary for $\varphi_q \sim 0$ or π.

A.5 RPA calculation of the fermion self-energy

The imaginary part of the fermion self-energy corrections at the FS, $\Sigma''(\vec{k}_F, \omega)$, scales with frequency (as $\omega \to 0$) as $\sim |\omega|^\mu$. When the scaling index μ is larger than 1, the low-energy theory of the fermions can be described by the Landau FL theory. But if μ is less than 1, the self-energy correction will dominate and the Landau FL theory will break down at low energies. As a result, the system will exhibit non-FL behavior.

A.5.1 The nematic-smectic QCP

To the one-loop level, for $\omega > 0$,the imaginary part of the fermion self-energy correction from Φ is

$$\Sigma''_S(\vec{k}_F, \omega) = \frac{g_S^2}{2} \int_{0<\epsilon(\vec{k}_F+\vec{Q}_S-\vec{q})<\omega} \frac{\mathrm{d}\vec{q}}{(2\pi)^2} B_S\left(\vec{q}, \omega - \epsilon\left(\vec{k}_F + \vec{Q}_S - \vec{q}\right)\right), \tag{A.30}$$

where $B_S(\vec{q}, \omega)$ is the spectral density of the smectic field. At the nematic-smectic QCP ($Q_S < 2k_F$) Eq. (3.36) gives

$$B_S(\vec{q}, \omega) = \frac{2C_0\omega}{C_0^2\omega^2 + (C_x q_x^2 + C_y q_y^2)^2}. \tag{A.31}$$

By substituting this to Eq. (A.30), we find that for the four points marked on Fig. 3.2(a), $\Sigma''_S \sim |\omega|^{1/2}$, while for all other points on the FS $\Sigma''_S \sim \omega^2$. For the special case of $C_x = C_y = C$, an analytical formula can be achieved. For the four special points, $\Sigma''_S = \sqrt{2|\omega|}/(4\pi\sqrt{CC_0})$ valid for $|\omega|C/C_0 \ll 1$. For other

points on the FS, $\Sigma''_S(\vec{k}_F) = \omega^2 v^2 C_0/(16\pi C^2\Delta^3)$, where the constants Δ and v comes from the expansion of the dispersion relation near $\vec{k}_F + \vec{Q}_S$ as $\epsilon(\vec{q}+\vec{k}_F+\vec{Q}_S) = \mu + \Delta + \vec{v}\cdot\vec{q} + \ldots$.

The nematic Goldstone mode has an $\omega^{2/3}$ contribution to Σ'' for most points on the FS except the four points in the main-axis directions where $\Sigma'' \sim |\omega|^{3/2}$ [150]. The $|\omega|^{2/3}$ behavior is dominant over a $\Sigma''_S \sim \omega^2$ scaling, but not over a $\Sigma''_S \sim |\omega|^{1/2}$ contribution. As a result, the four main-axis directions still have FL behavior. The special points shown in Fig. 3.2(a) will have $\Sigma'' \sim |\omega|^{1/2}$ non-FL behaviors. For all other part of the Fermi surface, $\Sigma'' \sim |\omega|^{2/3}$ due to the nematic Goldstone mode. If the nematic Goldstone mode is gapped due to a lattice background or an external field, the $\Sigma'' \sim |\omega|^{2/3}$ non-FL behavior will disappear. But the $\Sigma'' \sim |\omega|^{1/2}$ non-FL behavior at the four special points will persist.

The incommensurate CDW of $Q_S = 2k_F$ case has a relevant perturbation $\Phi^{5/2}$, so the critical theory will be controlled by microscopic details. RPA calculation will not be reliable in such a situation.

However we know that the commensurate CDW with $Q_S = 2k_F$ is a second order transition described by the Gaussian theory, so RPA is applicable. Here we follow the same approach mentioned above. For most part of the FS, this bosonic mode will provide a self-energy correction $\Sigma''_S \sim \omega^2$ for small ω. However for the special point $\vec{k} = \pm k_F \vec{e}_y$, Σ''_S is linear in ω when $\omega\kappa \ll 1$. $|\omega|^{2/3}$ term from the ϕ_N mode will not be present for the commensurate CDW due to the lattice background. Hence, the fermions at this critical point are described by a FL theory, except for fermions with $\vec{v}_F \parallel \vec{Q}_S$.

For the special case of the inflection points, by following the same procedures, we get $\Sigma'' \sim |\omega|^{13/12}$ at inflection points, where the FL picture is valid for the whole FS.

A.5.2 The electron smectic phase

In the smectic phase, for $\omega > 0$, the fluctuations of the smectic Goldstone boson ϕ_Φ will contribute to the fermion self-energy:

$$\Sigma''_{n,\phi_\Phi}(\vec{k},\omega) = \sum_{n'} \frac{|\bar{\Phi}|^2}{2} \int_{0<\epsilon_{n'}(\vec{k}-\vec{q})<\omega} \frac{\mathrm{d}\vec{q}}{(2\pi)^2} \left|\tilde{g}_S^{n,n'}(\vec{k},\vec{q})\right|^2 B_{\phi_\Phi}\left[\vec{q}, |\omega| - \epsilon_{n'}(\vec{k}-\vec{q})\right]. \tag{A.32}$$

Here $B_{\phi_\Phi}(\vec{q},\omega)$ is the spectral density function of the ϕ_Φ mode presented below, $\epsilon_n(\vec{k})$ is the dispersion relation for fermions in band n and the vertex is

$$\tilde{g}_S^{n,n'}(\vec{k},\vec{q}) = ig_S \sum_m \left[T_{n,m+1}(\vec{k}-\vec{q})T_{n',m}(\vec{k}) - T_{n,m}(\vec{k}-\vec{q})T_{n',m+1}(\vec{k})\right].$$

with $T_{n,m}$ being the matrix element of the orthogonal transformation defined in Eq. (A.18)

The energy gap between two different energy bands dictated that the contributions from the interband scatterings to Σ'' ($n \neq n'$) scale as ω^2 at small ω, which is subleading to the FL behavior. As for the intraband scatterings, the vertex vanishes linearly in the long wavelength limit ($q \sim 0$) as

$$\tilde{g}_S^{n,n}(\vec{k},\vec{q}) = i\sum_m \left[\nabla T_{n,m}(\vec{k})T_{n,m+1}(\vec{k}) - \nabla T_{n,m+1}(\vec{k})T_{n,m}(\vec{k})\right]\cdot\vec{q} + O(q^2). \tag{A.33}$$

This is because the Goldstone mode cannot couple directly to the fermion density but to its fluctuations, as required by the translational symmetry. As a consequence of this structure of the vertex, we found that the quasiparticle scattering rate from intraband scatterings are also subleading corrections to the FL behavior by numerically evaluating the integral in Eq. (A.32).

For an electron smectic without a lattice background, Eq. (3.50) gives

$$B_{\phi_\Phi}(\vec{q},\omega) = \frac{k_F}{g_S|\bar{\Phi}|N_S(0)}\,\frac{2A\omega\sqrt{\kappa_1\kappa_2^{-1}q_x^4+q_y^2}}{\left(A\omega\sqrt{\kappa_1\kappa_2^{-1}q_x^4+q_y^2}\right)^2 + \left(B\omega^2 - k_F g_S|\bar{\Phi}|(\kappa_1 q_x^4+\kappa_2 q_y^2)\right)^2}. \tag{A.34}$$

For most part of the FS, the intraband scatterings lead to a fermion scattering rate $\Sigma''_{\phi_\Phi} \sim \omega^2\log|\omega|$ in the small frequency limit. However for some special points, where the Fermi velocity is perpendicular to the stripe direction, $\Sigma''_{\phi_\Phi} \sim |\omega|^{3/2}$. This result suggests that the fermions will be described by a FL. For unpinned smectics with a lattice background, we have

$$B_{\phi_\Phi}(\vec{q},\omega) = \frac{k_F}{g_S|\bar{\Phi}|N_S(0)}\,\frac{2A(\phi_q)\omega q}{\left(A(\phi_q)\omega q\right)^2 + \left(B(\phi_q)\omega^2 - k_F g_S|\bar{\Phi}|\kappa_S(\phi_q)q^2\right)^2}, \tag{A.35}$$

and that $\lim_{\omega\to 0}\Sigma''(\omega) \sim \omega^2\log|\omega|$ at most part of the Fermi surface, while $\Sigma''(k_F,\omega)\sim\omega^2$ at the special points where $\tilde{g}_S^{n,n}(\vec{k},\vec{q})$ is independent of q_t to the linear order of $\vec{q}$, with q_t being the component of $\vec{q}$ parallel to the reconstructed Fermi surface.

Appendix B

B.1 Self energy in Hartree-Fock

Using the formula for the decomposition of a plane wave into a sum of spherical harmonics we can show that the Fourier transform of the dipolar interaction $V_d(\mathbf{r}) = (d^2/r^3)(1 - 3\cos^2\theta_{\mathbf{r}})$, can be written as

$$\begin{aligned} V_d(\mathbf{k}-\mathbf{k}') &= \int d^3 r e^{-i(\mathbf{k}-\mathbf{k}')\cdot\mathbf{r}} V_d(\mathbf{r}) \\ &= \sum_{lm;l'm'} V_{lm;l'm'}(k,k') Y^*_{lm}(\hat{\mathbf{k}}') Y_{l'm'}(\hat{\mathbf{k}}) \end{aligned}$$

Where

$$V_{lm,l'm'}(k,k') = -2d^2(4\pi)^2(-i)^l i^{l'} \left(\int \frac{dr}{r} j_l(kr) j_{l'}(k'r)\right) \left(\int d\Omega\, Y^*_{lm}(\hat{\mathbf{r}}) Y_{l'm'}(\hat{\mathbf{r}}) P_2(\hat{\mathbf{r}})\right)$$

In Hartree-Fock, the Hartree contribution to the self-energy vanishes because $V_d(\mathbf{q}=0) = 0$. The Fock term can be written as

$$\begin{aligned} \Sigma_{HF}(\mathbf{k}') &= -\int \frac{d^3k}{(2\pi)^3} V(\mathbf{k}-\mathbf{k}') n^0_k \\ &\equiv \sum_{lm} \sigma_{lm}(k) Y_{lm}(\hat{\mathbf{k}}') \end{aligned}$$

Where we defined

$$\sigma_{l,m}(k) = -\sum_{l'm'} \int \frac{d^3k}{(2\pi)^3} V_{lm,l'm'}(k,k') Y_{l'm'}(\hat{\mathbf{k}}) n^0_k$$

In perturbation theory we use the spherical distribution n_k^0 in momentum space. We only need to calculate the term $V_{00,lm}$. This term is readily calculated from its definition above. We then substitute to obtain

$$\sigma_{lm} = -\delta_{l,2}\delta_{m,0}\frac{4d^2}{\pi}\sqrt{\frac{4\pi}{5}}\int_0^{k_F^0} k'^2 dk' \int_0^\infty \frac{dr}{r} j_0(kr)\, j_2(k'r)$$

Where k_F^0 is the undistorter(spherical) Fermi wave vector. We conclude that the Hartree-Fock self-energy is $\sim P_2(\hat{\mathbf{k}})$ and is given by

$$\Sigma_{HF}(\mathbf{k}) = \sigma(k) P_2(\hat{\mathbf{k}})$$

where explicit calculation gives the smooth, slowly varying function of the magnitude k:

$$\sigma(k) \;=\; \frac{-d^2}{36\pi k^3}\left[3k^5 k_F^0 + 8k^3(k_F^0)^3 - 3k(k_F^0)^5 - 3(k^2-(k_F^0)^2)^3 \arctan(\frac{k_<}{k_>})\right]$$

This equation is valid for all k with $k_<$ being the least of k_F^0 and k. One can check that $\sigma(k)$ is continuous and twice differentiable at k_F^0. We conclude that the single particle dispersion relation is given

$$\begin{aligned}\epsilon_{\mathbf{k}} &= \epsilon_k^0 + \Sigma_{HF}(\mathbf{k}) \\ &= \frac{k^2}{2m} + \sigma(k) P_2(\cos\theta_k)\end{aligned}$$

In particular the Fermi wave vector can be written as

$$\mathbf{k}_F = \hat{\mathbf{n}} k_F^0 + \hat{\mathbf{n}}\delta k_F$$

To 1st order in the dipolar interaction ie. Hartree-Fock level, the chemical potential is unchanged $\mu = (k_F^0)^2/2m$. The first correction to the chemical potential is cuadratic. The change in Fermi wave vector is given by the wave vectors, $\mathbf{k}_F$, that satisfy

$$\frac{\mathbf{k}_F^2}{2m} + \sigma(k_F) P_2(\hat{\mathbf{k}}_F) = \mu$$

Solving to 1st order in δk_F we obtain

$$\delta k_F = \frac{m d^2 (k_F^0)^2}{9\pi} (3\cos^2\theta_{\mathbf{k}} - 1)$$

B.2 Self energy of an imbalanced two-component dipolar Fermi gas

Starting from the expression

$$\hbar\Sigma_{\alpha\beta}(\mathbf{k}) = -\int \frac{d^3k'}{(2\pi)^3} \frac{1}{\hbar\beta} \sum_{n'} \mathrm{e}^{i\omega_{n'}0^+} G^0_{\delta\gamma}(\mathbf{k}', i\omega_{n'}) V_{ij}(\mathbf{k}-\mathbf{k}') \sigma^i_{\alpha\delta} \sigma^j_{\gamma\beta},$$

and performing the spin indices summation and the Matsubara sums we obtain

$$\begin{aligned}
\hbar\Sigma_{11}(\mathbf{k}) &= -\frac{4\pi\mu^2}{3} \int \frac{d^3k'}{(2\pi)^3} (3\cos^2\theta_{\mathbf{k}-\mathbf{k}'} - 1) \left[n_F(\epsilon^0_{\mathbf{k}'} - \mu_1) - n_F(\epsilon^0_{\mathbf{k}'} - \mu_2) \right] \\
\hbar\Sigma_{12}(\mathbf{k}) &= -\frac{4\pi\mu^2}{3} \int \frac{d^3k'}{(2\pi)^3} 3\cos\theta_{\mathbf{k}-\mathbf{k}'} \sin\theta_{\mathbf{k}-\mathbf{k}'} \mathrm{e}^{-i\phi_{\mathbf{k}-\mathbf{k}'}} \left[n_F(\epsilon^0_{\mathbf{k}'} - \mu_1) - n_F(\epsilon^0_{\mathbf{k}'} - \mu_2) \right]
\end{aligned} \tag{B.1}$$

Moreover one can show that $\Sigma_{21} = \Sigma_{12}^*$ and $\Sigma_{22} = -\Sigma_{11}$. Note that these expressions vanish for a system with equal number of particles in each of the σ^z eigenstates. By expanding the dipolar interaction in spherical harmonics and using the unperturbed distribution of momentum, the integrals can be calculated analytically with the result

$$\begin{aligned}
\hbar\Sigma_{11}(\mathbf{k}) &= -f(k)(3\hat{\mathbf{k}}_z^2 - 1) \\
\hbar\Sigma_{12}(\mathbf{k}) &= -f(k) 3\hat{\mathbf{k}}_z (\hat{\mathbf{k}}_x - i\hat{\mathbf{k}}_y)
\end{aligned} \tag{B.2}$$

$f(k)$ is a smooth function of the magnitude of the wave vector,

$$f(k) = \frac{2\mu^2}{\pi} \int_0^\infty k'^2 dk' \int_0^\infty \frac{dr}{r} j_2(kr) j_0(k'r) \left[n_F(\epsilon^0_{\mathbf{k}'} - \mu_1) - n_F(\epsilon^0_{\mathbf{k}'} - \mu_2) \right]$$

The self energy can be expanded in Pauli matrices as

$$\hbar\Sigma(\mathbf{k}) \quad = \quad \begin{pmatrix} \hbar\Sigma_{11} & \hbar\Sigma_{12} \\ \hbar\Sigma_{12}^* & -\hbar\Sigma_{11} \end{pmatrix} = \Sigma_i \sigma^i$$

where $\Sigma_i(\mathbf{k}) = -f(k)(3\hat{\mathbf{k}}_i\hat{\mathbf{k}}_z - \delta_{i,z})$. We know obtain Eqn. B.2. From Eqn. B.1 we write

$$V_{20}(\mathbf{k}-\mathbf{k}') = \frac{4\pi\mu^2}{3}(3\cos^2\theta_{\mathbf{k}-\mathbf{k}'} - 1) = \sum_{lm}\sum_{l'm'} V_{20}^{lm;l'm'}(k,k')Y_{lm}^*(\hat{\mathbf{k}}')Y_{l'm'}(\hat{\mathbf{k}})$$

Substituting back into Eqn. B.1 we obtain

$$\hbar\Sigma_{11}(\mathbf{k}) = -\sum_{l'm'} \sigma_{l'm'}(k)Y_{l'm'}(\hat{\mathbf{k}})$$

Where we defined the functions, $\sigma_{l'm'}(k)$, that depend only on the magnitude of the wave vector,

$$\sigma_{l'm'}(k) = \sum_{lm}\int \frac{d^3k'}{(2\pi)^3}\, V_{20}^{lm;l'm'}(k,k')Y_{lm}^*(\hat{\mathbf{k}}')\left[n_F(\epsilon^0_{\mathbf{k}'} - \mu_1) - n_F(\epsilon^0_{\mathbf{k}'} - \mu_2)\right] \tag{B.3}$$

The angular integration is simplified because the unperturbed distribution function is spherically symmetric:

$$\sigma_{l'm'}(k) = \frac{\sqrt{4\pi}}{(2\pi)^3}\int k'^2 dk' V_{20}^{00;l'm'}(k,k')\left[n_F(\epsilon^0_{\mathbf{k}'} - \mu_1) - n_F(\epsilon^0_{\mathbf{k}'} - \mu_2)\right] \tag{B.4}$$

The terms, $V_{20}^{00;l'm'}(k,k')$, are found by noticing that the Fourier transform of $V_{20}(\mathbf{r}) = (\mu^2/r^3)(1-3\cos^2\theta_{\mathbf{r}})$ is $V_{20}(\mathbf{q}) = (4\pi\mu^2/3)(3\cos^2\theta_{\mathbf{q}} - 1)$. Hence one case write by definition

$$V_{20}(k-k') = \int dr^3 e^{-i(\mathbf{k}-\mathbf{k}')\cdot\mathbf{r}} V_{20}(\mathbf{r}) \tag{B.5}$$

Note that $V(\mathbf{r})$ can also be written as

$$V_{20}(\mathbf{r}) = -\frac{\mu^2}{r^3}\, 2\sqrt{\frac{4\pi}{5}} Y_{20}(\hat{\mathbf{r}})$$

and substituting the spherical wave expansion of a plane wave

$$e^{-i\mathbf{k}\cdot\mathbf{r}} = 4\pi \sum_{lm} (-i)^l j_l(kr) Y_{lm}(\hat{\mathbf{k}}) Y^*_{lm}(\hat{\mathbf{r}}) \tag{B.6}$$

into eqn B.5 we can read off the only non-vanishing coefficient

$$V_{20}^{00;20}(k,k') = (4\pi)^2 \mu^2 \, 2\sqrt{\frac{4\pi}{5}} Y_{00} \int_0^\infty \frac{dr}{r} j_2(kr) j_0(k'r).$$

Substituting back into B.4 we obtain the only non-vanishing coefficient

$$\begin{aligned} \sigma_{20}(k) &= \frac{2}{\pi}\mu^2 \, 2\sqrt{\frac{4\pi}{5}} \int k'^2 dk' \int \frac{dr}{r} \, j_2(kr) j_0(k'r) \left[n_F(\epsilon^0_{\mathbf{k}'} - \mu_1) - n_F(\epsilon^0_{\mathbf{k}'} - \mu_2) \right] \\ &= 2\sqrt{\frac{4\pi}{5}} f(k) \end{aligned} \tag{B.7}$$

at $T = 0$, the function $f(k)$ is explicitly given by given by $f(k) = g(k, k_{F1}) - g(k, k_{F2})$, where $g(x, y)$ depends on two parameters and is given by

$$g(x,y) = \frac{\mu^2}{76\pi} \frac{1}{x^3} \left[3x^5 y + 8x^3 y^3 - 3xy^5 - \frac{3}{2}(x^2 - y^2)^3 \ln \left| \frac{y+x}{y-x} \right| \right]$$

Finally,

$$\hbar \Sigma_{11}(\mathbf{k}) = -f(k)(3\cos^2\theta_{\mathbf{k}} - 1) = -f(k)(3\hat{\mathbf{k}}_z^2 - 1)$$

If $\mu_1 > \mu_2$ then $k_{F1} > k_{F2}$, where k_F are the unperturbed Fermi wave vectors. In this case $f(k) > 0$.

Appendix C

C.1 Mean field theory of nematic to biaxial-nematic phase transition

Consider a homogeneous system of Fermionic polarized dipoles. Consider a variational distribution function of fermions with two preferred directions.

$$f(\mathbf{k}) = \Theta\left(k_F^2 - \alpha^{-1}(\beta k_x^2 + \frac{1}{\beta}k_y^2) - \alpha^2 k_z^2\right).$$

The variational parameters are α and β. For $\alpha = 1$ and $\beta = 1$ the Fermi surface is a sphere, but for $\alpha \neq 1$ and $\beta \neq 1$ the FS is in general an ellipsoid with three unequal principal axes. i.e. it is not an ellipsoid of revolution. The advantage of using this wave function is that it allows consideration ,in a simple way, of *all* channels of the dipolar interaction.

Defining $k_{1x} = \alpha^{-1/2}\beta^{1/2}k_x$, $k_{1y} = \alpha^{-1/2}\beta^{-1/2}k_y$ and $k_{1z} = \alpha k_z$ we have that the volume element is conserved $d^3k_1 = d^3k$, i.e., an ellipsoid is topologically equivalent to a sphere. The number of particles is independent of the variational parameters α, β i.e.,

$$\int \frac{d^3k}{(2\pi)^3} f(\vec{k}) = \int \frac{d^3k}{(2\pi)^3}\Theta(k_F^2 - k^2) = \frac{k_F^3}{6\pi^2} \equiv n_f$$

The kinetic energy term is

$$
\begin{aligned}
E_{kin} &= \int d^3r \int \frac{d^3k}{(2\pi)^3}\,\frac{\hbar^2k^2}{2m}\,f(\mathbf{k}) \\
&= \frac{\hbar^2 V}{(2\pi)^3 2m}\int d^3k(\frac{1}{\beta}\alpha k_x^2+\alpha\beta k_y^2+\alpha^{-2}k_z^2)\Theta(k_F^2-k^2) \\
&= \frac{V\hbar^2k_F^5}{10m6\pi^2}\left[\frac{\alpha}{\beta}+\alpha\beta+\frac{1}{\alpha^2}\right]
\end{aligned}
$$

If $\beta = 1$ we recover our well know equation for the uniaxial distortions. As expected, the kinetic energy term is minimized for a spherical FS and penalizes any distortions of the FS.

The dipolar terms in Hartree-Fock are the direct term

$$
E_{hartree} = \frac{1}{2}\int d^3r \int d^3r'\, V_d(\vec{r}-\vec{r}')n(\vec{r})n(\vec{r}') = 0 \tag{C.1}
$$

Since we are considering the homogeneous density system. Note that in the semi-classical approach, the real space distribution of particles given by $n(\mathbf{r}) = (2\pi)^{-3}\int d^3\,k f(\mathbf{r},\mathbf{k})$. The exchange term is

$$
E_{fock} = -\frac{1}{2}\int d^3r \int d^3r' \int \frac{d^3k}{(2\pi)^3}\frac{d^3k}{(2\pi)^3}\,V_d(\mathbf{r}-\mathbf{r}')e^{i\,(\mathbf{k}-\mathbf{k}')(\mathbf{r}-\mathbf{r}')}f(\frac{\mathbf{r}+\mathbf{r}'}{2},\mathbf{k})f(\frac{\mathbf{r}+\mathbf{r}'}{2},\mathbf{k}')
$$

Which for homogeneous system become simply,

$$
E_{fock} = -\frac{V}{2}\int \frac{d^3k}{(2\pi)^3}\frac{d^3k'}{(2\pi)^3}\,V_d(\mathbf{k}-\mathbf{k}')f(\mathbf{k})f(\mathbf{k}')
$$

Where the Fourier transform of the dipolar interaction is

$$
V_d(\mathbf{k}-\mathbf{k}') = \frac{4\pi}{3}d^2(3\cos^2\theta_{\mathbf{k}-\mathbf{k}'}-1)
$$

Performing a change of variables and setting $\mathbf{k}_r = \mathbf{k}_1 - \mathbf{k}_2$ and $\mathbf{k}_m = \mathbf{k}_2$.

$$
\begin{aligned}
E_{fock} &= -\frac{V}{2}\frac{4\pi d^2}{3}\int \frac{d^3k_r}{(2\pi)^3}\frac{d^3k_m}{(2\pi)^3}\left[\frac{3k_{rz}^2}{\alpha^3\beta^{-1}k_{rx}^2+\alpha^3\beta k_{ry}^2+k_{rz}^2}-1\right] \\
&\qquad \times\Theta(k_F^2-|\mathbf{k_r}+\mathbf{k_m}|^2)\Theta(k_F^2-\mathbf{k_m^2}) \\
&= -\frac{V}{2}\frac{4\pi d^2}{3}\frac{1}{(2\pi)^6}\int d\phi d\theta\left[\frac{3\cos^2\theta}{\alpha^3\beta^{-1}\sin^2\theta\cos^2\phi+\alpha^3\beta\sin^2\theta\cos^2\phi+\cos^2\theta}-1\right] \\
&\quad \times\int k_r^2 dk_r\int\frac{d^3k_r}{(2\pi)^3}\Theta(k_F^2-|\mathbf{k_r}+\mathbf{k_m}|^2)\Theta(k_F^2-\mathbf{k_m^2})
\end{aligned}
\tag{C.2}
$$

The last integral is just the volume of intersection of two spheres of radius k_F whose centers are separated by a vector $\mathbf{k_r}$. Due to the spherical symmetry the result of this integration depends only on the distance k_r. In fact, one can show that

$$
\int\frac{d^3k_r}{(2\pi)^3}\Theta(k_F^2-|\mathbf{k_r}+\mathbf{k_m}|^2)\Theta(k_F^2-\mathbf{k_m^2})=\frac{2\pi}{3}(k_F-\frac{k_r}{2})^2(2k_F+\frac{k_r}{2})
$$

For $0<k_r<2k_F$ and equals 0 for $k_r>2k_F$. Performing the rest of integrations we arrive at

$$
E_{int}=-\frac{V\pi\, n_f^2 d^2}{3}I(\alpha,\beta)
$$

Where $I(\alpha,\beta)$ is

$$
I(\alpha,\beta)=\int_0^\pi d\theta\sin\theta\left[\frac{3\,\cos^2\theta}{\left(\alpha^3\beta\sin^2\theta+\cos^2\theta\right)^{1/2}\left(\alpha^3\beta^{-1}\sin^2\theta+\cos^2\theta\right)^{1/2}}-1\right]
$$

If $\beta=1$ we recover the result which agrees with the deformation function of ref. [140]. The total energy density $\mathcal{E}=\mathcal{E}_{kin}+\mathcal{E}_{int}$ is

$$
\frac{\mathcal{E}_{tot}}{\mathcal{E}_0}=\frac{1}{3}\left(\frac{\alpha}{\beta}+\alpha\beta+\frac{1}{\alpha^2}\right)-\frac{10\pi}{9(6\pi^2)^{2/3}}C_{dd}I(\alpha,\beta)
$$

where $\mathcal{E}_0=\hbar^2k_F^2 3n/10m$, $C_{dd}=a_d n^{1/3}$ and $a_d=md^2/\hbar^2$ is the dipolar dimensionless interaction strength. Numerically minimizing the total energy we find that for all reasonable values of C_{dd}, $\alpha<1$ and $\beta=1$, i.e.,

Only the uniaxial phase exist but nit the biaxial phase.

C.2 Biaxial-nematic in a trap

We can repeat the same calculation for a systems in a axially symmetric trap. It needs to be axially symmetric because we do not want to break the SO(2) rotational symmetry of the xy-plane. The trap potential has the form

$$U(r) = \frac{m}{2}[\omega_r^2(x^2+y^2) + \omega_z^2 z^2]$$

Following ref. [140] start by proposing a variational form of the Fermi wave vector that varies in space with axial symmetry.

$$k_F^2(\vec{r}) = (k_F^\lambda)^2 - \lambda^2 a_{ho}^{-4}(\beta(x^2+y^2) + \beta^{-2}z^2)$$

where $a_{ho} = 1/(m\omega)^{1/2}$ and $\omega = (\omega_r^2\omega_z)^{1/3}$. Then after a tedious calculations which are very similar to the ones above we get the total energy.

$$\epsilon(\alpha,\alpha',\beta,\lambda) = c_1\left[\lambda\left(\frac{\alpha'^3 + \alpha^3(1+\alpha'^3)}{\alpha^2\alpha'^2}\right) + \frac{1}{\lambda}\left(2\frac{\beta_0}{\beta} + \frac{\beta^2}{\beta_0^2}\right)\right] + c_2 c_{dd} N^{1/6}\lambda^{3/2}\big[I(\beta) - I(\alpha,\alpha')\big]$$

Where the biaxial nematic distortion is parametrized by α'. The dipolar interaction is parametrized by $c_{dd} = d^2/(a_{ho}^3\omega)$ which is the ratio of dipolar energy in the volume of the trap to the quantum energy for a trap. Finally, $\beta_0 = (\omega_r/\omega_z)^{2/3}$. Minimization of this energy shows that there is no region in the space or variational parameters where the biaxial-nematic is stable. The only stable being a uniaxial nematic distortion.

Appendix D

D.1 Fourier transform of dipole-dipole interaction

The dipole interaction is $V_d(r) = (d^2/r^3)(1 - 3\,\cos^2\theta)$ One shows that $V_d(0) = 0$ from

$$V_d(q=0) = d^2 \int r^2 \frac{1}{r^3} dr \int d\Omega \left(1 - 3\cos^2\theta\right) = 0$$

The Fourier transform of the dipolar interaction is simplified if we express the exponentials in terms of spherical harmonics, then: see also [111].

$$V(\vec{q}) = \int d^3r \exp^{-i\vec{q}\cdot\vec{r}} V_d(\vec{r})$$

But $V_d(\vec{r}) = (d^2/r^3)(1 - 3\,\cos^2\theta_r)$ and $\mathrm{e}^{i\vec{k}\cdot\vec{r}} = 4\pi \sum_{l,m} i^l Y^*_{lm}(\hat{k}) j_l(kr) Y_{lm}(\hat{r})$ hence

$$\begin{aligned} V(\vec{k}) &= (4\pi)(-2d^2)\sqrt{\frac{4\pi}{5}}(-i)^2 \int_b^\infty \frac{d\,r}{r} Y_{2,0}(\hat{k}) j_2(kr) \\ &= (4\pi)(2d^2)\left[\int_{bk}^\infty \frac{dx}{x} j_2(kr)\right] P_2(k) \\ &= (4\pi)(2d^2)\left[\frac{\sin kb}{(kb)^3} - \frac{\cos kb}{(kb)^2}\right] P_2(k) \end{aligned}$$

Where b is a short range cut off bellow which the dipolar interaction is not valid. For small b we have

$$\begin{aligned} V(\vec{k}) &= \frac{(4\pi)}{3}(2d^2)\left[1 - \frac{(kb)^2}{10}\right] P_2(k) \\ &= \frac{4\pi d^2}{3}\left[1 - \frac{(kb)^2}{10}\right](3\cos^2\theta_k - 1) \end{aligned}$$

The important point is that at long length scales i.e. $k \to 0$ the Fourier transform if the dipolar interaction depends only on angle not on the magnitude. Compare this behavior with long range potential such as

Coulomb where its Fourier component blow up as $k \to 0$ or with very short range potentials where only the Fourier components of $\sim q \sim 0$ are non-vanishing. Dipolar interaction, for which the limit $k \to 0$ is not defined,(but $V(\vec{q} = 0) = 0!$) is, in a sense, very pathological it is not so long ranged but not atological it is not so long ranged but not so short either!

Where θ is the polar angle between z and vector distance between the center of the dipoles assumed point-like objects. b is a natural cut off where the dipolar two body interaction stops being of the dipolar type. for $r < b$ one action stops being of the dipolar type. for $r < b$ one needs to take into account Coulomb repulsion between the atoms electronic clouds. For C_r it is quoted [207] that $b \sim 100a_0$. The important point is that there is a small length scale $b > 0$ that may play a role in the phenomena at low energies and densities. The above form of Fourier transform does not have a well defined limit $q \to 0$. If $\theta\pi/2$ $V(\hat{q}) = -4\pi d^2/3$ where as if $\theta = 0$, $V(\hat{q}) = 8\pi d^2/3$.

References

[1] Within two body physics, the interaction energy is more correctly given in terms of two-body phase shifts, rather than scattering lengths: $E_{\rm int} \simeq -4\pi\hbar^2\delta n/km$, where $k \lesssim k_F$ is an averaged relative momentum in the interaction, $\sim k_F$, and $\delta = -\tan^{-1}(ka)$ is the scattering phase shift. Thus in this case, we would write $ka_{\rm eff} \sim \tan^{-1}(ka)$, which is similar in structure to Eq. (2.11). This result corresponds to $\gamma = 2k/\pi k_F$.

[2] The term $iN^\dagger(\partial_x + i\partial_y)N^\dagger(\partial_x + i\partial_y)N + h.c.$ is not allowed due to chiral symmetry.

[3] A nematic-spin-nematic [103, 212] is a 2D invariant under a rotation by π followed by a spin flip. The uniaxial 3D ferro-nematic state discussed here does not have this property, as its up FS and down FS, although oppositely distorted, are not equivalent under a rotation.

[4] Sogo *et al* [189] estimated that the homogeneous fully polarized dipolar Fermi gas becomes unstable at a critical value of $C_{dd} \equiv (3\pi^2)^{2/3}(\lambda_d/2) \simeq 3.2$. The correct value is $C_{dd} \simeq 2.5$.

[5] G. Baym and T. Hatsuda, private communication (2009).

[6] P. Abbamonte, A. Rusydi, S. Smadici, G. D. Gu, G. A. Sawatzky, and D. L. Feng. Spatially modulated 'Mottness' in $La_{2-x}Ba_xCuO_4$. *Nature Phys.*, 1:155, 2005.

[7] B. L. Altshuler, L. B. Ioffe, and A. J. Millis. Critical behavior of the $T = 0$, $2k_F$, density-wave phase transition in a two-dimensional Fermi liquid. *Phys. Rev. B*, 52:5563, 1995.

[8] D. J. Amit. *Field Theory, the Renormalization Group and Critical Phenomena*. McGraw Hill, New York, NY, 1980.

[9] Y. Ando, K. Segawa, S. Komiya, and A. N. Lavrov. Electrical Resistivity Anisotropy from Self-Organized One-Dimensionality in High-Temperature Superconductors. *Phys. Rev. Lett.*, 88:137005, 2002.

[10] V. I. Anisimov, M. A. Korotin, A. S. Mylnikova, A. V. Kozhevnikov, Dm. M. Korotin, and J. Lorenzana. Computation of stripes in cuprates within the lda+u method. *Phys. Rev. B.*, 70:172501, 2004.

[11] Enrico Arrigoni, Eduardo Fradkin, and Steven A. Kivelson. Mechanism of High Temperature Superconductivity in a striped Hubbard Model. *Phys. Rev. B*, 69:214519, 2004.

[12] G.A. Baker. *Phys. Rev. C.*, 60:054311, 1999.

[13] M A Baranov. Theoretical progress in many-body physics with ultracold dipolar gases. *Physics Reports*, 464:71–111, 2008.

[14] H. Barath, M. Kim, J. F. Karpus, S. L. Cooper, P. Abbamonte, E. Fradkin, E. Morosan, and R. J. Cava. Quantum and classical mode softening near the charge-density-wave/superconductor transition of Cu_xTiSe_2: Raman spectroscopic studies. *Phys. Rev. Lett.*, 100:106402, 2008.

[15] Daniel G. Barci, Eduardo Fradkin, Steven A. Kivelson, and Vadim Oganesyan. Theory of the quantum Hall Smectic Phase. I. Low-energy properties of the quantum Hall smectic fixed point. *Phys. Rev. B*, 65(24):245319, Jun 2002.

[16] Sourish Basu and Erich J. Mueller. Stability of bosonic atomic and molecular condensates near a feshbach resonance. *Phys. Rev. A*, 78:053603, 2008.

[17] G. Baym and C. J. Pethick. *Phys. Rev. Lett.*, 76:6, 1996.

[18] Gordon Baym and Christopher Pethick. *Landau Fermi-Liquid Theory.* John Wiley & Sons, 1991.

[19] Erez Berg, Eduardo Fradkin, Eun-Ah Kim, Steven Kivelson, Vadim Oganesyan, John M. Tranquada, and Shoucheng Zhang. Dynamical layer decoupling in a stripe-ordered high T_c superconductor. *Phys. Rev. Lett.*, 99:127003, 2007.

[20] D. J. Bergman, T. M. Rice, and P. A. Lee. Fluctuations, coulomb effects, and long-range order in incommensurate charge-density-wave structures. *Phys. Rev. B*, 15(4):1706–1718, Feb 1977.

[21] R. A. Borzi, S. A. Grigera, J. Farrell, R. S. Perry, S. J. S. Lister, S. L. Lee, D. A. Tennant, Y. Maeno, and A. P. Mackenzie. Formation of a Nematic Fluid at High Fields in $Sr_3Ru_2O_7$. *Science*, 315:214, 2007.

[22] T. Bourdel, J. Cubizolles, L. Khaykovich, K. M. F. Magalh aes, S. J. J. M. F. Kokkelmans, G. V. Shyapnikov, and C. Salamon. *Phys. Rev. Lett.*, 91:020402, 2003.

[23] C.C. Bradley, C.A. Sackett, J.J. Tollett, and R.G. Hulet. *Phys. Rev. Lett.*, 75:1687, 1995.

[24] S. A. Brazovskii. Phase transition of an isotropic system to a nonuniform state. *Soviet Physics JETP*, 41:85, 1975.

[25] F. Brochard and P. G. de Gennes. Theory of magnetic suspensions in liquid crystals. *J. Physique (Paris)*, 31:691, 1970.

[26] V. Brouet, W. L. Yang, X. J. Zhou, Z. Hussain, N. Ru, K. Y. Shin, I. R. Fisher, and Z. X. Shen. Fermi Surface Reconstruction in the CDW State of $CeTe_3$ Observed by Photoemission. *Phys. Rev. Lett.*, 93:126405, 2004.

[27] G. M. Bruun and E. Taylor. Quantum phases of a two-dimensional dipolar Fermi gas. 2008.

[28] D. A. Butts and D. S. Rokhsar. *Phys. Rev. A*, 55:4346, 1997.

[29] E. W. Carlson, V. J. Emery, S. A. Kivelson, and D. Orgad. Concepts in High Temperature Superconductivity. In K. H. Bennemann and J. B. Ketterson, editors, *The Physics of Conventional and Unconventional Superconductors*, Berlin, 2004. Springer-Verlag.

[30] E. W. Carlson, D. Orgad, S. A. Kivelson, and V. J. Emery. Dimensional crossover in quasi one-dimensional and high t_c superconductors. *Phys. Rev. B*, 62:3422, 2000.

[31] J. Carlson, S.-Y. Chang, V. R. Pandharipande, and K. E. Schmidt. *Phys. Rev. Lett.*, 91:050401, 2003.

[32] Antonio H. Castro Neto and Eduardo Fradkin. Bosonization of the low energy excitations of fermi liquids. *Phys. Rev. Lett.*, 72:1393, 1994.

[33] Antonio H. Castro Neto and Eduardo Fradkin. Exact solution of the landau fixed point via bosonization. *Phys. Rev. B*, 51:4084, 1995.

[34] P. M. Chaikin and T. C. Lubensky. *Principles of Condensed Matter Physics.* Cambridge University Press, Cambridge, UK, 1998.

[35] S. Chakravarty, R. B. Laughlin, D. K. Morr, and C. Nayak. Hidden order in the cuprates. *Phys. Rev. B*, 63:094503, 2001.

[36] Ching-Kit Chan, Congjun Wu, Wei-Cheng Lee, and S. Das Sarma. Anisotropic fermi liquid theory of the ultra cold fermionic polar molecules: Landau parameters and collective modes. arXiv:0906.4403v4.

[37] R. Chicireanu et al. *Phys. Rev. Lett.*, 73:053406, 2006.

[38] A. V. Chubukov and D. V. Khveshchenko. The effect of Fermi surface curvature on low-energy properties of fermions with singular interactions. *Phys. Rev. Lett.*, 97:226403, 2006.

[39] Andrey V. Chubukov, Victor M. Galitski, and Victor M. Yakovenko. Quantum Critical Behavior Near a Density-Wave Instability in an Isotropic Fermi Liquid. *Phys. Rev. Lett.*, 94:046404, 2005.

[40] K. B. Cooper, J. P. Eisenstein, L. N. Pfeiffer, and K. W. West. Observation of narrow-band noise accompanying the breakdown of insulating states in high landau levels. *Phys. Rev. Lett.*, 90:226803, 2003.

[41] K. B. Cooper, M. P. Lilly, J. P. Eisenstein, T. Jungwirth, L. N. Pfeiffer, and K. W. West. An investigation of orientational symmetry-breaking mechanisms in high landau levels. *Sol. State Commun.*, 119:89, 2001.

[42] K. B. Cooper, M. P. Lilly, J. P. Eisenstein, L. N. Pfeiffer, and K. W. West. Onset of anisotropic transport of two-dimensional electrons in high Landau levels: Possible isotropic-to-nematic liquid-crystal phase transition. *Phys. Rev. B*, 65:241313, 2002.

[43] V. Cvetkovic. *Ann. Phys. (N. Y.)*, 310:181, 2007.

[44] V. Cvetkovic, Z. Nussinov, S. Mukhin, and J. Zaanen. Observing the fluctuating stripes in high Tc superconductors. *Euro. Phys. Lett.*, 81:27001, 2007.

[45] V. Cvetkovic, Z. Nussinov, and J. Zaanen. Topological kinematical constraints: quantum dislocations and glide principle. *Phil. Mag.*, 86:2995, 2006.

[46] Elbio Dagotto, Takashi Hotta, and Adriana Moreo. Colossal magnetoresistant materials: the key role of phase separation. *Phys. Rep.*, 344:1, 2001.

[47] Hongjie Dai, Huifen Chen, and Charles M. Lieber. Weak Pinning and Hexatic Order in a Doped Two-Dimensional Charge-Density-Wave System. *Phys. Rev. Lett.*, 66:3183, 1991.

[48] P. G. de Gennes and J. Prost. *The Physics of Liquid Crystals*. Oxford Science Publications, Oxford, 1993.

[49] B. Deb and L. You. Low-energy atomic collition with dipole interactions. *Phys. Rev. A*, 64:022717, 2001.

[50] Luca Dell'Anna and Walter Metzner. Fermi surface fluctuations and single electron excitations near Pomeranchuk instability in two dimensions. *Phys. Rev. B*, 73:45127, 2006.

[51] Q. M. Doan and E. Manousakis. Quantum nematic as ground state of a two-dimensional electron gas in a magnetic field. *Phys. Rev. B*, 75:195433, 2007.

[52] Nicolas Doiron-Leyraud, Cyril Proust, David LeBoeuf, Julie Levallois, Jean-Baptiste Bonnemaison, Ruixing Liang, D. A. Bonn, W. N. Hardy, and Louis Taillefer. Quantum oscillations and the Fermi surface in an underdoped high-T_c superconductor. *Nature*, 447:565–568, 2007.

[53] R. R. Du, D. C. Tsui, H. L. Störmer, L. N. Pfeiffer, K. W. Baldwin, and K. W. West. Strongly anisotropic transport in higher two-dimensional landau levels. *Solid State Comm.*, 109:389, 1999.

[54] R. A. Duine and A. H. MacDonald. Itinerant ferromagnetism in an ultracold atom fermi gas. *Phys Rev Lett*, 95:230403, 2005.

[55] V. J. Emery, E. Fradkin, S. A. Kivelson, and T. C. Lubensky. Quantum Theory of the Smectic Metal State in Stripe Phases. *Phys. Rev. Lett.*, 85:2160, 2000.

[56] V. J. Emery and S. A. Kivelson. Frustrated electronic phase separation and high-temperature superconductors. *Physica C*, 209:597, 1993.

[57] V. J. Emery, S. A. Kivelson, and O. Zachar. Spin-Gap Proximity Effect Mechanism of High Temperature Superconductivity. *Phys. Rev. B*, 56:6120, 1997.

[58] A. Fang, N. Ru, I. R. Fisher, and A. Kapitulnik. STM Studies of Tb Te_3: Evidence for a Fully Incommensurate Charge Density Wave. *Phys. Rev. Lett.*, 99:046401, 2007.

[59] Chen Fang, Hong Yao, Wei-Feng Tsai, Jian Ping Hu, and Steven A. Kivelson. Theory of Electron nematic Order in LaOFeAs, 2008.

[60] William Fogle and Jerome H. Perlstein. Semiconductor-to-Metal Transition in the Blue Potassium Molybdenum Bronze, $K_{0.30}$ MoO_3; Example of a Possible Excitonic Insulator. *Phys. Rev. B*, 6(4):1402–1412, Aug 1972.

[61] I. A. Fomin, C. J. Pethick, and J. W. Serene. Influence of internal fields on magnetic and electric orientational effects in superfluid ^{3}he. *Phys Rev. Lett.*, 40:1144, 1978.

[62] E. Fradkin and S. A. Kivelson. Liquid-Crystal Phases of Quantum Hall Systems. *Phys. Rev. B*, 59:8065, 1999.

[63] E. Fradkin, S. A. Kivelson, E. Manousakis, and K. S. Nho. Nematic phase of the two-dimensional electron gas in a magnetic field. *Phys. Rev. Lett.*, 84:1982, 2000.

[64] E. Fradkin, S. A. Kivelson, and V. Oganesyan. Discovery of a Nematic Electron Fluid in a Transition Metal Oxide. *Science*, 315:196–197, 2007.

[65] Benjamin M. Fregoso and Gordon Baym. Stability of trapped fermionic gases with attractive interactions. *Phys. Rev. A*, 73:043616, 2006.

[66] Benjamin M. Fregoso and Eduardo Fradkin. Unconventional magnetism in imbalanced fermi systems with magnetic dipolar interactions. arXiv:1001.4167v1 (2010).

[67] Benjamin M. Fregoso and Eduardo Fradkin. Ferronematic ground state of the dilute dipolar fermi gas. *Phys. Rev. Lett.*, 103:205301, 2009.

[68] Benjamin M. Fregoso, Kai Sun, Eduardo Fradkin, and Benjamin L. Lev. Biaxial nematic phases in ultracold dipolar fermi gases. *New J. Phys.*, 11:103003, 2009.

[69] H. Frohlich. On the Theory of Superconductivity: The One-Dimensional Case. *Proc. Roy. Soc (London) Series A*, 223:296–305, May 1954.

[70] M. E. Gehm, S. L. Hemmer, S. R. Granade, K. M. O'Hara, and J. E. Thomas. *Phys. Rev. A.*, 68:011401, 2003.

[71] P. Ghaemi, A. Vishwanath, and T. Senthil. Finite temperature properties of quantum lifshitz transitions between valence-bond solid phases: An example of local quantum criticality. 72:024420, 2005.

[72] M. Granath, V. Oganesyan, S. A. Kivelson, E. Fradkin, and V. J. Emery. Nodal quasi-particles and coexisting orders in striped superconductors. *Phys. Rev. Lett.*, 87:167011, 2001.

[73] A. G. Green, S. A. Grigera, R. A. Borzi, A. P. Mackenzie, R. S. Perry, and B. D. Simons. Phase bifurcation and quantum fluctuations in sr_3 ru_2o_7. *Phys. Rev. Lett.*, 95:086402, 2005.

[74] A. Griesmaier et al. *Phys. Rev. Lett.*, 94:160401, 2005.

[75] S. A. Grigera, R. S. Perry, A. J. Schofield, M. Chiao, S. R. Julian, G. G. Lonzarich, S. I. Ikeda, Y. Maeno, A. J. Millis, and A. P. Mackenzie. Magnetic field-tuned quantum criticality in the metallic ruthenate $sr_3ru_2o_7$. *Science*, 294:329, 2001.

[76] G. Grinstein and Robert A. Pelcovits. Anharmonic Effects in Bulk Smectic Liquid Crystals and Other "One-Dimensional Solids". *Phys. Rev. Lett.*, 47:856–859, Sep 1981.

[77] G. Grüner. The dynamics of charge-density waves. *Rev. Mod. Phys.*, 60:1129, 1988.

[78] G. Grüner. The dynamics of spin-density-waves. *Rev. Mod. Phys.*, 66:1, 1994.

[79] C. J. Halboth and W. Metzner. d-wave superconductivity and Pomeranchuk instability in the two-dimensional Hubbard model. *Phys. Rev. Lett.*, 85:5162, 2000.

[80] F. D. M. Haldane. Luttinger's Theorem and Bosonization of the Fermi surface. In J. R. Schrieffer and R. Broglia, editors, *Proceedings of the International School of Physics "Enrico Fermi," course 121, Varenna, 1992*, New York, 1994. North-Holland.

[81] B. I. Halperin, T. C. Lubensky, and S-K Ma. First-Order Phase Transitions in Superconductors and Smectic-*A* Liquid Crystals. *Phys. Rev. Lett.*, 32:292–295, Feb 1974.

[82] T. Hanaguri, C. Lupien, Y. Kohsaka, D. H. Lee, M. Azuma, M. Takano, H. Takagi, and J. C. Davis. A 'checkerboard' electronic crystal state in lightly hole-doped $Ca_{2-x}Na_xCuO_2Cl_2$. *Nature*, 430:1001, 2004.

[83] H. Heiselberg. *Phys. Rev. A.*, 63:043606, 2001.

[84] John A. Hertz. Quantum critical phenomena. *Phys. Rev. B*, 14:1165, 1976.

[85] A. Himeda, T. Kato, and M. Ogata. Stripe States with Spatially Oscillating d-Wave Superconductivity in the two-dimensional $t - t' - J$ model. *Phys. Rev. Lett.*, 88:117001, 2002.

[86] V. Hinkov, P. Bourges, S. Pailhés, Y. Sidis, A. Ivanov, C.T. Lin, D.P. Chen, and B. Keimer. In-plane anisotropy of spin excitations in the normal and superconducting states of underdoped $YBa_2Cu_3O_{6+y}$. unpublished, 2006.

[87] V. Hinkov, D. Haug, B. Fauqué, P. Bourges, Y. Sidis, A. Ivanov, C. Bernhard, C. T. Lin, and B. Keimer. Electronic liquid crystal state in superconducting $YBa_2Cu_3O_{6.45}$. *Science*, 319:597, 2008.

[88] T.-L. Ho and E. J. Mueller. *Phys. Rev. Lett.*, 92:160404, 2004.

[89] C. Honerkamp, M. Salmhofer, and T. M. Rice. Flow to strong coupling in the two-dimensional Hubbard model. *Euro. Phys. J. B*, 27:127, 2002.

[90] M. Houbiers, R. Ferwerda, H. T. C. Stoof, W. I. McAlexander, C. A. Sackett, and R. G. Hulet. *Phys. Rev. A*, 56:4864, 1997.

[91] A. Houghton, H. J. Kwon, and J. B. Marston. Multidimensional Bosonization. *Adv. Phys.*, 49:141, 2000.

[92] A. Houghton and J. B. Marston. Bosonization and fermion liquids in dimensions greater than one. 48:7790, 1993.

[93] C. Howald, H. Eisaki, N. Kaneko, M. Greven, and A. Kapitulnik. Periodic density of states modulations in superconducting $Bi_2Sr_2CaCu_2O_{8+\delta}$. *Phys. Rev. B*, 67:014533, 2003.

[94] Yoseph Imry and Shang-Keng Ma. Random-field instability of the ordered state of continuous symmetry. *Phys. Rev. Lett.*, 35(21):1399–1401, Nov 1975.

[95] Reza Jamei, Steven Kivelson, and Boris Spivak. Universal aspects of Coulomb-frustrated phase separation. *Phys. Rev. Lett.*, 94:056805, 2005.

[96] Gyu-Boong Jo, Ye-Ryoung Lee, Jae-Hoon Choi, Caleb A. Christensen, Tony H. Kim, Joseph H. Thywissen, David E. Pritchard, and Wolfgang Ketterle. Itinerant ferromagnetism in a fermi gas of ultracold atoms. *Science*, 325:1521 – 1524, 2009.

[97] S. Jochim, M. Bartenstein, A. Altmeyer, G. Hendl, S. Riedl, C. Chin, J. Hecker Denschlag, and R. Grimm. *Science*, 302:2101, 2003.

[98] K. B. Cooper et al. Onset of anisotropic transport of two-dimensional electrons in high Landau levels: Possible isotropic-to-nematic liquid-crystal phase transition. 65:241313, 2002.

[99] Y. Kamihara, T. Watanabe, M. Hirano, and H. Hosono. *J. Am. Chem. Soc.*, 130:3269, 2008.

[100] M. Kato, K. Machida, H. Nakanishi, and M. Fujita. *J. Phys. Soc. Jpn.*, 59:1047, 1990.

[101] Hae-Young Kee, Eugene H. Kim, and Chung-Hou Chung. Signatures of an electronic nematic phase at the isotropic-nematic phase transition. *Phys. Rev. B*, 68(24):245109, Dec 2003.

[102] Igor Khavkine, Chung-Hou Chung, Vadim Oganesyan, and Hae-Young Kee. Formation of an electronic nematic phase in interacting fermion systems. *Phys. Rev. B*, 70:155110, 2004.

[103] S. A. Kivelson, I. P. Bindloss, E. Fradkin, V. Oganesyan, J. M. Tranquada, A. Kapitulnik, and C. Howald. How to detect fluctuating stripes in the high-temperature superconductors. *Rev. Mod. Phys.*, 75:1201, 2003.

[104] S. A. Kivelson, E. Fradkin, and V. J. Emery. Electronic liquid-crystal phases of a doped mott insulator. *Nature*, 393:550, 1998.

[105] Steven A. Kivelson and Eduardo Fradkin. How optimal inhomogeneity produces high temperature superconductivity. In J. Robert Schrieffer and J. Brooks, editors, *Treatise of High Temperature Superconductivity*, pages 569–595, Berlin, 2007. Springer-Verlag.

[106] Steven A. Kivelson, Eduardo Fradkin, and Theodore H. Geballe. Quasi-1d dynamics and the nematic phase of the 2d emery model. *Phys. Rev. B*, 69:144505, 2004.

[107] Y. Kohsaka, C. Taylor, K. Fujita, A. Schmidt, C. Lupien, T. Hanaguri, M. Azuma, M. Takano, H. Eisaki, H. Takagi, S. Uchida, and J. C. Davis. An Intrinsic Bond-Centered Electronic Glass with Unidirectional Domains in Underdoped Cuprates. *Science*, 315:1380–1385, 2007.

[108] A. L. Korzhenevskii and B. N. Shalaev. Effect of fluctuations on the properties of the phase transition from a nematic liquid crystal to an isotropic liquid. *Sov. Phys. JETP*, 49:1094, 1979.

[109] J. M. Kosterlitz and D. J. Thouless. Order, metastability and phase transitions in two-dimensional systems. *J. Phys. C: Solid State Phys.*, 6:1181, 1973.

[110] A. A. Koulakov, M. M. Fogler, and B. I. Shklovskii. Charge Density Wave in Two-Dimensional Electron Liquid in Weak Magnetic Field. *Phys. Rev. Lett.*, 76:499, 1996.

[111] G. Krzysztof, K. Rzazewski, and T. Pfau. Bose-einsten condensation with magnetic dipole forces. *Phys. Rev. A*, 61:051601(R), 2000.

[112] L. D. Landau. *Phys. Z. Sowjet Union*, 2:26, 1937.

[113] J. Laverock, S. B. Dugdale, Zs. Major, M. A. Alam, N. Ru, I. R. Fisher, G. Santi, and E. Bruno. Fermi surface nesting and charge-density wave formation in rare-earth tritellurides. *Phys. Rev. B*, 71:085114, 2005.

[114] Michael J. Lawler, Daniel G. Barci, Victoria Fernández, Eduardo Fradkin, and Luis Oxman. Nonperturbative behavior of the quantum phase transition to a nematic Fermi fluid. *Phys. Rev. B*, 73:085101, 2006.

[115] Michael J. Lawler and Eduardo Fradkin. Quantum Hall smectics, sliding symmetry, and the renormalization group. *Phys. Rev. B*, 70:165310, 2004.

[116] Michael J. Lawler and Eduardo Fradkin. Local Quantum Criticality in the Nematic Quantum Phase Transition of a Fermi Fluid. *Phys. Rev. B*, 75:033304, 2007.

[117] P. A. Lee, T. M. Rice, and P. W. Anderson. Conductivity from charge or spin density waves. *Sol. State Commun.*, 14:703, 1974.

[118] Anthony James Leggett. *Quantum Liquids: Bose Condensation and Cooper Pairing in Condensed-Matter Systems*. Oxford University Press, USA, 2006.

[119] Q. Li, M. Huecker, G. D. Gu, A. M. Tsvelik, and J. M. Tranquada. Two-Dimensional Superconducting Fluctuations in Stripe-Ordered $La_{1.875}Ba_{0.125}CuO_4$. *Phys. Rev. Lett.*, 99:067001/1–4, 2007.

[120] M. P. Lilly, K. B. Cooper, J. P. Eisenstein, L. N. Pfeiffer, and K. W. West. Anisotropic states of two-dimensional electron systems in high Landau levels: effect of an in-plane magnetic field. *Phys. Rev. Lett.*, 83:824–827, 1999.

[121] M. P. Lilly, K. B. Cooper, J. P. Eisenstein, L. N. Pfeiffer, and K. W. West. Evidence for an Anisotropic State of Two-Dimensional Electrons in High Landau Levels. *Phys. Rev. Lett.*, 82:394, 1999.

[122] Chungwei Lin, Erhai Zhao, and W. Vincent Liu. Liquid crystal phases of ultracold dipolar fermions on a lattice. arXiv:0909.5267v2.

[123] J. Lorenzana, C. Castellani, and C. Di Castro. Mesoscopic frustrated phase separation in electronic systems. *Euro. Phys. Lett.*, 57:704, 2002.

[124] J. Lorenzana and G. Seibold. Metallic mean-field stripes, incommensurability, and chemical potential in cuprates. *Phys. Rev. Lett.*, 89:136401, 2002.

[125] Mingwu Lu, Seo Ho Youn, and Benjamin L. Lev. Trapping ultracold dysprosium: a highly magnetic gas for dipolar physics. *Phys. Rev. Lett.*, 104:063001, 2010.

[126] J.M. Luttinger and L. Tisza. Theory of dipole interaction in crystals. *Phys. Rev.*, 70:954–964, 1946.

[127] A. H. MacDonald and M. P. A. Fisher. *Phys. Rev. B*, 61:5724, 2000.

[128] K. Machida. *Physica C*, 158:192, 1989.

[129] Adrian Del Maestro and Subir Sachdev. Thermal melting of density waves on the square lattice. *Phys. Rev. B*, 71:184511, 2005.

[130] Dmitrii L. Maslov, Andrey V. Chubukov, and Ronojoy Saha. Nonanalytic magnetic response of fermi and non-fermi liquids. *Physical Review B*, 74(22):220402, 2006.

[131] M. Matsuda, M. Fujita, S. Wakimoto, J. A. Fernandez-Baca, J. M. Tranquada, and K. Yamada. Magnetic Excitations of the Diagonal Incommensurate Phase in Lightly-Doped $La_{2-x}Sr_xCuO_4$. unpublished, 2008.

[132] J. J. McClelland and J. L. Hanssen. *Phys. Rev. Lett.*, 96:143005, 2006.

[133] W. L. McMillan. Landau theory of charge density waves in transition-metal dichalcogenides. *Phys. Rev. B*, 12:1187, 1975.

[134] W. L. McMillan. Theory of discommensurations and the commensurate-incommensurate charge-density-wave phase transition. *Phys. Rev. B*, 14:1496, 1976.

[135] C. Menotti, P. Pedri, and S. Stringari. *Phys. Rev. Lett.*, 89:250402, 2002.

[136] W Metzner, D. Rohe, and S. Andergassen. Soft fermi surfaces and breakdown of fermi-liquid behavior. *Phys. Rev. Lett.*, 91:066402, 2003.

[137] A. J. Millis. Effect of a nonzero temperature on quantum critical points in itinerant fermion systems. *Phys. Rev. B*, 48:7183, 1993.

[138] A. J. Millis, A. J. Schofield, G. G. Lonzarich, and S. A. Grigera. Metamagnetic Quantum Criticality. *Phys. Rev. Lett.*, 88:217204, 2002.

[139] Andrew J. Millis and M. R. Norman. Antiphase Stripe Order as the Origin of Electron Pockets Observed in 1/8-Hole-Doped Cuprates. *Phys. Rev. B*, 76:220503(R), 2007.

[140] Takahiko Miyakawa, Takaaki Sogo, and Han Pu. Phase-space deformation of a trapped dipolar fermi gas. *Phys. Rev. A*, 77:061603, 2008.

[141] Akiharu Miyanaga and Hiroyuki Yamase. Orientational symmetry-breaking correlations in square lattice t-J model. *Phys. Rev. B*, 73:174513, 2006.

[142] R. Moessner and J. T. Chalker. Exact results for interacting electrons in high landau levels. *Phys. Rev. Lett.*, 54:5006, 1996.

[143] H. A. Mook, Pengcheng Dai, F. Doğan, and R. D. Hunt. One-dimensional nature of the magnetic fluctuations in $YBa_2Cu_3O_{6.6}$. *Nature*, 404:729, 2000.

[144] E. Morosan, H. W. Zandbergen, B. S. Dennis, J. W. Bos, Y. Onose, T. Klimczuk, A. P. ramirez, N. P. Ong, and R. J. Cava. Superconductivity in Cu_xTiSe_2. *Nature Phys.*, 2:544, 2006.

[145] G. Mu, X. Zhu, L. Fang, L. Shan, C. ren, and H. H. Wen, 2008.

[146] E. Mueller and G. Baym. *Phys. Rev. A*, 62:053605, 2000.

[147] D. R. Nelson and B. I. Halperin. *Phys. Rev. B*, 19:2457, 1979.

[148] David R. Nelson and John Toner. Bond-orientational order, dislocation loops, and melting of solids and smectic-*A* liquid crystals. *Phys. Rev. B*, 24:363, 1981.

[149] Johan Nilsson and A. H. Castro Neto. Heat Bath Approach to Landau Damping and Pomeranchuk Quantum Critical Points. *Phys. Rev. B*, 72:195104, 2005.

[150] Vadim Oganesyan, Steven A. Kivelson, and Eduardo Fradkin. Quantum theory of a nematic fermi liquid. *Phys. Rev. B*, 64:195109, 2001.

[151] K. M. O'Hara, S. L. Hemmer, M. E. Gehm, S. R. Granade, and J. E. Thomas. *Science*, 298:2179, 2002.

[152] E. Olsson and C. J. Pethick. Multipolar contributions to the spin response of nuclear matter. *Phys. Rev. C.*, 66:065803, 2002.

[153] S. Ospelkaus et al. *arXiv:0811.4618*, 2008.

[154] W. Pan, R. R. Du, H. L. Störmer, D. C. Tsui, L. N. Pfeiffer, K. W. Baldwin, and K. W. West. Strongly anisotropic electronic transport at landau level filling factor $\nu = 9/2$ and $\nu = 5/2$ under tilted magnetic field. *Phys. Rev. Lett.*, 83:820, 1999.

[155] Kwon Park and Subir Sachdev. Bond-operator theory of doped antiferromagnets: From Mott insulators with bond-centered charge order to superconductors with nodal fermions. *Phys. Rev. B*, 64:184510, 2001.

[156] G. B. Partridge, W. Li, R. I. Kamar, Y. Liao, and R. G. Hulet. *Science*, 311:503, 2006.

[157] G. B. Partridge, K. E. Strecker, R. I. Kamar, M.W. Jack, and R.G. Hulet. *Phys. Rev. Lett.*, 95:020404, 2005.

[158] R. E. Peierls. *Annales de l'Institut Henri Poincaré*, 5:177, 1935.

[159] R. S. Perry, K. Kitagawa, S. A. Grigera, R. A. Borzi, A. P. Mackenzie, K. Ishida, and Y. Maeno. Multiple first-order metamagnetic transitions and quantum oscillations in ultrapure $Sr_3Ru_2O_7$. *Phys. Rev. Lett.*, 92:166602, 2004.

[160] C. J. Pethick and H. Smith. *Bose-Einstein condensation in dilute gases*. Cambridge University Press, New York, 2008.

[161] V. Poénaru and G. Toulouse. The crossing of defects in ordered media and the topology of 3-manifolds. *J. Physique*, 8:887, 1977.

[162] D. Poilblanc and T. M. Rice. *Phys. Rev. B*, 39:9749, 1989.

[163] I. Ia. Pomeranchuk. *Sov. Phys. JETP*, 8:361, 1958.

[164] R. G. Priest and T. C. Lubensky. Critical properties of two tensor models with application to the percolation problem. *Phys. Rev. B*, 13:4159, May 1976.

[165] Leonid P. Pryadko, Steven A. Kivelson, and Oron Zachar. Incipient order in the t-J model at high temperatures. *Phys. Rev. Lett.*, 92:067002, 2004. Erratum: *ibid* **98**, 069901 (2007).

[166] J. Quintanilla and A. J. Schofield. Pomeranchuck and topological fermi surface instabilities from central interactions. *Phys. Rev. B*, 74:115126, 2006.

[167] Jorge Quintanilla, Sam T. Carr, and Joseph J. Betouras. Meta-nematic, smectic and crystalline phases of dipolar fermions in an optical lattice. 2008.

[168] R. A. Borzi et al. Formation of a Nematic Fluid at High Fields in . *Science*, 315:214–217, 2007.

[169] Marcin Raczkowski, Manuela Capello, Didier Poilblanc, Raymond Frésard, and Andrzej M. Oleś. Unidirectional d-wave superconducting domains in the two-dimensional $t - J$ model. *Phys. Rev. B*, 76:140505(R), 2007.

[170] L. Radzihovsky and A. T. Dorsey. Theory of Quantum Hall Nematics. *Phys. Rev. Lett.*, 88:216802, 2002.

[171] Leo Radzihovsky and Ashvin Vishwanath. Quantum liquid crystals in imbalanced Fermi gas: fluctuations and fractional vortices in Larkin-Ovchinnikov states.

[172] S. R. Renn and T. C. Lubensky. Abrikosov dislocation lattice in a model of the cholesteric-to-smectic-A transition. *Phys. Rev. A*, 38(4):2132–2147, Aug 1988.

[173] Peter Ring and Peter Schuck. *The Nuclear Many-Body Problem*. Springer-Verlag New York Inc, 1980.

[174] Shai Ronen and John L. Bohn. Zero sound in dipolar fermi gases. arXiv:0906.3753v2.

[175] M. Rübhausen, S. Yoon, S. L. Cooper, K. H. Kim, and S. W. Cheong. Anisotropic optical signatures of orbital and charge ordering in $Bi_{1-x}Ca_xMnO_3$. *Phys. Rev. B*, 62:R4782, 2000.

[176] P. A. Ruprecht, M. J. Holland, K. Burnetts, and M. Edwards. *Phys. Rev. A*, 51:4704, 1995.

[177] A. Rusydi, S. Smadici, J. C. Lee, S. Wang, P. Abbamonte, M. Enoki, M. Fujita, M. Rübhausen, and K. Yamada. Unidirectional charge order near room temperature in Zn-doped $La_{2-x}Sr_xCuO_4$. unpublished, 2007.

[178] A. Sacchetti, E. Arcangeletti, A. Perucchi, L. Baldassarre, P. Postorino, S. Lupi, N. Ru, I. R. Fisher, and L. Degiorgi. Pressure Dependence of the Charge-density-Wave Gap in Rare-Earth Tritellurides. *Phys. Rev. Lett.*, 98:026401, 2007.

[179] A. Sacchetti, L. Degiorgi, T. Giamarchi, N. Ru, and I. R. Fisher. Chemical pressure and hidden one-dimensional behavior in rare-earth tri-telluride charge-density-wave compounds. *Phys. Rev. B*, 74:125115, 2006.

[180] Subir Sachdev. *Quantum Phase Transitions*. Cambridge University Press, Cambridge, UK, 1999.

[181] Subir Sachdev. Order and quantum phase transitions in the cuprate superconductors. *Rev. Mod. Phys.*, 75:913, 2003.

[182] Subir Sachdev, Andrey V. Chubukov, and Alexander Sokol. Crossover and scaling in a nearly antiferromagnetic fermi liquid in two dimensions. *Phys. Rev. B*, 51(21):14874–14891, Jun 1995.

[183] H. J. Schulz. Incommensurate antiferromagnetism in the 2-dimensional Hubbard model. *Phys. Rev. Lett.*, 64:1445, 1990.

[184] G. Seibold and J. Lorenzana. Stability of metallic stripes in the one-band extended Hubbard model. *Phys. Rev. B*, 69:134513, 2004.

[185] M Seul and D Andelman. Domain shapes and patterns: The phenomenology of modulated phases. *Science*, 267:476, 1995.

[186] L. J. Sham and Bruce R. Patton. Effect of impurity on a peierls transition. *Phys. Rev. B*, 13(7):3151–3153, Apr 1976.

[187] T. Shi, J.-N. Zhang, C.-P. Sun, and S. Yi. Singlet and triplet bcs pairs in a gas of two-species fermionic polar molecules. arXiv:0910.4051v1.

[188] C. S. Snow, J. F. Karpus, S. L. Cooper, T. E. Kidd, and T.-C. Chiang. Quantum Melting of the Charge-Density-Wave State in 1T-$TiSe_2$. *Phys. Rev. Lett.*, 91:136402, 2003.

[189] T Sogo, L He, T Miyakawa, S Yi, H Lu, and H Pu. Dynamical properties of dipolar fermi gases. *New J. Phys.*, 11:055017, 2009.

[190] C. Stock, W. J. L. Buyers, R. Liang, D. Peets, Z. Tun, D. Bonn, W. N. hardy, and R. J. Birgeneau. Dynamic stripes and resonance in the superconducting and normal phases of $YBa_2Cu_3O_{6.5}$ ortho-II superconductor. *Phys. Rev. B*, 69:014502, 2004.

[191] H. T. C. Stoof, M. Houbiers, C. A. Sackett, and R. G. Hulet. *Phys. Rev. Lett.*, 76:10, 1996.

[192] K.E. Strecker, G.B. Partridge, and R.G. Hulet. *Phys. Rev. Lett.*, 91:080406, 2003.

[193] K. Sun, B. M. Fregoso, M. J. Lawler, and E. Fradkin. Fluctuating stripes in strongly correlated electron systems and the nematic-smectic quantum phase transition. *Phys. Rev. B*, 78:085124, 2008.

[194] John Toner and David R. Nelson. Smectic, cholesteric, and rayleigh-benard order in two dimensions. *Phys. Rev. B*, 23(1):316–334, Jan 1981.

[195] J. M. Tranquada, B. J. Sternlieb, J. D. Axe, Y. Nakamura, and S. Uchida. Evidence for stripe correlations of spins and holes in copper oxide superconductors. *Nature*, 375:561, 1995.

[196] J. M. Tranquada, H. Woo, T. G. Perring, H. Goka, G. D. Gu, G. Xu, M. Fujita, and K. Yamada. Quantum Magnetic Excitations from Stripes in Copper-Oxide Superconductors. *Nature*, 429:534, 2004.

[197] John M. Tranquada. Neutron scattering studies of antiferromagnetic correlations in cuprates. In J. R. Schrieffer and J. Brooks, editors, *Treatise of High Temperature Superconductivity*, pages 257–298, New York, 2007. Springer-Verlag.

[198] V. Hinkov et al. Electronic liquid crystal state in superconducting $YBa_2Cu_3O_{6.45}$. *Science*, 319:597, 2008.

[199] Hilbert v. Löhneysen, Achim Rosch, Matthias Vojta, and Peter Wölfle. Fermi-liquid instabilities at magnetic quantum phase transitions. *Rev. Mod. Phys.*, 79:1015, 2007.

[200] C. M. Varma. A Theory of the Pseudogap State of the Cuprates. *Philos. Mag.*, 85:1657, 2005.

[201] G. Veeravalli et al. *Phys. Rev. Lett.*, 101:250403, 2008.

[202] I. Vekhter and A. V. Chubukov. Non-Fermi liquid behavior in itinerant antiferromagnets. *Phys. Rev. Lett.*, 93:016405, 2004.

[203] M. Vershinin, S. Misra, S. Ono, Y. Abe, Y. Ando, and A. Yazdani. Local ordering in the pseudogap state of the high-t_c superconductor $bi_2sr_2cacu_2o_{8+\delta}$. *Science*, 303:1005, 2004. arXiv:cond-mat/0402320.

[204] Ashvin Vishwanath and David Carpentier. Two-dimensional anisotropic non-Fermi-liquid phase of coupled Luttinger liquids. *Phys. Rev. Lett.*, 86:676, 2001.

[205] M. Vojta and S. Sachdev. Charge order, superconductivity, and a global phase diagram of doped antiferromagnets. *Phys. Rev. Lett.*, 83:3916, 1999.

[206] M. Vojta, Y. Zhang, and S. Sachdev. Renormalization group analysis of quantum critical points in d-wave superconductors. *Int. J. Mod. Phys. B*, 14:3719, 2000.

[207] Daw-Wei Wang. An effective many-body theory for strongly interacting polar molecules. *New Journal of Physics*, 10:053005, 2008.

[208] C. Wexler and A. Dorsey. Disclination Unbinding Transition in Quantum Hall Liquid Crystals. *Phys. Rev. B*, 64:115312, 2001.

[209] S. R. White and D. J. Scalapino. *Phys. Rev. B*, 61:6320, 2000.

[210] E. P. Wigner. On the Interaction of Electrons in Metals. *Phys. Rev.*, 46(11):1002–1011, Dec 1934.

[211] P. Wolfle and A. Rosch. Fermi liquid near a quantum critical point. *J. Low Temp. Phys.*, 147:165, 2007.

[212] C. J Wu, Kai Sun, Eduardo Fradkin, and S.-C Zhang. Fermi liquid instabilities in the spin channel. *Phys. Rev. B*, 75:115103, 2007.

[213] Cenke Xu, Markus Müller, and Subir Sachdev. Ising and Spin orders in Iron-based Superconductors, 2008.

[214] H. Yamase. Magnetic excitations in La-based cuprate superconductors: slave-boson mean-field analysis of the two-dimensional t-J model. *Phys. Rev. B*, 75:014514, 2007.

[215] H. Yamase and H. Kohno. *J. Phys. Soc. Jpn.*, 69:2151, 2000.

[216] Hiroyuki Yamase, Vadim Oganesyan, and Walter Metzner. Mean-field theory for symmetry-breaking surface deformation on a square lattice. *Phys. Rev. B*, 72:035114, 2005.

[217] Hong Yao, John A. Robertson, Eun. Ah Kim, and Steven A. Kivelsonn A. Kivelson. Theory of stripes in quasi-two-dimensional rare-earth tritellurides. *Phys. Rev. B*, 74:245126, 2006.

[218] S. Yi and L. Lou. Trapped condensates of atoms with dipole interations. *Phys. Rev. A*, 63:053607, 2001.

[219] S. Yi and H. Pu. *Phys. Rev. Lett.*, 97:020401, 2006.

[220] L. You and M. Marinescu. Prospect for p-wave paired bardeen-cooper-schrieffer states of fermionic atoms. *Phys. Rev. A*, 60:2324, 1999.

[221] A. P. Young. *Phys. Rev. B*, 19:1855, 1979.

[222] J. Zaanen and O. Gunnarsson. Charged magnetic domain lines and the magnetism of high T_c oxides. *Phys. Rev. B*, 40:7391, 1989.

[223] J. Zaanen, Z. Nussinov, and S. I. Mukhin. Duality in 2+1 D Quantum Elasticity: superconductivity and Quantum Nematic Order. *Annals of Physics*, 310:181, 2004.